Zeitschrift: Helvetica Physica Acta
Band: 63 (1990)
Heft: 4

Artikel: Proceedings of the PSI workshop on intense slow positron beams and applications in condensed matter physics
Autor: [s.n.]
DOI: https://doi.org/10.5169/seals-116227

Proceedings of the PSI Workshop on Intense Slow Positron Beams and Applications in Condensed Matter Physics

EDITOR: W.B. Waeber

EDITORIAL

In November 1989 an international workshop on 'Intense Beams of Slow Positrons and Applications in Condensed Matter Physics and Other Scientific Disciplines' was held at PSI. 38 scientists from Japan, USA, USSR and Europe as well as 28 scientists from this country attended the meeting, which has been co–sponsored by PSI and the University of Geneva. We would like to express our appreciation to Mrs. E. Huber, PSI for her skilful organizational efforts towards a very successful meeting.

The following proceedings highlight the topics that have been treated in the workshop. We are grateful to all invited speakers of the workshop, without their efforts it would not have been possible to publish the proceedings in time. The contribution on 'Defect Studies by Positron Annihilation' has been included in an extended form in these proceedings. It meets the general philosophy of PSI by expressing encouraging perspectives for future developments in positron annihilation applied to defect physics.

We would also like to thank the Editor of Helvetica Physica Acta and the Birkhäuser Verlag, who have supported the idea of publishing the proceedings in one of the current volumes of the journal.

W.B. Waeber, PSI

Helvetica Physica Acta
Vol. 63 (1990)

0018-0238/90/040377-01$1.50+0.20/0

FOREWORD

This collection of reports is the result of an evaluation concerning the installation of an intense e^+-source at PSI and will serve as the basis for a corresponding proposal. This evaluation was mainly undertaken, because e^+-beams with intensities that are not available at present might open new research possibilities such as e^+-microscopy, mainly for defect studies, and e^+-spectroscopy of electronic structures in metals. The development of a working e^+-microscope is a challenge by itself, and e^+-spectroscopy at the envisaged intensities would call for new types of detectors; i.e., advancement of future technology.

The contributions to this volume which are written versions of talks that were delivered at a special workshop organized at PSI on November 20, 1989, discuss the possibilities for realizing such a facility and also reveal some of its future applications. We are especially indebted to our outside colleagues in Switzerland and particularly to those from abroad who show interest in our plans and lent us their expertise and know-how. Special thanks go to Prof. M. Peter of the University of Geneva, who enthusiastically supported the project from its beginning. Last but not least I should like to thank the members of PSI's defect-physics group who made this evaluation possible, together with various members of the Research Division F1, whose contributions are also gratefully acknowledged. In this sense the project could become a major task whose success would heavily depend on a close collaboration between different research divisions of PSI.

Professor H.R. Ott
Head of Research Division F3

Helvetica Physica Acta
Vol. 63 (1990)
0018-0238/90/040378-07$1.50+0.20/0

THE PULSED POSITRON BEAM IN MUNICH AND A HIGH INTENSE POSITRON SOURCE AT GRENOBLE

W. Triftshäuser, G. Kögel,
Institut für Nukleare Festkörperphysik, Universität der Bundeswehr München,
8014 Neubiberg, Fed. Rep. of Germany,
K. Schreckenbach, B. Krusche,
Institut Laue–Langevin, 38042 Grenoble, France.

A pulsing system for a low energy positron beam of variable energy has been set up. The system consists of a beam chopper and a beam buncher. Presently, a time resolution of 135 ps is achieved for the pulsing system at positron energies in the range between 0.5 keV and 28 keV.

A high intense positron beam is proposed at the high flux nuclear reactor using ^{113}Cd. Positrons are produced by pair production from the γ–rays of ^{114}Cd after neutron capture. Outside of the reactor a low energy positron beam of 10^{10} positrons/s is expected.

1. INTRODUCTION

Positron annihilation is a standard method to study microscopic properties in condensed matter [1]. Positron lifetime measurements are particularly valuable because they allow, in principle, the quantitative identification of several structural defects that are present simultaneously [2]. With the standard lifetime method using a radionucleus (e.g. ^{22}Na), the time difference between an annihilation quantum and a γ–ray following the positron emission is measured. However, due to the large penetration depth (20–200 μm) of the positrons from radioactive isotopes only bulk properties can be studied. Monoenergetic positrons of variable energy [3,4] have to be used to control the mean penetration depth of the positrons in order to obtain information about surface, surface layers and damage regions. Such monoenergetic positrons are obtained by slowing down the positrons from a radioactive source in an appropriate moderator material and accelerating the reemitted ones to the desired energy. However, the time correlation, as described above, is destroyed due to the moderation process. In order to regain a time correlation, the positron beam is chopped to 1 ns pulses and a subsequent buncher compresses the pulses, in the present state, to 135 ps at the target position [5,6]. Since the coincidence count rate in such a lifetime system is equal to the single count rate in only one detector, there is almost no principle limitation on the primary intensity of the positron source. When intense positron beams are available (e.g. 10^{10} positrons/s), lifetime spectra can be obtained in fractions of a second, and it will be possible to study dynamical processes on very short time scales. One possibility for a high intense positron beam based on ^{113}Cd inside a nuclear reactor will be proposed and discussed.

2. THE PULSED LOW ENERGY POSITRON SYSTEM (PLEPS)

The concept of beam pulsing was first developed for heavy ion beams [5–8]. With a chopper a continuous beam is deflected across an aperture in order to cut out a certain part of the positron beam and to suppress the rest [9]. A disadvantage, however, is the reduction of the average beam intensity as well as the additional energy spread arising when a pulse width is created. With a subsequent beam buncher the positrons may be accelerated or decelerated by alternating longitudinal electric fields resulting in a time focus at the target position. There is no loss in the average beam intensity. Due to non-ideal modulation voltages, however, there is always a finite background intensity remaining. Therefore the combination of chopper and buncher is the best approach. A more detailed description of the complete system can be found in ref. [10]. The schematics of PLEPS is shown in fig. 1. The whole system is mounted vertically in order to allow also the investigation of liquid targets.

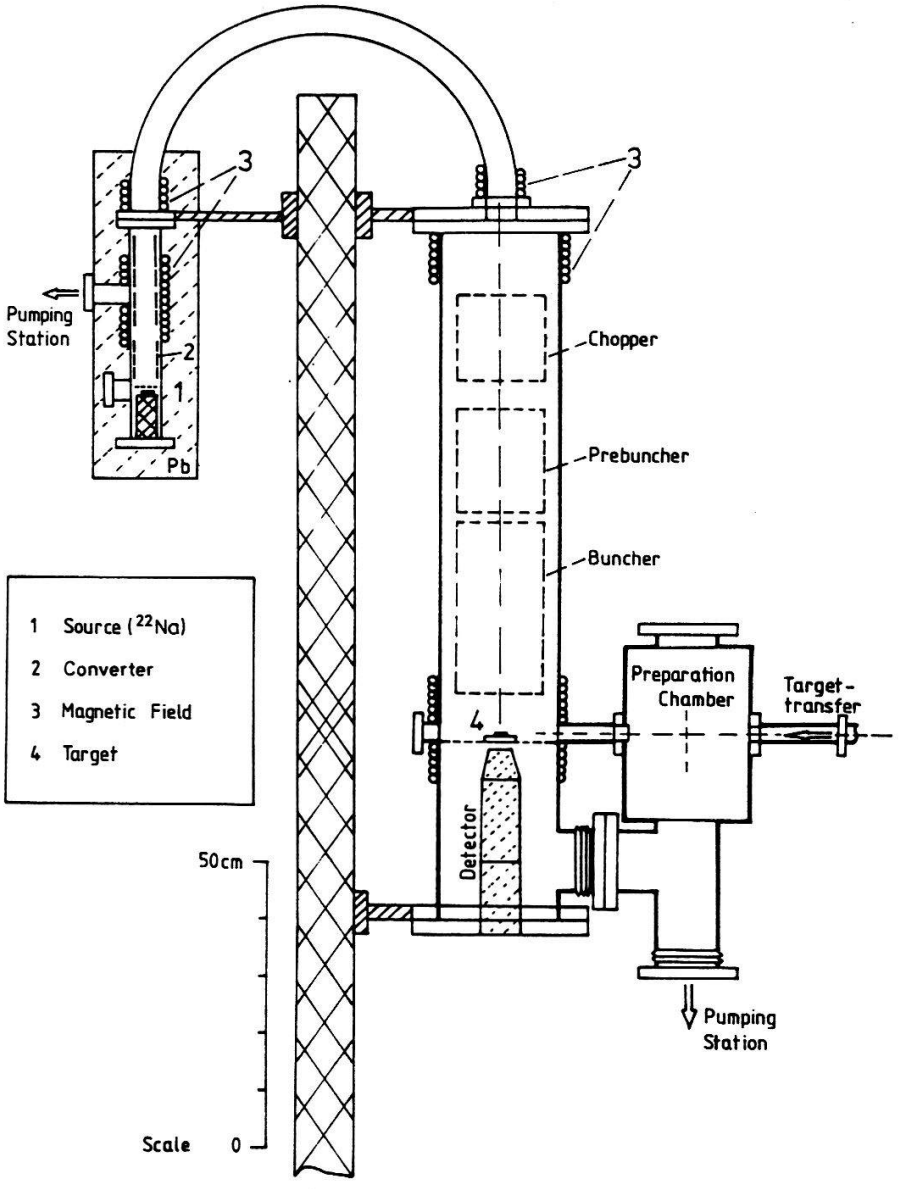

Fig. 1. The pulsed low energy positron system (PLEPS)

The beam pulsing unit and the corresponding time structure in the beam is shown schematically in fig. 2. For the in situ treatment and the transfer of the target a preparation chamber is connected to the vacuum system. The PLEPS is in operation for several years [11,12].

Positron lifetimes in various materials ranging from carbon to tantalum have been investigated at positron energies from 0.5 keV up to 28 keV. Most recently the positron lifetime at clean metallic surfaces has been measured [13]. The total time resolution for the 3 mm diameter positron beam, as deconvoluted by standard fitting procedures from the measured distribution, is 225 ps (FWHM). The time resolution of the detector (BaF_2 scintillator coupled to an XP 2020 Q photomultiplier) and the subsequent electronics was determined to ≈ 180 ps. This results in a time resolution of the pulsing system of about 135 ps.

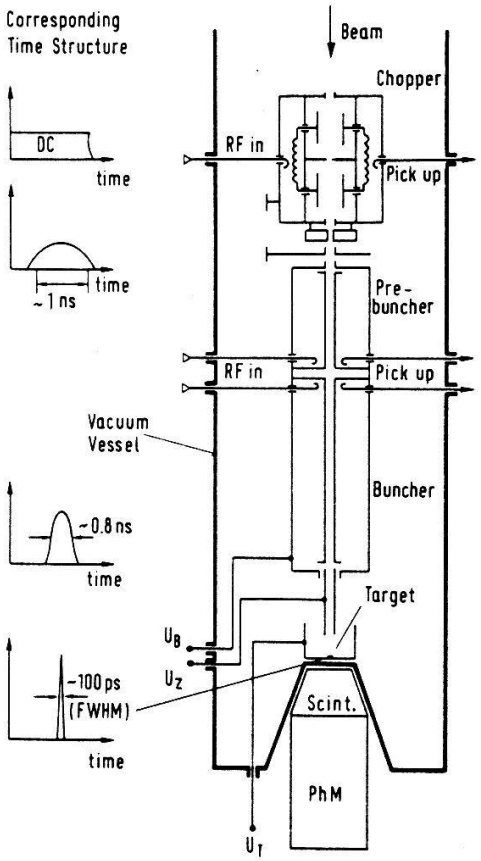

Fig. 2. Schematics of the beam pulsing unit and the corresponding time structure of the beam.

Presently several procedures are under way for upgrading the existing PLEPS.

i) The insertion of a pulsed remoderation stage will reduce the beam diameter to about 1 mm. Due to resulting less energy spread the pulsing time resolution is estimated to 50 ps FWHM and the final positron energy could be as low as 50 eV.

ii) Before the remoderation stage the positron beam will be bunched to 1.5 ns pulses. Thus no total intensity loss is expected inspite of the remoderation process. iii) The pulse repetition rate will be expanded from presently 5 ns to 20 ns so that longer positron lifetimes can be determined.

3. THE PROJECTED HIGH INTENSE POSITRON BEAM

For the high flux reactor at Grenoble a new type of a high intense positron source is being discussed. The source is based on the pair production process from neutron capture γ–rays. A first type of such a source was already operated for a tunable positron beam in the energy range between 2 and 3 MeV. A target of a 3.3 mm thick titanium plate (area 5 cm x 10 cm) covered with a 0.25 mm thick platinum converter was placed at the in–pile target site of the BILL beta spectrometer at a neutron flux of $3.3 \cdot 10^{14}$ neutrons/cm^2s. The beta spectrometer served as monochromator and focussed the positrons in the focal plane at a distance of 14 m away from the target. The measured positron flux in the available area of 10 cm · 1 cm in the focal plane was $3 \cdot 10^6$

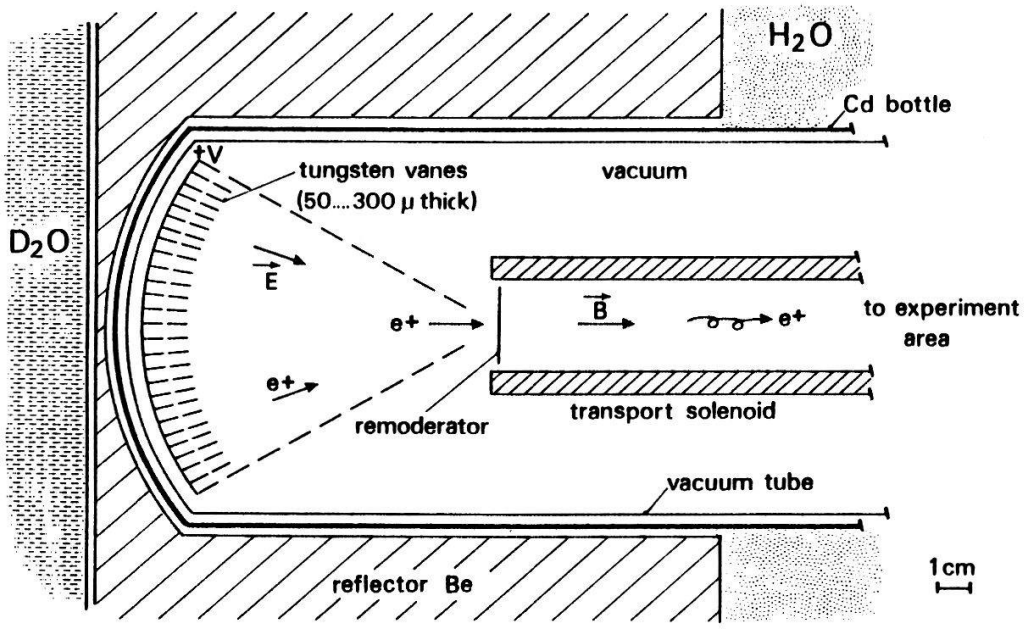

Fig. 3. Arrangment of the positron source inside the reactor in form of an "electron gun".

positrons/s at an energy of 2.5 MeV. Due to the relative momentum dispersion of $1.5 \cdot 10^{-3}$ per cm of the beta spectrometer, the 10 cm length of the focal plane correspond to an energy range of 30 keV at 2.5 MeV [14]. The total positron intensity at the target position was estimated as 10^{10} positrons/s for the total size of the plate. A further intensity increase is in principle possible with thicker targets provided the self heating problem can be solved. A series of positron–electron (Bhabha) scattering experiments have been performed with this source system in search for possible resonances in this process as a possible interpretation of observed correlated positron–electron peaks in heavy ion reactions [14,15].

The combination titanium target and platinum converter yields primary positrons of relatively high energy (maximum intensity around 2.5 MeV). This is not optimal for moderating positrons when used as a primary source. The combination of neutron capture in cadmium and the conversion of the subsequent γ–rays in tungsten is better suited for this purpose. The isotope ^{113}Cd (natural abundance 12%) has a very high cross section of 27 000 barn for capturing thermal neutrons. Therefore a layer of 1 mm natural cadmium is totally absorbing for thermal neutrons. The γ–ray spectrum in cadium after neutron capture is "softer" than in the case of titanium. In a layer of tungsten the γ–rays can be converted into electron–positron pairs and the produced high energy positrons are moderated in the same layer to low energy positrons. In this way an intense source of low energy positrons is created. This process is similar to the low energy positron source at a LINAC, but with very important differences: i) The heat produced in the converter is much less. ii) A continuous positron beam is being

produced. iii) The energy distribution of the primary positrons is at lower energies. Calculations and measurements of the produced primary positron spectrum give adistribution with a maximum at about 800 keV. For a plane geometry of 1 mm cadmium covered by 200 μm tungsten, the absorption of 100 neutrons would yield about 1 positron [16]. A possible layout for a source of low energy positrons using this method is shown in fig. 3. The arrangement will work best if it is placed in a high thermal neutron flux without fast neutrons in order to prevent radiation damage especially in the tungsten moderator. In addition to the production of the γ–rays, the cadmium layer protects the tungsten from neutron activation. The produced isotope ^{114}Cd is stable. Therefore the whole system will not remain too radioactive when it will be moved out of the neutron flux. A large thermal neutron flux is normally available at a reactor. The problem arises to collect efficiently the moderated positrons from a large surface and to from a narrow positron beam. The source shown here uses a focussing arrangment similar to an electron gun. In order to improve the beam quality (good energy homogeneity, small diameter) and to facilitate the beam transport, a remoderator may be used at the entrance of the magnetic transport field. At the high flux reactor at Grenoble the cadmium bottle could be placed in the light water pool just outside the heavy water tank. With a flux of about $4 \cdot 10^{13}$ neutrons/cm^{2}s at this position, a flux of remoderated positrons in the transport solenoid of the order of 10^{10} positrons per second is expected with a beam diameter of less than 1 cm. For this estimate moderator and remoderator efficiencies of $5 \cdot 10^{-4}$ and $1.5 \cdot 10^{-1}$ are assumed, respectively.

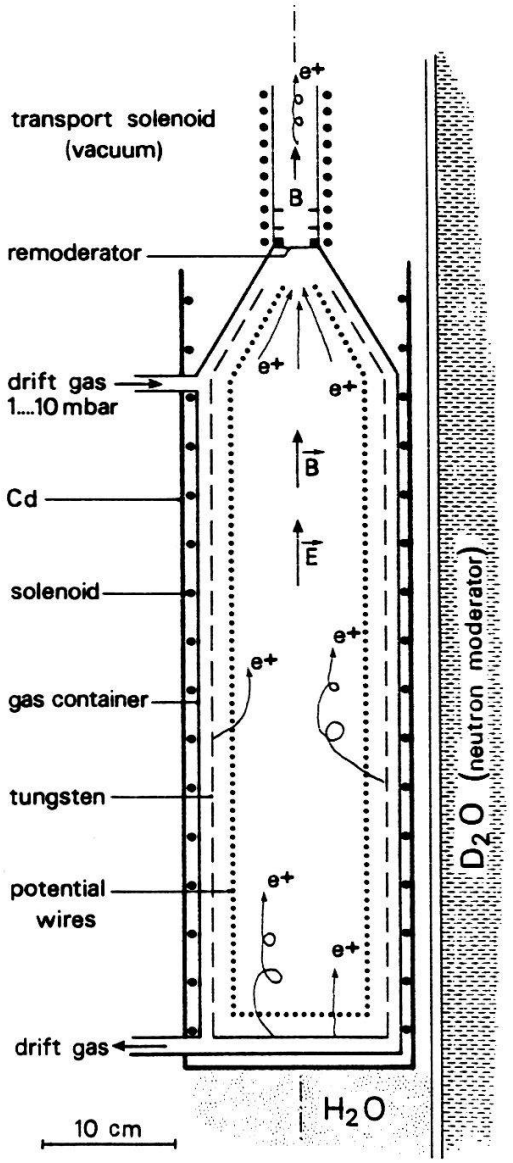

Fig. 4. A positron drift chamber as low energy positron source. The tracks illustrate the drift of moderated positrons and the gas moderation, respectively.

A still higher intensity of positrons could be achieved if positrons from an even larger source area can be focussed to a narrow beam. The electrostatic focussing is limited by the initial transversal momentum of the positrons when leaving the moderator. One possibility to solve this problem may be the use of a drift tube as shown in fig. 4. The moderated positrons drift along the electric field lines without acceleration and below the energy threshold for positronium formation. Under these conditions the annihilation probability is rather low. For suitable gas pressures corresponding to a mass density of about 5 $\mu g/cm^3$ (equivalent to 28 mbar He, 4 mbar N_2 or 2.5 mbar CO_2) the positron survival time is of the order of 40 μs [17,18]. Typical drift velocities are 1 to 2 cm/μs. Some additional premoderation of positrons in the keV region is also likely. For molecular gases the positrons are slowed down via rotational exitations. The positrons are finally collected and focussed onto a remoderator. Certainly a number of problems arise for the verification of such a positron drift chamber. It may not even work in this way, in particular, in the presence of the high radiation level present at the necessary position inside the reactor. However, it is worthwhile to be investigated further and it can stimulate discussions whether the drift principle could provide an effective way of collecting moderated positrons. A similar principle has been already successfully used for trapping positrons [19].

4. CONCLUSIONS

With a pulsed positron beam it has been proven to obtain a time resolution of 135 ps, and with further upgrading even 50 ps will be possible. In contrast to a conventional positron lifetime system where coincidences between a high energy γ–ray (start–detector) and an annihilation quantum (stop–detector) have to be measured, enables the PLEPS positron lifetime measurements with only one detector. Therefore there are no principal limitations for the positron source intensity whereas in the other case the accidental coincidences limit the maximum source activity ($\sim$ 50 μCi).

The realization of a continuous high intense beam of low energy positrons seems feasable. With suitable geometries and collection processes intensities even larger than 10^{10} low energy positrons/s are not unrealistic. However, further investigations are necessary in this field.

Acknowledgements

This project is partly supported by the Deutsche Forschungsgemeinschaft.

REFERENCES

[1] W. Triftshäuser in Microscopic Methods in Metals, ed. U. Gonser, Topics in Current, ed. U. Gonser, Topics in Current Physics, Vol. 40 (Springer, Berlin–Heidelberg–New York, 1986) p. 249

[2] B. Viswanathan, W. Triftshäuser and G. Kögel, Radiat. Eff. 78 (1983) 231

[3] K.G. Lynn, J. Phys. C 12 (1979) 1435

[4] W. Triftshäuser and G. Kögel, Phys. Rev. Lett. 48 (1982) 1741

[5] R. Zierl, W. Czech, P. Kienle, H.J. Körner, K.E. Rehm, P. Sperr and W. Wagner, Nucl. Instr. and Meth. 164 (1979) 219

[6] D. Schödlbauer, K. Rudolf, U. Lenz and S.J. Skorka, Nucl. Instr. and Meth. A 244 (1986) 180

[7] F.J. Lynch, R.N. Lewis, L.M. Bollinger, W. Henning and O.D. Despe, Nucl. Instr. and Meth. 159 (1979) 245

[8] U. Ratzinger, R. Geier, W. Schollmeier, S. Gustavsson and E. Nolte, Nucl. Instr. and Meth. 205 (1983) 381

[9] W. Korndahl and R.W. Richter, Nucl. Instr. and Meth. 68 (1969) 298

[10] D. Schödlbauer, P. Sperr, G. Kögel and W. Triftshäuser, Nucl. Instr. and Meth. in Phys. Res. B 34 (1988) 258

[11] D. Schödlbauer, G. Kögel, P. Sperr and W. Triftshäuser, Phys. Status Solidi 102 (1987) 549

[12] G. Kögel, D. Schödlbauer, W. Triftshäuser and J. Winter, Phys. Rev. Lett. 60 (1988) 1550

[13] R. Steindl, G. Kögel and W. Triftshäuser, to be published

[14] H. Tsertos, C. Kozhuharov, P. Armbruster, P. Kienle, B. Krusche and K. Schreckenbach, Phys. Rev. D 40 (1989) 1397

[15] S. Judge et al, to be published

[16] B. Krusche and K. Schreckenbach, to be published in Nucl. Instr. and Meth.

[17] G.R. Heyland, M. Charlton, T.C. Griffith and G.L. Wright, Can. J. Phys. 60 (1982) 503

[18] M. Charlton, J. Phys. B 18 (1985) L 667

[19] C.M. Surko, M. Leventhal and A. Passner, Phys. Rev. Lett. 62 (1989) 901

Helvetica Physica Acta
Vol. 63 (1990)

0018-0238/90/040385-04$1.50+0.20/0

PRESENT AND FUTURE POSITRON BEAMS IN JAPAN

Shoichiro Tanigawa

Institute of Materials Science, University of Tsukuba,
Tsukuba, Ibaraki 305, Japan

Introduction

The field of low energy positron physics has significantly expanded in recent years to include not only particle and atomic physics but also solid state and surface physics or materials science. The interaction of a positron with matter shows a wide variety. Roughly speaking, the use of a positron as a probe in materials science can be grouped into four categories: 1) an electronic structure probe, 2) a lattice defect probe, 3) a surface/interface probe, and 4) a micro probe. The advances in positron beam technology from an uncontrolled use as a white beam as born from radioactive nuclei to a well controlled use as a slow/monoenergetic and a high brightness beam expanded an object of study from the bulk to the depth specified surface/interface region and further to the three–dimensionally specified small region.

In this report, I will review the status of present and future positron beams in Japan. At present, two slow positron facilities using Linacs as a slow positron generator are in operation. Several radioisotope–based laboratory beams are in operation.

I begin with a survey of conditions surrounding positron beams in Japan. A second section will summarize several ways for the generation of positrons. Emphasis will be placed on three types of planned beams: 1) a Linac–based full scale factory, 2) a cyclotron–based mini–factory, and 3) a radioisotope–based laboratory beam dedicated to industrial research.

Conditions Surrounding Positron Beams in Japan

There have been big circumstantial changes around positron research in Japan in the last few years. One of them is a new trend for the investment of research funds, especially to basic research fields. The government changed his mind from the applied research oriented policy to the basic one based on the consideration of the trade imbalance with other countries and on its contribution to the world via creative basic research. The applied research will easily produce useful results and is very helpful for the promotion of industries. The basic research, however, is future–oriented and not directly useful at the moment. Although positron colleagues persist that positrons are very useful particles, the word "positron" sounds very basic and mysterious.

Second, there is a big demand on a probe for lattice defects near surface/interfaces in materials engineering. The well defined and controlled surface/interface will provide a new source of high–performance materials. The characterization of surface/interfaces is a key requisite. Electrons, ions, photons, and so on have been successfully used as a probe of atomistic arrangements and element compositions near surface/interface. More important is the defect analysis near a surface/interface. We have had no suitable probe for defects

until the physical process to create a low and/or monoenergetic positron was discovered. This excellent feature of slow positron beams has attracted the interest of industrial people, especially in semiconductor based devices. Some companies are planning to construct their own beams.

The third is the recent guideline on "Advanced Use of Radiations" in the atomic energy fund. Of course, a positron is nominated as one of promising candidates for useful radiations. According to the guideline, the Japan Atomic Energy Research Institute (JAERI) has started drafting a construction plan of a positron factory, in which high–intensity energy–controllable monoenergetic positron beams are generated from the pair production reaction caused by high–energy electrons from a Linac.

The fourth is the rapid spread of small cyclotrons, over 30 machines in hospitals and laboratories for the purpose of the positron CT. The positron CT has intensively been evaluated in the functional tomography, especially in brains. Also in the experiments on small animals, one can save the number of animals without killing by the use of the CT. This advantage has attracted the interest of engineers of automobiles. They are planning to see the flow of lubricants in the interior of engines without cutting. Roughly speaking, in the medical science, even a very expensive method is approved if it can save the life of a patient. The same is true in industries accompanied with mass production, i.e., automobiles, VLSI and so on.

The above mentioned situations have been much encouraging positron people in Japan. A few of our colleagues are rather afraid of the lack of accumulated human resources in this field and push us, university people, to supply many well educated students to the positron field.

Survey on Production Methods of Positrons

How can we get positrons? We have only two ways, the use of positron emitting radioisotopes and the use of positron–electron pair production. Depending on the manners of utilization, I will classify the methods to generate positrons into the following five groups:

1) Use of long–lived radioisotopes

Until now, ^{22}Na of $\sim$ 100 mCi and ^{58}Co of $\sim$ 500 mCi have been conveniently used for laboratory beams. The number of slow positrons varies from 10^4 to 5 x 10^6 e^+/sec. This number is enough for usual uses except for 2D–ACAR, microscopes, LEPD, and so on. Although the number of particles will be increased by the upgrade of moderation methods, it is also a clever way to employ high–efficiency detectors. This type of beam can be easily converted to a desktop beam and is planned to be introduced into industry laboratories in Japan.

2) Use of rather short–lived radioisotopes

Successful use of high–intense ^{64}Cu has been realized at Brookhaven. The number of slow positrons attains 10^8 e^+/sec. It needs a high–flux reactor near the beam site because of the half–life of 12.7 hours. In Japan, this method is not realistic due to the severe

regulation on unsealed radioisotopes. That is, the Japanese regulation expects that one per cent of the activity will diffuse into air.

3) Use of ultra short–lived radioisotopes

In the field of medical science, the positron CT method has rapidly advanced. In this field, ^{11}C (20.4 min), ^{13}N (10 min), ^{15}O (122 sec), and ^{18}F (110 min) are used as positron emitters which are supplied from a closely placed compact cyclotron. As far as I know, only Stein et al. utilized this type of ultra short–lived isotopes for the creation of slow positrons. A compact cyclotron is very cheap as compared with a high–flux reactor and an electron Linac. A Japanese group, including me, is now planning the on–line use of this machine to create ultra short–lived isotopes, such as ^{17}F (62 sec), ^{23}Mg (12 sec). ^{27}Si (4 sec), ^{30}P (150 sec), and so on. Due to their short life, the production yield cannot be determined by the usual measurement of radioactivity, but by a direct counting of positrons themselves after having transported them to a distant place from high radiation areas. This requires automatically the construction of a slow positron beam line. In an efficient nuclear reaction of a proton, a deuteron, and α–particles one positron emitter can be produced per 100 incidents. The maximum positron energies are ranging from 1.5 to 4 MeV. Since the positron emitter and a moderator can be separated in case of the back–reflecting geometry, the conversion efficiency of 10^{-4} can be expected at the lowest. The advance in a H^- cyclotron has made possible the use of 1 mA incident proton beam. Therefore, I myself expect that a slow positron beam of 1 nA is not impossible by this method.

4) Use of positron–electron pair production by radiations from an electron Linac

There have been many efforts to use an electron Linac for the production of slow positrons. It has been established that one incident electron of 50 – 120 MeV can produce 10^{-7} – 10^{-6} positrons. The operation mode of most Linacs is a pulsed one with the repetition of 50 – 1000 Hz. Therefore, produced positrons are also in a pulsed mode. Many experiments require a continuous DC beam because of the saturation of detectors. The conversion from a pulsed beam to a continuous one has been successfully realized by the use of a Penning trap. This conversion process loses 90 % of positrons at most, due to the inhomogeneous magnetic field and their collisions with gasses. In the case of a 1 mA Linac we can expect a sub–nA beam by the present state of the art.

5) Use of positron–electron pair production by γ radiations from the (n, γ) reaction in an atomic reactor

Cd, which is used as a thermal neutron absorber in an atomic reactor, absorbs neutrons by (n, γ) reaction with the cross section over 20.000 barns. In other words, Cd in a reactor is just the strong γ source to create positrons via pair production as proposed by European colleagues. In Japan, however, this method seems not to be realistic again in view of the regulation on atomic reactors.

The above listed ways of positron generation provide a continuous beam except for

the use of a pulsed Linac (4). The advantage of the methods (2) and (5) is a parasitic use of a reactor. Methods (3) and (4) require the monopoly of an accelerator at the beam time.

Present Status of Positron Beams in Japan

At this writing, two slow positron facilities are in operation. One is at the Electrotechnical Laboratory (ETL) in Tsukuba and the other is at the Japan Atomic Energy Research Institute (JAERI) in Tokai. At ETL, the conversion efficiency of 6 x 10^{-7} has been attained by 75 MeV electrons. Storage and stretching of slow positron pulses have been successfully performed using a Penning trap in order to fully utilize the high–intensity of the Linac–based beams. The obtained half–life for the storage for a positron of 10 eV was 5 – 10 msec. At JAERI, the degradation of tungsten moderators was found and was attributed to the radiation damage.

Two magnetically guided radioisotope–based beams are in operation: one at the University of Tsukuba and the other at the University of Tokyo. To our knowledge, at least two electrostatic beams and two microscopes are under construction.

Future Positron Beams in Japan

The future plans on beams in Japan can be grouped into three categories: 1) a Linac–based positron factory, 2) a cyclotron–based mini factory, and 3) a desktop beam for industrial applications. The Takasaki Radiation Chemistry Research Establishment of JAERI embarked on drafting a construction plan of a positron factory with a dedicated Linac. The planned specification for a high–power electron Linac is as follows: maximum energy 100 MeV, pulse width 1 μs, repetition 1000 pps, maximum current 1 mA. It is also planned to furnish the equipment for use of radioisotopes additionally to the factory, which enables to perform research on surface magnetism, etc. by using polarized beams which are difficult to obtain by the Linac. The University of Tsukuba group embarked on the preliminary search for the selection of nuclear reactions in a small cyclotron. At least two industrial companies plan to introduce their own desktop beams.

Helvetica Physica Acta
Vol. 63 (1990)

0018-0238/90/040389-08$1.50+0.20/0

RECENT PROGRESS IN ANNIHILATION RELATED STUDIES BY SLOW POSITRONS

K.G. Lynn

Brookhaven National Laboratory, Upton, NY 11973 USA

The field of slow–positron physics has expanded significantly in the last few years to include particle and atomic physics but has been most extensive in those associated with condensed matter or material science. This can primarily be attributed to the development of more efficient moderators (conversion of fast–to–slow positrons). These moderators have been associated with both laboratory– and facility based beams. In this paper I will focus only on the material–science aspects however. Positrons can and are being used to examine all of the various fields. I feel the contribution in all these areas will be significant. Owing to the space constraints, I will primarily discuss those developments that have been developed in the area of interface science; a field that has both scientific and technological importance and has a limited number of nondestructive probes used in studying a buried interface. Interfaces are technologically important for applications such as electrical properties (semiconductor devices) and mechanical properties (adhesion). Such applications help to motivate the fundamental research of interface properties and dynamics, which is necessary to develop the basic understanding of new types of interfaces. The role of the interface is also important (i.e. grain boundaries) since it contributes to the strength of a solid. I will only discuss this area owing to the limited length of this paper, however those interested can read recent reviews by Schultz and Lynn [1] for solid–state studies and for atomic physics reviews by Charlton [2], and Stein and Kauppila [3].

Results will be presented on interface studies that have occurred in the last year, including some unpublished results obtained at Brookhaven over the last year. This field is in the early stages and I expect that the full utilization of this relatively new probe can be anticipated in the next few years. I expect that future studies will be made using laboratory–based beams (10^6 positrons/sec), as well as those based on intense positron beams ($> 5 \times 10^7$ positrons/sec) which require both small and high brightness positron beams.

The research on interfaces with variable–energy positron beams can be reduced, at least in the first instance, to measurements of the γ–rays resulting from annihilation of positrons in delocalized, trapped, or Ps states. Occasionally other signals are employed such as direct Ps detection, characteristic x–rays, secondary or Auger electrons. In this review most of the data will be that obtained with high resolution semiconductor detectors [intrinsic Ge or Ge(Li)]. The annihilation line–shape can be deconvoluted to extract the electron momentum distribution, but more often it is simply quantified by a line–shape parameter such as "S", which is the ratio of counts in a central portion of the annihilation photopeak to the total counts in the peak.

In order to utilized variable–energy positrons to study overlayers and their interfaces one must be able to adequately describe the positron implantation profile. The requirement to adequately describe the stopping profile in typical positron beam experiments is more demanding than previous electron studies. It is not surprising that the

interaction of an energetic positron is different from electrons with similar velocities. The differences can be associated with the relative differential and total elastic cross-sections, and also with the different energy loss processes for the two particles. These variations are partly associated with the opposite charge, and partly with the fact that there is no Fermi sea of positrons in the sample so that there is no exchange part to the potential.

Results of the positron implantation profile are shown in Fig. 1 for four different incident positron energies. Typically 4,000 - 10,000 particles are needed to accurately define the profile. From these results we find the backscattered fractions (not shown in the figure) are a sensitive test of the relative weighting of the elastic to inelastic mean-free paths. Moreover, there is still a disagreement between the backscattered fraction determined from the Monte Carlo and those determined experimentally (Baker and Coleman [4] and Nielsen and Lynn [5]). This discrepancy is not fully understood but could be associated with an inaccurate description of correlation of positrons to the electron gas as well as the angle variation associated with inelastic collision. It is worth noting that agreement is generally good in determining the electron backscattered fraction.

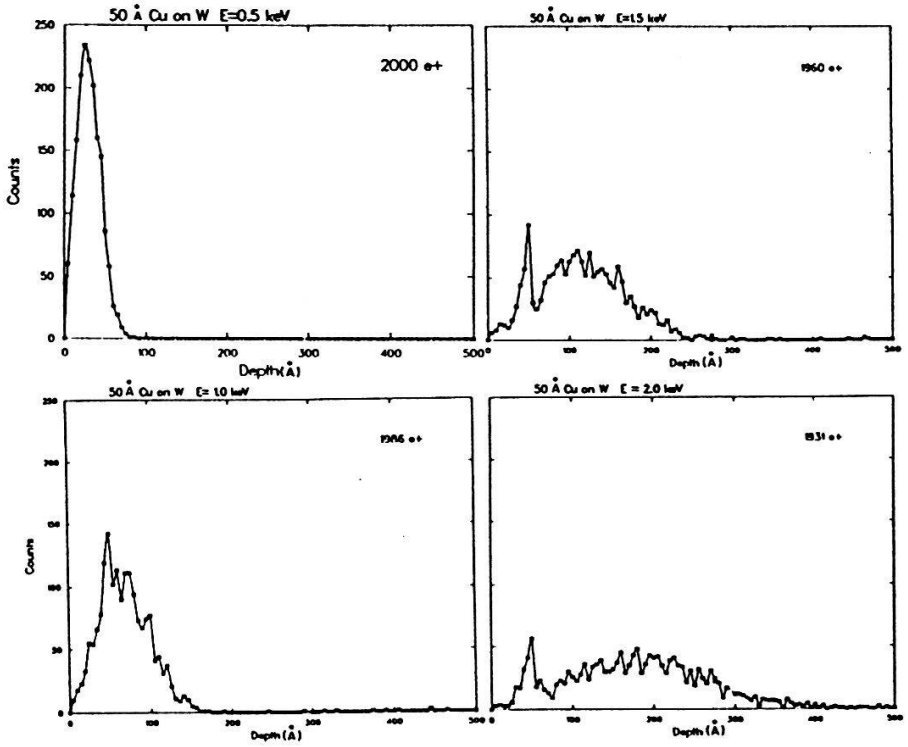

Figure 1: *Monte Carlo simulations of positron stopping profiles for Cu.*

The curves shown by Lynn and McKeown [6] in Fig. 1 can be approximately represented by a derivative of a Gaussian as noted by Valkealahti and Nieminen [7]. However, work on parameterizing these profiles in various multilayer systems is necessary so that experimenters can utilize analytical expressions of the implantation profiles for various composite systems.

Figure 2 shows a highly simplified schematic of positron interface trapping. The first observation that positrons were trapped at interfacial defects was for copper overlayers on a W (110) crystal (Schultz, Lynn, Frieze, and Vehanen [8]). The Cu, which forms an epitaxial overlayer of Cu (111), takes up strain of the lattice mismatch in the first two

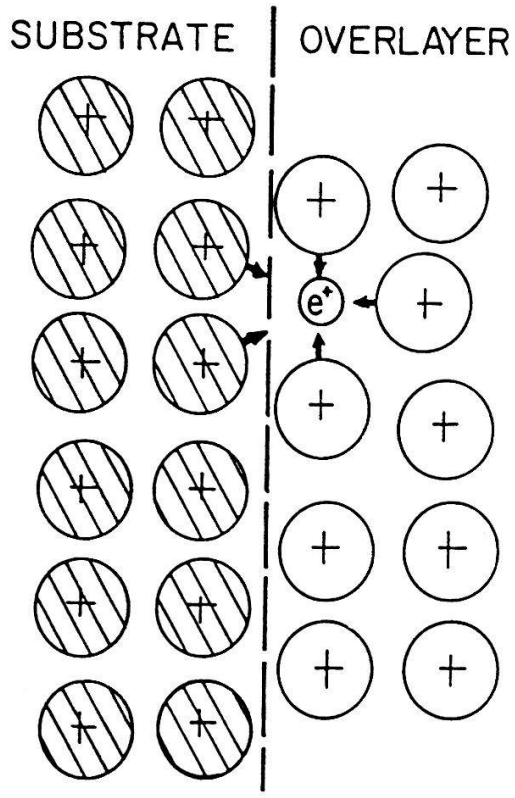

Figure 2: *Schematic representation of positron trapping at an open-volume defect at an interface.*

atomic layers. From the results shown in Fig. 3, it can be seen that the yield of 2-keV incident positrons reemitted from the Cu(111) overlayer is only ~30% of the anticipated yield. This reduced yield continued until the Cu/W (110) system was annealed to above 1222 K, which is very close to the temperature required to thermally activate the first atomic layer of Cu on W (110) (Bauer et al. [9]) and is well above the temperature required to anneal out any point defects in the bulk Cu itself.

The observed recovery of the interfacial defects at the Cu/W (110) interface was supplemented with measurements of the yield versus energy in the as-deposited state. These results showed approximately a 50% decrease in the reemitted yield for incident positron energies above $\sim$ 1 keV, which is consistent with the interfacial trapping.

An example of a "trapping" overlayer on a crystalline substrate, in which the positron diffuses, is that of SiO_2 on Si. Iwase, Uedono, and Tanigawa [10] first reported qualitative measurements in this system, showing an increase in the overfall fraction of positrons trapped following γ irradiation. More recently Nielsen, Lynn, Chen, and Welch [11] have made measurements in SiO_2 on Si (110) which fit with a superposition of parameters, including the diffusion in the substrate. Their results, shown in Fig. 4, yield the same value for L_+ as unmodified Si (110) for the portion at energies $\geq$ 7.5 keV, and the interface is seen very clearly to be near 7 keV. Using Eq. (1) for the mean penetration length, this corresponds to 3200 A, which is in adequate agreement with the known thickness of 3500 A.

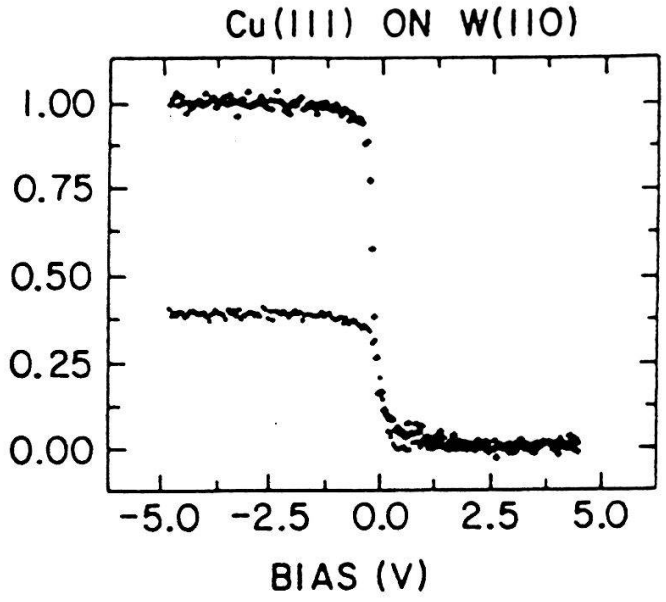

Figure 3: *Reemitted positron energy distribution for epitaxial Cu(111) evaporated on a W(110) substrate. The data are normalized to the defect–free yield of 30 % reemission (upper curve), which was observed only after the as–evaporated system (lower curve) was briefly annealed to temperatures above 1225 K (from Schultz, Lynn and Vehanen, 1983).*

$$L_+ = (D_+\pi_{eff})^{1/2} = (A/A')E_0^n \,, \tag{1}$$

In another study of this type, Nielsen, Lynn, Leung et al. [12] found a different behavior when a 520–Å oxide was grown on a Si (100) substrate. To reduce the effects of the electric field, the authors measured the sample at 500°C, obtaining the data shown in Fig. 5. At depths greater than the interface, the bulk diffusion length for the data shown was consistent with the field–free value. The increase of the line–shape parameter observed at the SiO_2/Si interface indicates positron trapping in open–volume defects. We have associated this increase with 3γ annihilations, suggesting the o–Ps is being formed in large open–volume spaces (voids) near the interface.

A different example is epitaxially grown semiconductor/semiconductor interfaces. An example described above (Fig. 4) illustrated the sensitivity of the variable–energy positron technique to the SiO_2/Si(110) interface. New studies presently underway are investigating some of the structural and electronic properties of heterostructures that are nominally epitaxial, grown using standard MBE (molecular–beam epitaxy) techniques (e.g., Bean [13]). Materials presently being investigated with variable–energy positrons include GaAs and Si_xGe_y alloys, which have (among others) applications as potential optical sources or detectors that can be matched to existing fiber optics. Other experiments have been performed for Si/Si superlattices, revealing new information about both electric field effects introduced by electrically active impurities in the epilayers and structural properties associated with the MBE fabrication of the material. Fig. 6(a) shows data for a $\sim$ 3000–Å epilayer grown on an N–type Si (100) substrate. The results are only slightly different from those for "bulk" material due to a layer of boron trapped at the interface,

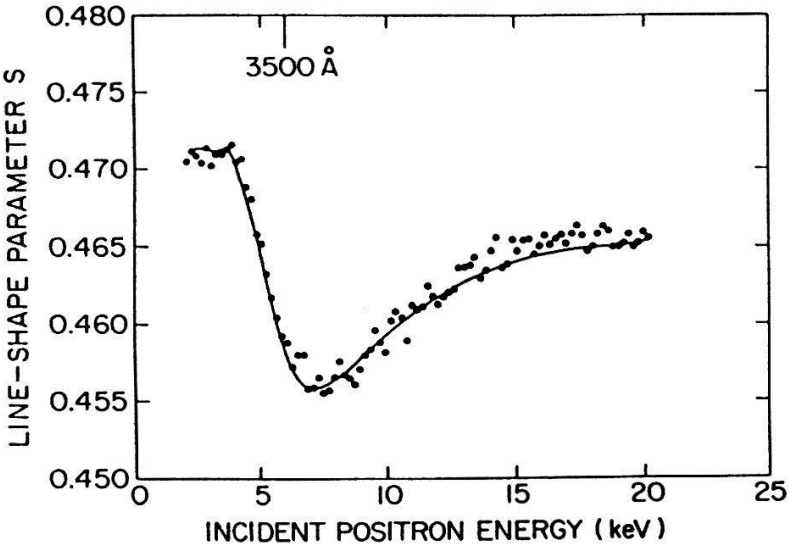

Figure 4: *Doppler–broadening parameter "S" as a function of incident positron energy in SiO_2 on Si (110). The curvature for energy greater than ~7 keV corresponds to positron diffusion in the crystalline Si. The influence of the interface is observable in the limiting value of the line–shape parameter, which the curve approaches (Nielsen, Lynn, Chen, and Welch [11]).*

which results in a bipolar field of $\sim 2 \times 10^3$ V/cm directed towards the interface. The data in Figs. 6(b) to 6(d) are for a ~ 3500–Åepilayer on Si (100) that contains oxide-like defects near the interface. The various data sets shown in Fig. 6(b) at 20°C (as grown), Fig. 6(c) at 300°C, and Fig. 6(d) after returning to 20°C. The solid curves through the data are the result of the interative modeling of the diffusion equation discussed above. Included in the modeling are the effects of positron drift velocity and trapping in defects, observed to be concentrated at the interface and spread (dilutely) throughout the overlayer. The figure also shows the bipolar potential calculated for this sample, and the defect distribution used in the model (Schultz, Tandberg, et al. [14]).

One of the important considerations for positron trapping in semiconductors is the charge state of the defect. For example, the data in Fig. 5 show clear signs of trapping in defects at the interface, which implies that they are either neutral or negatively charged. On the other hand, studies of thick silicon epilayers (4-6 μm) on Si substrates containing varying numbers of dislocations (from $\sim 5 \times 10^3$ to $\geq 10^8$ cm^{-2}) show no signs of positron trapping, indicating that these defects are positively charged. It is clear that more detailed studies of the charge states for various defects will be pursued in the future, and in particular studies will investigate whether or not the electric fields associated with charged defects are leading to prethermalized trapping of positrons. Puska et al. [15] have discussed some theoretical aspects of positron states in defects in semiconductors, and Dlubek and Krause [16] and Dannefear [17] have reviewed some of the bulk solid studies of semiconductors that have been conducted with positrons.

In a more recent study of Pd-Ta on Si (100) G.J. Van der Kolk et al. [18] have used Auger electron spectroscopy, RBS and positrons to study applicability of Pd_xTa_{1-x}

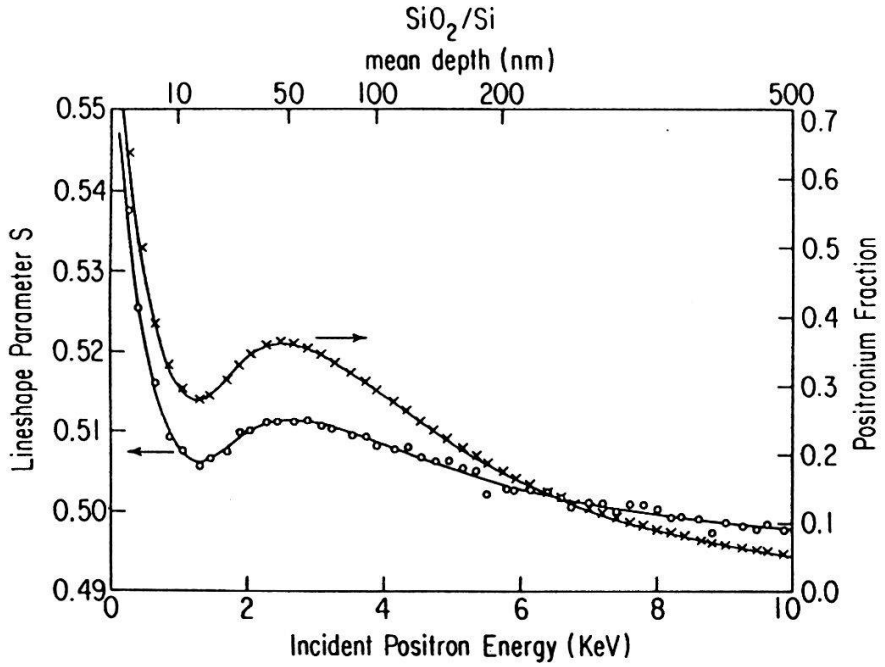

Figure 5: *Positron line-shape parameter S (open circles) and Ps-fraction (crosses) vs incident energy in Si with a thermally grown 52 nm overlayer of SiO_2. The sample had been heated at 970 C and the measurements were made at 800 K.*

as a diffusion barrier on Si. The positron data shows the defect concentrations in the as-deposited state is very high where the positron diffusion length is of the order of 1 nm. The reaction of the metal overlayer with Si is easily detectable with positrons (see Fig. 7). The changes that occur before 600°C is associated with annealing out point defects and the alloy formation occurs between 600 - 700°C.

Although still preliminary, studies of this type are providing the groundwork for using positrons to determine nondestructively depth profiles in defects in the near surface region of a solid. It is already possible to solve the problem without assuming a functional form for the defect profile, but without significant advancements in the numerical procedure the technique is limited by the experimental precision of the data. These concerns, and the correlation of defect and implantation profiles, will eventually establish the limits to which a profile of unknown defects can be uniquely determined experimentally.

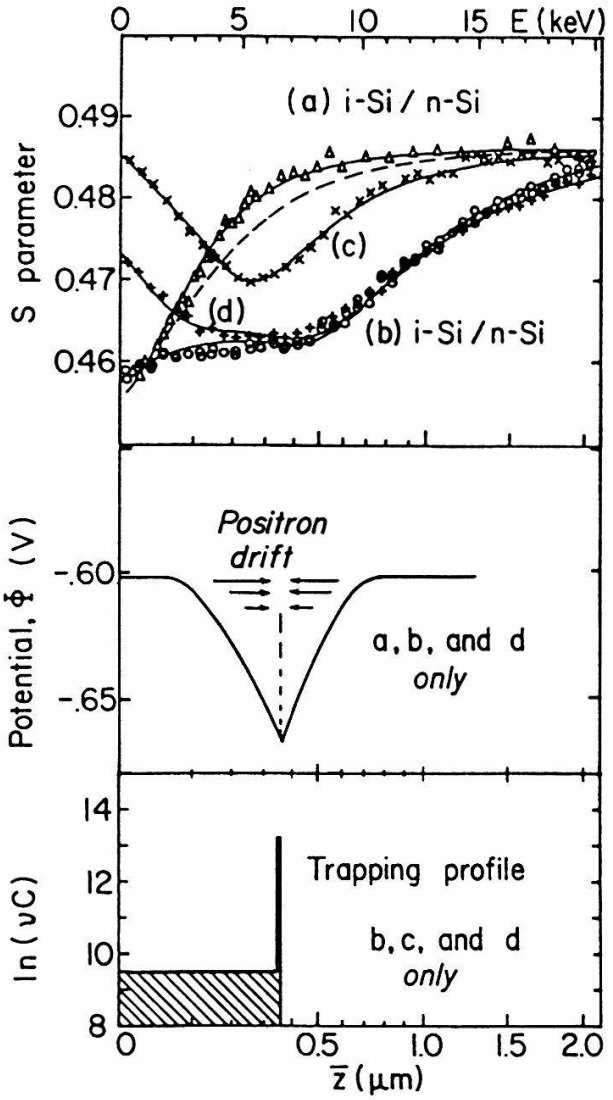

Figure 6: *S–parameters data for MBE–grown intrinsic Si epilayers on n–type Si (100). Data are (a) without defect trapping, and (b) to (d) for a sample containing oxide–type defects. All data are for samples at 20°C, except (c), which is at 300°C. The solid curves are obtained by iteratively solving the diffusion equation, including both defect trapping [profile νC(z)] and positron drift. The dashed curve is for bulk material. From Schultz, Tandberg et al., 1988.*

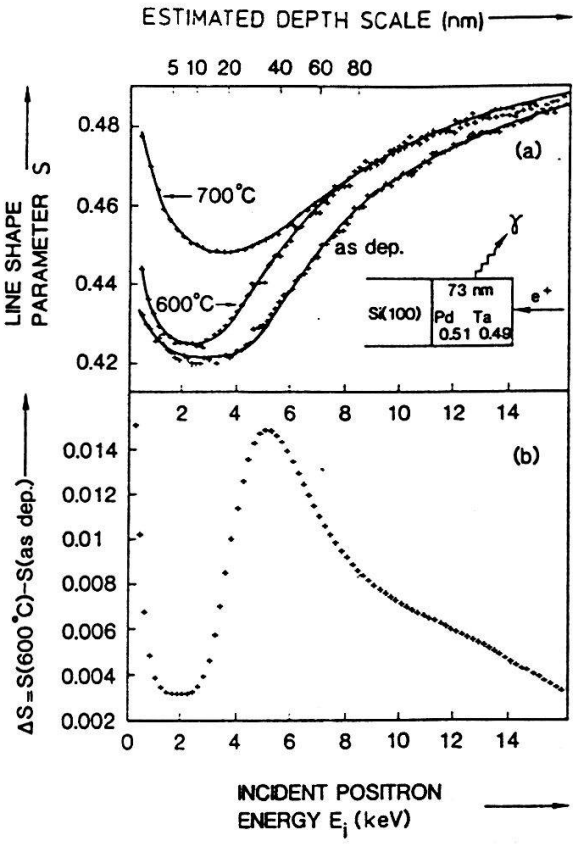

Figure 7: *(a) Line–shape parameter S of the 511 keV annihilation gamma peak as a function of the energy of a positron beam, incident on a 73 nm thick $Pd_{0.51}Ta_{0.49}$ overlayer on Si (100); as–deposited and after annealing at 600°C and 700°C. Lines are drawn to guide the eye. (b) $\Delta S = S$ (600 C) minus S (as–deposited).*

ACKNOWLEDGEMENTS

The author thanks useful collaboration with B. Nielsen, D.O. Welch, M. McKeown, P.J. Schultz and G. Rubloff on the studies presented in this paper. This work was performed under the auspices of the U.S. Department of Energy under Contract No. DE–AC02–76CH00016.

References

[1] P.J. Schultz and K.G. Lynn, Rev. Mod. Phys. 60, 701 (1988).

[2] M. Charlton, Rep. Prog. Phys. 48, 737 (1985).

[3] T.S. Stein and W.E. Kauppila, Adv. At. Mol. Phys. 18, 53 (1982).

[4] J.K. Baker and P.G. Coleman, J. Phys. C: Solid State Phys. 21, L875 (1988).

[5] B. Nielsen and K.G. Lynn, J. Appl. Phys. (June 1989) to be published.

[6] K.G. Lynn and M. McKeown, unpublished.

[7] S. Valkealahti and R.M. Nieminen, Appl. Phys. A 32, 51 (1984).

[8] P.J. Schultz, K.G. Lynn, W.E. Frieze, and A. Vehanen, Phys. Rev. B. 27, 6626 (1983).

[9] E. Bauer, H. Poppa, G. Todd, and F. Bonczek, J. Appl. Phys. 45, 5164 (1974).

[10] Y. Iwase, A. Uedono, and S. Tanigawa, in ICPA85, p.977, 1985; see also A. Uedono, S. Tanigawa, and Y. Ohsi, Phys. Letts. A 133, 82 (1988).

[11] B. Nielsen, K.G. Lynn, Yen-C. Chen, and D.O. Welch, Appl. Phys. Lett. 51, 1022 (1987).

[12] B. Nielsen, K.G. Lynn, T.C. Leung, D.O. Welch, and G. Rubloff, in 'Defects in Electronic Materials', edited by M. Stavola, S.J. Pearton, and G. Davies (Materials Research Society Symposia Proceedings, Boston, MA 1987).

[13] J. Bean, Physics Today 39 No. 10, 36 (1986).

[14] P.E. Schultz, E. Tandberg, K.G. Lynn, Bent Nielsen, T.E. Jackman, M.W. Denhoff, and G.C. Aers, Phys. Rev. Lett. 1988 (in press).

[15] M.J. Puska, O. Jepsen, O. Gunnarsson, and R.M. Nieminen, Phys. Rev. B 34, 2695 (1986).

[16] G. Dlubek and R. Krause, Phys. Status Solidi (a) 102, 443 (1987).

[17] S. Dannefaer, Phys. Statud Solidi (a) 102, 481 (1987).

[18] G.J. Van der Kolk, A.E.T. Kuiper, J.P.W.B. Cuschateau, M. Willemsen, B. Nielsen, K.G. Lynn, J. Vac. Sci. Technol. **A7**, (1989) 1601.

Helvetica Physica Acta
Vol. 63 (1990)
0018-0238/90/040397-06$1.50+0.20/0

Need of Intense Positron Beams for Solid State Applications of Positron Annihilation

A. A. Manuel and M. Peter
Département de Physique de la Matière Condensée, Université de Genève,
24 quai E. Ansermet, CH-1211 Genève 4, Switzerland

Abstract: We discuss the need of high intensity positron beams for 2D-ACAR measurements in solids. We outline 1) the difficulties often encountered to grow single crystals large enough to efficiently use standard radioactive sources, 2) the small amplitude of signals which are either the signature of a Fermi surface in metals with large numbers of electrons per unit cell, or due to the magnetic ordering, 3) the requirements for future high counting rate detectors.

Since one decade 2D-ACAR measurements (2D Angular Correlation of the (positron) Annihilation Radiation) are used to study electronic properties of solids. We discuss why and how intense positron beams facilities shall provide a new impulse to the technique. We divide the discussion in three sections: 1) materials, 2) signals and 3) detectors.

1. Materials

Single crystals are required to investigate electron momentum distributions. Size and quality are the two dominant parameters concerning the crystals.

The size of single crystals is the first important parameter in the measurement of angular correlations. This becomes clear if one consider the source of positrons. With traditional radioactive positron emitters, the active surface has to be large enough to keep low the fraction of positron annihilating in the source itself. For example, usual surfaces of the ^{22}Na sources is of the order of 5 to 10mm^2, for an activity of 50-100 mCi. A magnetic field lying along the source-sample axis may be used to guide positrons toward the sample along helical orbits. This leads to an increase of the positron flux on the sample by factors up to 10 (depending on the distance between the source and the sample, and also on the sample size). Such homogenous magnetic fields cannot focus particles, therefore the positron flux is limited by the source strength and the only way to increase the counting rate is to increase the surface of the material to study up to a surface equal to the one of the positron source. This criterion cannot always be reached. For many compounds the crystal growth is a delicate procedure. We give two examples:

1) In high T_c superconductors, it is often difficult to obtain single crystals of more

than $1mm^3$ [1]. Moreover when it is possible, the bulky nature of the samples makes difficult the diffusion of oxygen which is often required to obtain an homogeneous stochiometry over the whole volume.

2) Some phases are only synthesized through a solid state transformation. In these situations, the size of crystalites is intrinsically small and only epitaxial growth may overcome this difficulty, but only films up to 1 μm thick may be grown in that way.

It is clear that in these cases, which are nowadays very frequent, the use of radioactive emitters is far to be ideal. The availability of intense positron beams is the only way to study many new materials using the angular correlation method. Beyond the need of high intensities, which is discussed in the next section, small beam sections and a variable energy of the almost monoenergetic positrons are the interesting and often crucial factors.

A very promising way to create thin positrons beams is the technique of brightness enhancement which has been proposed by Mills [2] and is discussed by Waeber in this volume. A positron beam of a section down to $1mm^2$ shall make possible 2D-ACAR measurements on many systems which are actually beyond our possibilities. Let us mention for example untwinned high-T_c superconducting $YBa_2Cu_3O_7$ [3] and other superconducting oxides which are difficult (maybe impossible) to grow with large sizes, Guinier-Preston zones in metals, the semiconducting beta phase of the disilicide $FeSi_2$ which is formed via a solid state phase transition.

To have at our disposal monoenergetic positron beams with the possibility to select the energy of the positrons up to 60 keV should open other fields of investigation. Let us mention for example the possibility to study momentum distributions in samples made of films grown by epitaxy on a substrate. A proper tuning of the positron energy should permit to implant the positron in the film, keeping the fraction of annihilation in the substrate as low as possible.

Let us now focus briefly on the structural quality of the crystals. The quality of single crystals is a crucial factor which merits attention before 2D-ACAR measurements. It is usually not sufficient to obtain sharp X-rays patterns to certify that a crystal is good enough to be used for the study of the electronic properties of the bulk material. Knowledge of the spectrum of positron lifetimes is required to be sure that positrons do not annihilate in vacancies or other types of structural defects. From positron lifetime measurements, it is generally possible to control if positrons annihilate with Bloch electrons. For a discussion of the potential advantages of positron beams in the determination of positron lifetimes, we refer to the contributions of A. Seeger and W. Triftshäuser, in this volume.

2. Signals

The impact of the intensity of the positron beams is straightforward: a decrease of the counting time. But, maybe more important is the possibility to significantly increase the statistics of the data within a finite and fixed measuring time. The required statistics depends on many parameters, among them: 1) the resolution of the spectrometer, 2) the size of the Brillouin zone, 3) the number of bands, 4) magnetic effects and 5) the nature of the positron wavefunction.

1) Resolution: With a resolution of about 0.3x0.3mrad^2, the mesh of experimental points has to be typically of 0.01mrad^2. Let us do a rough estimation of the total statistics required: Suppose we want to have 1% precision for a 2D distribution extending over 100mrad^2 (10^4 pixels), we need 10^8 counts. This number is a minimum threshold, it neglects the statistical error added by the determination of the efficiency resolution function and it assumes a constant distribution limited to 100mrad^2, which is clearly not the case.

2) Size of Brillouin zones: Today, interesting systems to investigate are compounds and their total number of atoms per unit cell is increasing over the years. As a consequence, the size of Brillouin zones is continuously decreasing and, therefore, the angular resolution of 2D-ACAR spectrometers has to increase (at least at the same rate [4]), requiring a continuous increase of the number of pixels then, jointly, of the global statistics.

3) Number of bands: An other consequence of the large number of atoms per unit cell is an increase of the number of electronic bands. For metallic systems this leads to a decrease of the amplitude of the Fermi surface breaks[5]. An increase of the statistical accuracy is also required for this reason. This makes our estimation of the total counts rather undervalued.

4) Magnetic effects: Small signals are also the signature of magnetic effects, studied with polarized positron beams. One example: in Cr, differences between paramagnetic and antiferromagnetic states have been observed [6] and successfully interpreted as a modification of the Fermi surface by the magnetic order. With the actual positrons sources (^{22}Na isotopes), the signal was not far from the limit of detection and it was not possible to perform a quantitative analysis of the phenomenon.

5) Positron wavefunction: 2D-ACAR measurements are determined by the behaviour of the positron wavefunction. While the positive charge of the positron keeps it in the interstitial region, hence reducing the contribution of the (less interesting) core electrons, the Coulomb repulsion may have some drawback. It is the case in the study of strongly ionic materials. Here, the positron will not sample uniformly the valence electronic states. In $YBa_2Cu_3O_7$ for example, it is thought that the Fermi surface is mainly due to the electronic states of the so called Cu-O planes, where positron density is small [7] compared to those

of the Cu-O chains. Therefore, the inhomogeneous positron distribution may be an extra factor contributing to decrease the amplitude of the interesting signals. It strengthens the data acquisition of very high statistics.

When we add all these factors, we realize that statistics for a compound like the high-T_c superconductor $YBa_2Cu_3O_7$ should be more than 10^9 counts. This is not achievable actually within reasonable measuring time. We show in the section 3 that intense positrons beams are needed to reach this criterion.

3. Detectors

Actual 2D-ACAR machines are based either on Anger cameras, multi-scintillators systems or high density proportional chambers (HDPC). We use this last technology [8] characterized mainly by a high spatial resolution (1-2mm^2) and reasonable detection efficiency of the gamma rays (15-18%). An important limitation of these detectors is the slow time resolution (200ns). This make the random coincidence rate too large when the true coincidence rate is higher that 1 kcps. The situation is improved with Anger cameras (coincidence time of 25-50ns) [9].

Anger cameras are very promising candidates for 2D-ACAR measurements using high intensity positron beams. They are commercially available, fully optimized and equiped with dedicated electronic read-out. There are some outsiders: barium fluoride scintillator and TAME filled wire chambers [10], BGO arrays and position sensitive photomultipliers [11], thin solid-state converters [4] and microchannel plates [12].

To emphasize the impact of intense positron beams on 2D-ACAR measurements, we give estimations of the coincidence rate C and the signal to noise ratio S for various source/detector configurations. For radioisotopes, the positron flux on samples I is calculated from the source intensity i (taking account for self-absroption) from the source-sample solid angle A [13]. R, the rate of gamma rays on a detector is given by

$$R = 2 \cdot i \cdot \beta \cdot A \cdot O \cdot \varepsilon$$

where ε is the efficiency of the detectors, β the positron yield (0.89 for ^{22}Na and 0.15 for ^{58}Co) and O the solid angle sustended by the detectors. The coincidence rate C is given by

$$C = R \cdot \varepsilon.$$

N, the noise rate, is expressed as

$$N = 2 \cdot \tau \cdot R_1 \cdot R_2,$$

where τ is the coincidence time of the detectors and $R_1=R_2=R$. Finally, S is calculated as

$$S = C / (f \cdot N)$$

where f is a factor (we take f=8) to account for lake of energy resolution of the detectors.

A) HDPC 30x30cm^2, at 7.75m; ε=15%; τ=400ns	
^{22}Na 50mCi:	I = 3.7 10^6 cps
	C = 20 cps
	S = 180
^{58}Co 1Ci:	I = 1.2 10^7 cps
	C = 66 cps
	S = 50
positron beam:	I = 10^{10} cps (expected value)
	S < 1
B) Improved detector 7x7 cm^2, at 7.75m; ε=20%; τ=5ns	
positron beam:	I = 10^{10} cps (expected value)
	C = 5200 cps
	S = 100
^{22}Na 50mCi:	I = 3.7 10^6 cps
	C = 2 cps

(for radioisotopes, the following parameters have been used: sample: 1 mm^2; radioactive sources: 10x1 mm^2, self-absorption: 50%, sample-source: 3 mm, no magnetic field to guide positrons.)

Table 1: Estimated counting rates C and signal to noise ratio S for various detectors and sources configurations (I is the positron flux on the sample)

The table outlines the need of improved detectors to take full advantage of intense positrons beams. These detectors have to have a fast coincidence time (τ< 5ns). Such detectors offer the possibility to accumulate 10^9 counts within 2 days (smaller acquisition time should be obtained with larger detectors), while the same statistics is achieved after ~100 days using HDPC's and a magnetic field to guide positrons from a ^{22}Na source.

These rough estimations clearly point out the necessity and the interest to develop a beam of 10^{10} positrons per second.

Conclusions

We have outlined the important characteristics of a positron beam to be efficiently used for the investigation of the electronic properties of solids by the 2D-ACAR technique,

namely: a) the beam size, required to measure small single crystals, b) the high intensity of the beam, which is needed to get the large statistics required for a precise determination of the electron-positron momentum distributions in solids, c) the possibility to vary the energy of the positrons impinging on the sample which shall make possible to adjust the penetration depth of the positrons for the study of epitaxial films as well as multilayers. Finally, we have shown that intense positron beams require a new generation of detectors characterized by a high resolving time as well as high counting rates capabilities.

As a last word, let us state the ideal beam facility we would like to have to our disposal for 2D-ACAR measurements: A permanently available DC beam of 10^{10} polarized positrons per second (or more) with a section of $1mm^2$ (or less) and the possibility to select the energy of the positrons between 2 and 60keV.

Acknowledgements:

We are very grateful to W. Waeber and U. Zimmermann for stimulating discussions and to L. Hoffmann and P. Genoud for a critical reading of the manuscript.

References:

1. W. Sadowski and H.J. Scheel, *J. Less Common Met.* **150**, 219 (1989)
2. A.P. Mills, Jr., *Appl. Phys.* **23**, 189 (1980)
3. H. Schmid, E. Burkhardt, B.N. Sun and J.P. Riviera, *Physica C* **157**, 555 (1989)
4. An interesting idea has been proposed by V.I. Baskakov et al. to develop 2D gamma rays detectors with a resolution of 5 μm x 1 mm: V.I. Basakakov, V.N. Belyaev, K.F. Zainulin, A.N. Mikheev, A.I. Skuratov and A.N. Tikhomirov, submitted to *Rev. of Scient. Instr*, (1989).
5. M. Peter and A.A. Manuel, *Physica Scripta* **T29** 106 (1989)
6. A.K. Singh, A.A. Manuel and E. Walker, *Europhys. Lett.* **6**, 67 (1988)
7. E.C. von Stetten, S. Berko, X.S. Li, R.R. Li, J. Brynestad, D. Singh, H. Krakauer, W.E. Pickett and R.E. Cohen, *Phys. Rev. Lett.* **60**, 2198 (1988)
8. A.P. Jeavons, D.W. Townsend, N.L. Ford, K. Kull, A.A. Manuel, O. Fischer and M. Peter, *IEEE Trans. Nucl. Sci.* **25**, 164 (1978)
9. T. Chiba, private communication.
10. P. Miné, J.C. Santiard, D. Scigocki, M. Suffert, S. Tavernier and G. Charpak, *NIM in Phys. Res.* **A273**, 881 (1988)
11. H. Uchida, T. Yamashita, M. Ida and S. Muramatsu, *IEEE Trans. Nucl. Sci.* **33**, 464 (1986)
12. B.T.A. McKee, A. Linhananta and A.T. Stewart, *NIM in Phys. Res.* **A275**, 911 (1988).
13. J. Cook, *Nucl. Instr. and Meth.* **178**, 561 (1980)

Helvetica Physica Acta
Vol. 63 (1990)

0018-0238/90/040403-26$1.50+0.20/0

Defect Studies by Positron Annihilation — Techniques, Achievements, Problems, Perspectives

Alfred Seeger and Florian Banhart

Universität Stuttgart, Institut für theoretische und angewandte Physik,
and
Max-Planck-Institut für Metallforschung, Institut für Physik,
Heisenbergstr. 1, D-7000 Stuttgart 80, Germany

Abstract

The paper reviews the general background and the principal experimental techniques developed for the study of defects in crystals or, more generally, of inhomogeneities in condensed matter by means of positron annihilation. The various versions of the so-called trapping model that have been developed for the analysis of such experiments are described and critically considered. It is emphasized that in order to extract reliable information on defects in crystals from positron annihilation measurements detailed information on the thermalization, the diffusion, and the capture of the positrons by the defects acting as traps is required.

The great potential of an intense beam of relativistic positrons for positron lifetime spectroscopy and age-momentum correlation measurements is pointed out. Such a beam should be spin-polarized in order to facilitate measurements of the positron spin relaxation rate in ferro- and ferrimagnets as well as of the formation of ortho- and para-positronium.

1 Introduction

During the past two decades positrons have developed into important probes for studying inhomogeneities in condensed matter, in particular *lattice defects in crystals.* They may be characterized as "active" internal probes [1]. The attribute "active" alludes to the fact that, owing to their small mass, positrons in condensed matter are usually very mobile and hence capable of scanning a fairly large volume in spite of their short mean life. (Their "lives"are terminated by annihilation with electrons; in condensed matter the mean positron life is of the order of magnitude $2 \cdot 10^{-10}$ s.) This property enables positrons implanted into condensed matter to roam and to find inhomogeneities in the host sample even when their concentration is rather low. In order for the positrons to act as *probes* for inhomogeneities of the sample they must be able to "decorate" them. This requires an attractive interaction between positrons and inhomogeneities that is large enough for the positrons to be *trapped.* In quantum mechanical language this means that the positrons must possess at least one bound state localized at each inhomogeneity and that the positron binding energy in that state must be large enough for the positrons to spend a time comparable with or larger than their mean lifetime in that state.

Many different inhomogeneities may act as traps for positrons. Even if for the time being we confine ourselves to crystalline materials, the list of possible traps includes a very wide variety of defects: vacancies, voids, bubbles, foreign atoms, dislocations, grain boundaries, and phase boundaries. The power of positrons as probes is that they can give us *quantitative information on the nature of the traps* and that, in particular, they are capable of *distinguishing* between different traps. However, a prerequisit for this is that before the trapping the positrons are in a *standard state* so that differences in their behaviour may be attributed directly to different properties of the traps. It is indeed usually assumed that positrons implanted into condensed matter become part of the thermal equilibrium so quickly that the thermalization period may be disregarded. It should be borne in mind that this is an assumption that is difficult to verify. We must therefore be prepared to encounter situations in which it is not admissable.

From the preceding discussion it is clear that we have to address ourselves to the following questions:

1. What happens during the implantation of positrons in condensed matter? How long does it take for them to reach thermal equilibrium?
2. How do the positrons reach the traps after they have been thermalized?
3. What happens at the traps? How can we obtain quantitative information on the traps?

The present survey is not a review in the usual sense, aiming at covering the literature on the subject (the available space forbids this), but rather an attempt to provide the reader with a background knowledge on the techniques and the main achievements of the investigation of defects in condensed matter by means of positron annihilation, to draw his attention to a number of open problems, and to point out the potential of several new techniques, particularly those related to high-energy and /or spin-polarized positron beams.

2 Positron Thermalization and Diffusion

In positron annihilation studies of condensed matter positrons (e^+) are implanted into the sample with kinetic energies that exceed the thermal energy $k_B T$ considerably. (The e^+ kinetic energies are typically 10^2 to 10^3 keV in the case of unmoderated e^+ from external or internal radioactive sources, a few MeV in the case of positrons coming from accelerators, or of the order of magnitude of 1 keV in the case of "slow" positrons obtained by moderation and emission from surfaces with negative e^+ work functions.) In view of the rather short life of e^+ in condensed matter it is important to have some information on the time it takes for the positrons to *thermalize*, i.e. to reach average kinetic energies $3k_BT/2$. There is little doubt that in condensed matter the positrons lose most of their kinetic energy very rapidly by the excitation of electron-hole pairs [2,3]. Our detailed knowledge on the final thermalization process, which is governed by the interaction between phonons and positrons, is rather limited, however. Under circumstances under which the trapping rate is particularly large ("resonance trapping", cf. Sect. 4) we cannot exclude the possibility that positrons are trapped before they are fully thermalized. More direct experimental information is needed.

For the following discussion let us assume that the thermalization process is *not* suddenly terminated by the capture of the positrons in (possibly metastable) localized states. In analogy

to holes (= defect electrons) in semiconductors the movement of the thermalized e^+ may then be characterized by a *diffusivity* D^+ and a *mobility* μ^+. These two quantities are related by

$$D^+ = k_B T \mu^+. \tag{1}$$

The e^+ diffusivity determines how fast the thermalized positrons reach the traps. For the present subject the knowledge of $D^+(T)$ is therefore of paramount importance.

In 1972 one of the present authors [4,5] proposed that the e^+ diffusion in solids is limited by the scattering of phonons by the positrons. Under the simplest assumptions (isotropic phonon spectrum with linear dispersion curve, elastic scattering) this gives for the mean free path of the positrons (see, e.g. [6,7])

$$l^+ = \pi \hbar^4 c_l^2 \rho_0 / m_+^2 \epsilon_d^2 k_B T \tag{2}$$

and for their mobility

$$\mu^+ = 2(\pi m_+ k_B T/2)^{-1/2}/3l^+. \tag{3}$$

Here ρ_0 and c_l denote density and longitudinal sound velocity of the material, ϵ_d the deformation potential constant for positrons, and m_+ the effective mass of the positrons. $\hbar$ has the usual meaning of Planck's constant h divided by 2π. The positron diffusivity follows from (1 - 3) as

$$D^+ = \frac{2^{3/2}\pi^{1/2}\rho_0 c_l^2 \hbar^4}{3 m_+^{5/2} \epsilon_d^2 (k_B T)^{1/2}}. \tag{4}$$

A further prediction was [5] that (2 - 4) should cease to hold at temperatures below a critical temperature

$$T_0 = 12 m_+ c_l^2 / k_B. \tag{5}$$

Below T_0 the phonon-positron scattering ceases to be elastic, and the effectivity of the phonons in limiting the positron mean free path is drastically reduced. In pure materials this should lead to a rapid increase of D^+ with decreasing temperature (cf. Fig. 1). In pure metals at low enough temperatures the scattering of the e^+ by the conduction electrons might come into play and reduce the temperature dependence of D^+. In the following we estimate this effect from a treatment of the diffusivity of positive muons by Jäckle and Kehr [8].

Jäckle and Kehr [8] consider positive particles of effective mass m_+ that interact with the conduction electrons through a screened Coulomb potential with Thomas-Fermi screening. Their final result for the diffusivity of these particles may be written as

$$D^+ = \frac{3}{[2\zeta(3) + \pi^2/3]\,\pi^2} \frac{\epsilon_F}{k_B T} \frac{h}{m_e} \left(\frac{m_e}{m_+}\right)^2. \tag{6}$$

In (6) m_e denotes the electrons mass, ϵ_F the Fermi energy of the conduction electrons, and $\zeta(3) = 1.20$ a value of Riemann's zeta function. The quantity $h/m_e = 7.274 \cdot 10^{-4} \mathrm{m^2 s^{-1}}$ is known as the "quantum of circulation". Since Jäckle and Kehr [8] had in mind the application to positive muons, for which $m_+/m_e \gg 1$, they made assumptions whose validity for e^+ is not entirely clear. Nevertheless, (6) should give the right order of magnitude for e^+ as well. After inserting numerical values it reads

$$D^+ = 4 \cdot 10^{-5} \left(\frac{\epsilon_F}{k_B T}\right) \left(\frac{m_e}{m_+}\right)^2 \frac{\mathrm{m}^2}{\mathrm{s}}, \tag{7a}$$

or with $m_+/m_e = 1.5$ and $\epsilon_F = 10$ eV,

$$D^+ = 2T^{-1}\mathrm{Km^2s^{-1}}. \tag{7b}$$

Measurements of D^+ are by no means straightforward. At the present time, for metals the most promising method is based on the "slow-positron beam technique"[9]. Positrons with variable kinetic energies between, say, 0.1 keV and 30 keV are implanted into high-quality single crystals with well-polished surfaces. The back-diffusion of the implanted positrons is monitored by measuring the positronium yield at the surface. The data analysis requires several assumptions which may affect somewhat the final outcome.

Soisinen et al. [10] have recently summarized their measurement on four metals (Al, Mo, Cu, Ag). The temperature dependence of D^+ was found to be close to the $T^{-1/2}$ law predicted by (4) over fairly wide temperature ranges (16 K to 505 K for Al, 34 K to 1400 K for Mo). Possible deviations in the direction of a slightly stronger temperature dependence might be caused on the low-temperature side ($T \leq T_0$) by the ineffectiveness of elastic e^+– phonon collisions mentioned above, on the high-temperature side by the curvature of the phonon dispersion curves, which was not taken into account in the derivation of (4).

Typical room-temperature values of D^+ lie between $1 \cdot 10^{-4}\mathrm{m^2s^{-1}}$ and $2 \cdot 10^{-4}\mathrm{m^2s^{-1}}$. As discussed by Soisinen et al. [10], this is in agreement with (4), measured elastic constants, and reasonable values for the effective positron mass m_+ (about 1.5 times the electron mass m_e), and the deformation-potential constant ϵ_d. One must keep in mind, however, that even for cubic materials the assumption of elastic isotropy, on which (2 - 5) are based, may be grossly violated. In such cases the characterization of the deformation potential involves a second constant in addition to ϵ_d. A theoretical investigation of this effect is under way.

Comparison of (7) and (4) shows that even in metals the phonon scattering dominates over the electron scattering at all accessible temperatures with the possible exception of $T/T_0 \gg 1$. However, at such low temperatures l^+ is presumably limited by residual impurities even in the purest metals available.

In *semiconductors* and *insulators* the possibility exists to obtain the positron mobility from drift experiments in applied electric fields. By observing the Doppler shift of the 2γ-annihilation radiation (cf. Sect. 5.2) Mills and Pfeiffer measured the drift velocities of positrons in strong electric bias fields in Ge [11] and Si [12] and deduced e^+ mobilities from them. Table 1 shows the diffusivities calculated from these by means of (1). They are of the same order of magnitude as in the metals discussed above. Whereas the temperature dependence in Si is compatible with (4), that in Ge is substantially weaker, indicating that in this case impurity scattering might have played a rôle.

We may use (3) to extract the *mean free path* l^+ of the positrons from the experimental values of D^+ or μ^+. The assumptions $D^+(293\mathrm{K}) = 2 \cdot 10^{-4}\ \mathrm{m^2s^{-1}}$ and $m_+ = 1.5m_e$ give us the room temperature value of the mean free path of the positrons $l^+(293K) = 6.9$ nm and l^+ (30 K) = 69 nm. These values may be compared with the mean diffusion length during the positron lifetime τ,

$$L_D = (2D^+\tau)^{1/2}. \tag{8}$$

With $D^+ = 2 \cdot 10^{-4}\ \mathrm{m^2\ s^{-1}}$ and a positron lifetime $\tau = 2 \cdot 10^{-10}$s we obtain $L_D = 0.28\mu$m. We see that over the entire range over which (2 - 4) is applicable we have $L_D \gg l^+$, so that the diffusion picture for the motion of the positrons is indeed appropriate in both metals and semiconductors.

T[K]	36 ± 5	80 ± 5	93 ± 5	184
Ge	1.08 ± 0.15	-	0.99 ± 0.146	-
Si	-	3.17 ± 0.14	-	2.74 ± 0.24

Table 1: Positron diffusivities D^+ in units of 10^{-4} m^2s^{-1} in germanium and silicon as deduced from drift measurements [11,12].

Following ideas of Norton and Levinstein [13] and of Mills and Pfeiffer [11,12], knowing D^+ allows us to obtain a lower limit for the thermalization time. A particle with effective mass m^*, velocity v, and kinetic energy $\epsilon = m_+v^2/2$ loses energy by the emission of acoustic phonons at the rate [14,15]

$$\frac{d\epsilon}{dt} = -\frac{\epsilon_d^2\, m_+^4\, v^3}{\pi\, \rho_0\, \hbar^4} = -\frac{8}{3}\frac{c_l^2}{D^+}(\pi\, k_B\, T)^{-1/2}\epsilon^{3/2}. \tag{9}$$

In (9) the deformation potential constant has been eliminated using (4). Integrating (9) between the limits $\epsilon_d = 3k_BT/2$ and $\epsilon_1 \gg \epsilon_2$ gives us for the thermalization time associated with the *emission* of thermal phonons

$$\Delta t_{em} = \left(\frac{3\pi}{8}\right)^{1/2}\frac{D^+}{c_l^2}. \tag{10}$$

[Eq.(10) differs by a factor of 4 from the corresponding one of Mills and Pfeiffer [11], which we believe to contain a numerical error.] Taking Al as an example and using the D^+ data of Soisinen et al. [10], we obtain Δt_{em} (20K) = 37ps and Δt_{em} (500K) = 5 ps. We emphasize that these estimates are based on the *emission of phonons only* and that they disregard both the excitation of electron-hole pairs (which reduces the thermalization times only slightly) and the *absorption* of phonons, which leads to gains in the kinetic energy and therefore lengthens the thermalization period. The latter effect is more pronounced at higher temperatures.

Under certain conditions measurements of *positron trapping rates* (cf. Sect. 3) can be used to determine the temperature dependence of D^+. Provided that the rate at which positrons that have arrived at the traps by diffusion are captured in the bound state is sufficiently fast, in cubic materials the trapping rate per unit trap concentration (measured in atomic units) may be written as [16]

$$\sigma = 4\pi r_0 D^+/V_A. \tag{11}$$

Here r_0 denotes the effective capture radius of the traps and V_A the atomic volume. If the trap concentration C_t is temperature-independent, the temperature dependence of D^+ may be obtained from measurements of the trapping rate σC_t as a function of temperature, provided that we know the temperature dependence of r_0. We may assume r_0 to be independent of temperature if the range of the interaction between positrons and traps is short (e.g., comparable with the interatomic distance as in the case of vacant sites in metals or electrically neutral vacancies in semiconductors). If the interaction is long-range, the temperature dependence of r_0 may be estimated by considering the drift of the positrons due to the force exerted on them by the traps.

An example of the technique outlined in the preceding paragraph is provided by the work of Shirai and Takamura [17] on the trapping of positrons by stacking-fault tetrahedra in Au.

The stacking-fault tetrahedra (introduced by quenching from high temperatures and subsequent moderate annealing) are rather stable so that the temperature variation of σC_t could be measured between 4.2 K and 400 K, yielding a $T^{-1/2}$-law above 50 K. This is in agreement with (4) since to a good approximation the effective capture radius of stacking-fault tetrahedra may be taken as temperature-independent. Below 50 K the temperature variation is stronger, possibly due to the suppression of elastic positron-phonon scattering below T_0.

The discussions of the present section have so far been based on the picture of weak positron-phonon interactions, which can be handled by a scattering formalism and contributions to the effective positron mass m_+. However, it is well known that in some solids electrons and positive holes (= defect electrons) may interact strongly with optical phonons, forming *polarons*. As Gol'danskii and Prokop'ev [18] pointed out in *ionic crystals* positrons should form polarons, too.

In contrast to the situation prevailing in insulators and semiconductors, owing to the screening of the e^+ charge by conduction electrons *positrons in metals* do not give rise to long-range electric fields. An analogue to the above-mentioned optical polaron, the "acoustic polaron", is nevertheless conceivable.

In order to introduce the idea of *acoustic polarons* in metals (or valence crystals), let us compare the positron Bloch waves in a rigid or only slightly deformed metal crystal with a situation where the positron charge density in the interstices is drastically increased and at the same time the ion cores have moved away from the positrons. The "localization" of the positron wavefunction leads to an *increase* of the e^+ kinetic energy, the increase of the positron-ion separation to a *decrease* of the potential energy of the system. In addition there is an energy *increase* due to the deformation of the lattice. The following situations may arise [19,20].

(a) The formation of a state consisting of strongly localized positively charged particles surrounded by "deformation clouds" (= *acoustic* e^+ *polarons*) leads to a *lowering* of the total energy of the system. Then acoustic polarons are *stable*. They may be considered as "quasi-particles" with an effective mass m_+ that is large compared with the electron mass m_e. There is so far no evidence that for *positrons* this situation might prevail in any metal. The analogous polaron state of the heavier "isotopes" of the e^+, viz. the positive muon μ^+, the positive pion π^+, and the hydrogen nuclei, however, is always stable owing to the much bigger masses of these particles.

(b) The formation of acoustic polarons leads to an *enhancement* of the total energy of the system. Acoustic e^+ polarons may then be either mechanically *metastable* (b_1) or mechanically *unstable* (b_2). In the case (b_1) an interesting situation arises if the decay rate of the metastable state is smaller than or comparable with the e^+ annihilation rate. Since owing to their large effective mass the lowest energy band of the acoustic polarons is very narrow, at elevated temperatures acoustic-polaron states may be partially occupied. This means that on the average the positrons spend a temperature-dependent fraction f of their life in one of the metastable states. (For details see [19,20]). The consequences for positron diffusion will be treated presently. In the context of e^+ diffusion case (b_2) is of no interest and will hence not be considered further. Irrespective of whether the acoustic e^+ polarons are stable or metastable, i.e., whether case (a) or case (b_1) is realized, their high-temperature diffusion proceeds by the "adiabatic mechanism" [21,22].

For this mechanism the hopping frequency may be approximately written as

$$\nu = \nu_D \exp(-H^+/k_B T), \tag{12}$$

where ν_D denotes the Debye frequency of the host metal and $H^+ > 0$ a small activation energy. The positron diffusivity will then be given by

$$D^+ = (1 - f)\, D_1^+ + f\, \nu_D\, d^2 \exp(-H^+/k_B T). \tag{13}$$

Here d is of the order of magnitude of the distance between interstices and D_1^+ the "ordinary" positron diffusivity given by, e.g., (4). Since $\nu_D d^2$ cannot be much larger than 10^{-7} $m^2 s^{-1}$, the positron diffusivity will be dominated by the first term of (13) unless f is very close to unity. Fig. 1 indicates qualitatively the temperature variation of the positron diffusivity one might expect from (13). For the sake of clarity the example chosen is not very realistic, though. In practice this

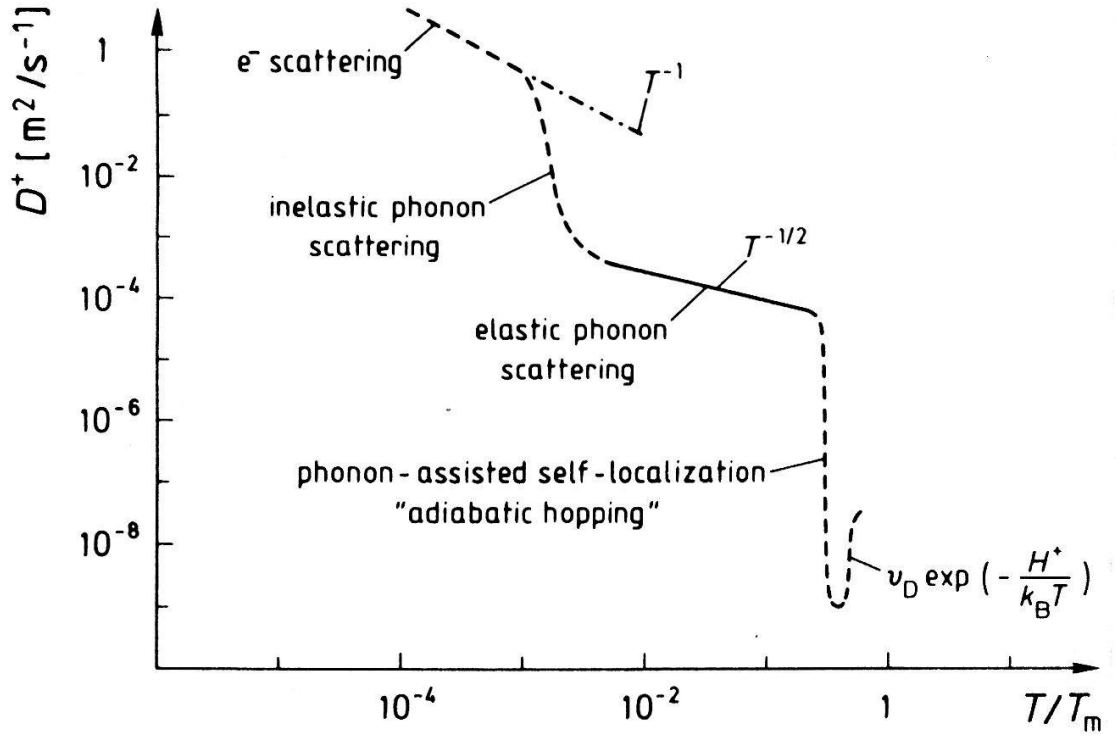

Figure 1: Schematized temperature dependence of the positron diffusivity D^+ in metals (logarithmic scales). The different mechanisms limiting the positron diffusivity and their temperature dependence are indicated.

means that it will be difficult to identify acoustic e^+ polarons by means of diffusivity measurements. Chances are better for e^+-lifetime or e^+e^--momentum measurements (Sect. 5) since the situation of an acoustic e^+ is reminiscent to that of a positron trapped in a vacancy (cf. Sect. 3).

From the point of view of predictive theory the distinction between (b_1) and (b_2) is a rather delicate matter. There is strong experimental evidence [23,24,25,26] that in cadmium (b_1) is realized (with complications connected with the hexagonal crystal structure). A similar "prevacancy effect" found in some cubic metals (e.g. Fe [27]) might also be due to metastable acoustic e^+ polarons.

3 Positron Trapping

The importance of positron annihilation for the study of defects and disorder rests on the fact that positrons may be *trapped by inhomogeneities* in condensed matter. This is illustrated by Fig. 2 for the case of a vacancy in a metal. In a perfect crystal the potential energy U of the positrons is periodic with the periodicity of the lattice. The e^+ wavefunctions are Bloch functions. They describe an e^+ probability distribution which possesses lattice periodicity, too. The admissable e^+ energies form "bands". The bottom of the "e^+ conduction band", ϵ_c, is indicated in Fig. 2. Removal of an ion core plus redistribution of the conduction electrons (= formation of a vacant lattice site) results in a local lowering of the e^+ potential energy. In most metals the ensuing potential well is deep and wide enough to give rise to at least one bound state for positrons. As indicated in Fig. 2 by a full line, the positron wavefunction associated with such a bound state is localized at the vacant site with some overlap into the neighbouring lattice cells. Electron density and momentum distribution, too, are modified at the lattice inhomogeneities. As a consequence, the trapping of positrons in the bound state affects the annihilation characteristics profoundly. This allows us to distinguish positrons annihilating in bound states (="trapped e^+") from those annihilating in Bloch states (= "free e^+"). Positrons may thus serve to *decorate* lattice defects and other inhomogeneities. The 1964 paper by Dekhtyar et al. [28] on the angular correlation of

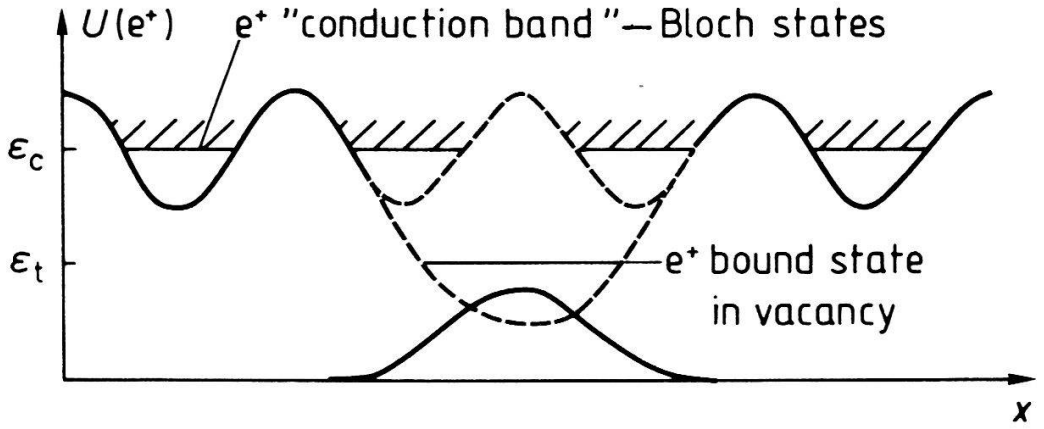

Figure 2: Lattice potential acting on positrons in a metal containing a monovacancy. The bottom of the conduction band of e^+ propagating in Bloch states is indicated by ϵ_c, the energy level of e^+ trapped in a vacancy by ϵ_t.

the e^+ annihilation radiation (= ACAR) in plastically deformed Ni-Fe alloys appears to contain the first indication of the strong effects of lattice defects (in this case presumably of dislocations) on positron annihilation. At about the same time Gol'danskii and Prokop'ev [18] proposed that in alkali halide crystals e^+ might be trapped by negative charged interstitial ions as well as by vacancies on the cation sublattice. Not much later Berko and Erskine [29] noted the effect of plastic deformation of Al on ACAR and interpreted it in terms of dislocation trapping.

The early work of e^+ annihilation in plastically deformed metals received little attention. The same was true of the observation of the rather strong temperature dependence of ACAR at elevated temperatures in In, Zn, and Cd [30], which, as we now know, was due to the trapping of e^+ by vacancies present in high-temperature thermal equilibrium.

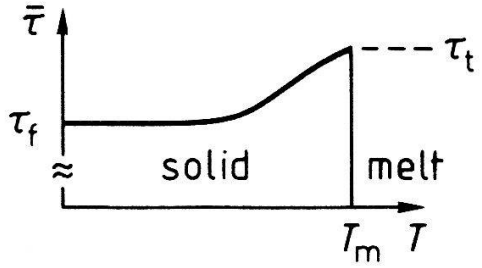

Figure 3: Schematic temperature dependence of the mean positron lifetime $\bar{\tau}$ in a metal. τ_f and τ_t denote the lifetimes of free (untrapped) e^+ and of e^+ trapped in vancancies. T_m = melting temperature.

The break-through came with the experiments of MacKenzie, Khoo, McDonald, and McKee [31], who observed on four metals (Al, In, Zn, Cd) at elevated temperatures a reversible rise of the mean e^+ lifetime, $\bar{\tau}$, with increasing temperature (Fig. 3). The authors recognized that the rise had to do with lattice vacancies formed in thermal equilibrium at high temperatures (hence the reversibility!) but the definitive explanation was given only two years later by Bergersen and Stott [32] as well as Connors and West [33], who applied the two-state trapping model to the data of MacKenzie et al [31]. Shortly before that, Grosskreutz and Millett [34] had interpreted the increase of e^+ lifetimes in cyclically deformed Al and Cu in terms of e^+ trapping by the dislocation cores.

The essentials of the *two-state trapping model* are as follows: The positrons may be in either one of two states: The "free" state, in which they annihilate with a rate τ_f^{-1}, and a trapped state, in which they annihilate with a rate $\tau_t^{-1} < \tau_f^{-1}$. Immediately after thermalization (see Sect. 2) virtually all e^+ are supposed to be in the free state; from there they may be trapped with a trapping rate σC_t, where C_t denotes the trap concentration and σ the trapping rate per unit concentration.

The lifetime spectrum following from the two-state trapping model consists of two components with decay times τ_0 and τ_1. The time spent by a positron in the free state may end either by annihilation or by being trapped, hence the decay time of the free positron population is given by

$$\tau_0 = \frac{1}{\tau_f^{-1} + \sigma\, C_t}. \tag{14}$$

The simple two-state trapping model as described above disregards the possibility of e^+ escaping from the traps (="detrapping"); hence it gives for the decay time of the trapped positron population

$$\tau_1 = \tau_t. \tag{15}$$

The relative intensities of the two components, I_0 and I_1 ($I_0 + I_1 = 1$), are given by

$$I_0 = \frac{\tau_t - \tau_f}{\tau_t(1 + \tau_f \sigma C_t) - \tau_f}, \qquad I_1 = \frac{\tau_t \tau_f\, \sigma C_t}{\tau_t(1 + \tau_f \sigma C_t) - \tau_f}, \tag{16}$$

the mean lifetime by

$$\bar{\tau} = \tau_0 I_0 + \tau_1 I_1 = \tau_f \frac{1 + \tau_t \sigma C_t}{1 + \tau_f \sigma C_t}. \tag{17}$$

The mean lifetime shows a sigmoidal behaviour as a function of the trap concentration. It increases from the lifetime of the free e^+, τ_f, at trap concentrations $C_t \ll (\tau_t \tau_f \sigma^2)^{-1/2}$ to the lifetime of

the trapped positrons, τ_t, at $C_t \gg (\tau_t \tau_f \sigma^2)^{-1/2}$. The observations of MacKenzie et al. [31] may thus indeed be understood in terms of e^+ trapping by vacancies in thermal equilibrium since their concentration increases exponentially with temperature (Fig. 4).

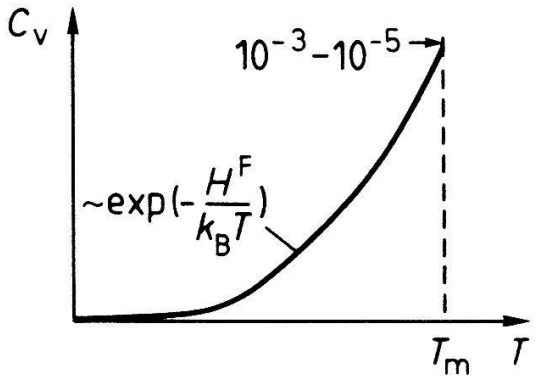

Figure 4: Concentration C_V of vacancies in a metal as a function of temperature (schematic). H^F = vacancy formation enthalpy

The mean positron lifetime is easily obtained from the measured lifetime spectrum and most of the early lifetime studies of e^+ were based on it. More information may be deduced, however, by *lifetime spectroscopy*, i.e., the decomposition of the lifetime spectrum into (exponentially decaying) components with decay times τ_0, τ_1, τ_2 etc. Provided the simple two-state trapping model outlined above is valid, the three quantities deducible from a two-component decomposition of the lifetime spectrum, τ_0, τ_1, and I_0/I_1, allow us to derive τ_f, τ_t, and σC_t. Applied to vacancies in thermal equilibrium this means that we may deduce, in addition to the lifetime τ_f of free positions, the lifetime of positrons annihilating in the vacancies and, from

$$H^F_{eff} = -\frac{\mathrm{d}\ \ln \sigma C_t}{\mathrm{d}(1/\ k_B T)}, \tag{18}$$

an *effective* enthalpy of vacancy formation.

The preceding example may serve to illustrate some of the characteristic features of the study of lattice defects by e^+ annihilation:

(i) The technique is *specific*, since the lifetime τ_t of the trapped positrons depends on the nature of the traps. Within the limits set by the resolving power the technique allows different traps to be distinguished from each other.

(ii) The technique is *sensitive*. Typical values for atomic defects are $(\tau_f\ \tau_t)^{1/2} = 2 \cdot 10^{-10}$s; $V_A/r_0 = 5 \cdot 10^{-20}$ m^2. Considering vacancies in thermal equilibrium and assuming $D^+ = 0.5 \cdot 10^{-4}$ m^2 s^{-1} gives us $(\tau_f\ \tau_t\ \sigma^2)^{-1/2} = 4 \cdot 10^{-5}$, hence a lower limit for the detectable vacancy concentration of about 10^{-7}. This has been confirmed experimentally on a number of metals in which C_t would be estimated independently. In low-temperature experiments, where D^+ is larger, the sensitivity is even greater.

(iii) Variations in the trap concentration as required, e.g., for the determination of defect formation enthalpies (cf.(19)), can be followed only through a *concentration window* centred at $(\tau_t \tau_f \sigma^2)^{-1/2}$ and extending about one and a half powers of ten in either direction. Outside this window one either has "saturation trapping", hence no dependence of the annihilation signal on the *concentration* of the traps, or no trapping at all since the positrons are too short-lived in order to reach the traps.

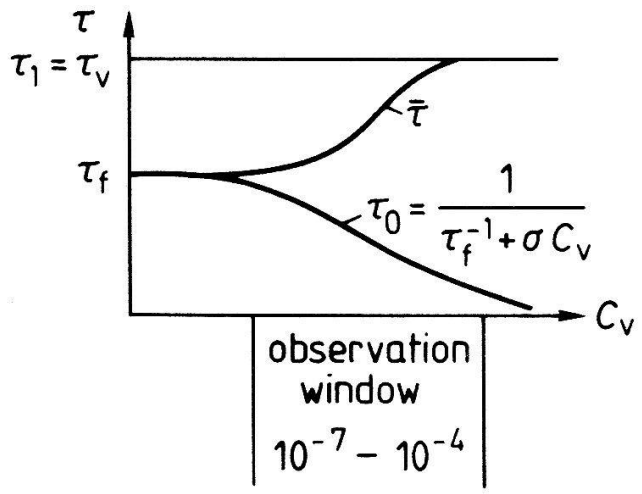

Figure 5: Positron lifetimes in a metal as a function of the vacancy concentration according to Eqs. (14), (15), and (17). The window of observable vacancy concentrations is indicated.

(iv) For quantitative investigations of the trap concentration one has to know the e^+ *diffusivity* D^+. (An estimate of the capture radius r_0 can often be obtained by simple arguments.) For obtaining accurate values of the defect formation enthalpies one must at least know the temperature dependence of the diffusivity. E.g., if in thermal-equilibrium studies monovacancies are the only defects that have to be taken into account and if r_0 is treated as temperature-independent we have, making use of (11),

$$-\frac{\mathrm{d}\ \ln \sigma\, C_t}{\mathrm{d}\ (1/k_B\, T)} = H_{1V}^F - \frac{\mathrm{d}\ \ln D^+}{\mathrm{d}(1/k_B\, T)}, \tag{19}$$

where H_{1V}^F is the enthalpy of monovacancy formation. Eq. (4) gives us $\mathrm{d}\ \ln D^+/\mathrm{d}\ (1/k_B\, T) = k_B\, T/2$. In this case the difference between H_{1V}^F and H_{eff} is small but, as a rule, not negligible. The difference can become quite large if acoustic polarons (cf. Sect. 2) have to be taken into account.

High-temperature positron annihilation measurements and their analysis in terms of the trapping model are at present the most powerful technique for determining enthalpies of *monovacancy formation* in metals and alloys. Recent reviews of this field have been published by Schaefer [35,36]; for earlier reviews see [7,37].

Notwithstanding the fact that some of the pioneering work on e^+ trapping was done on plastically deformed metals and alloys, our knowledge on e^+–dislocation interactions has remained rather vague. E.g., the influence of the dislocation character (edge vs. screw dislocations) and of the dislocation splitting on e^+ trapping and annihilation has not been established with any degree of reliability. Another point which is awaiting clarification is the rôle of special sites along the dislocation lines, e.g., of jogs and constrictions.

4 Critique and Extensions of the Simple Two-State Trapping Model

The trapping model may be considered as the back-bone of defect studies by means of e^+ annihilation. The basic physical concept appears to have been conceived in 1965 independently by several groups (Gol'danskii and Prokop'ev [18], Berko and Erskine [29], Brandt [38]). The mathematical formulation of the simple two-state trapping model, on which the equations of Sect. 3 are based, have been given simultaneously by Bergersen and Stott [32] and by Connors and West [33].

Successful as it has been especially in the study of vacancies in thermal equilibrium, the *simple two-state trapping model* has several serious limitations.The most important ones are briefly discussed in this section.

(i) Because of the sensitivity of the method we can only rarely expect that it suffices to take into account one kind of traps only. E.g., after plastic deformation not only vacancies but also different types of dislocations will act as traps. In low-temperature experiments impurities will in general have to be taken into account. The extension of the simple two-state trapping model to N different traps with lifetimes τ_j and trapping rates $\sigma_j C_j$ $(j = 1, \ldots, N)$ is straightforward [37].

(ii) The expressions of Sect. 2 and their extensions mentioned in (i) are based on the assumption that the specific trapping rates σ_j are independent of the time the positrons have spent in the material since their implantation. This is strictly true only if the trapping rate is "capture limited", i.e. if the diffusion is so fast that it may be neglected compared with the quantum-mechanical transition rate from the positron "band states" into the bound states. In the opposite limiting case [to which (11) pertains] the above-mentioned assumption is only approximately true since it neglects the fact that as the reaction between traps and positrons proceeds, the trap positron pair correlation function changes in the direction of the depletion of short trap-positron separations.

In the case of *negligible detrapping* [cf.(i)] it is not difficult to take the time dependence of the trapping rate into account [7]. Corrections for the time dependence have to be made only if

$$\frac{16\,\pi\,\tau_0\,\tau_1 D^+}{(\tau_1 - \tau_0)} \cdot \left[\frac{r_0\,C_t}{V_A}\right]^2 \geq 1, \tag{20}$$

i.e., for fairly high trap concentrations. (For the generalization of (20) to more than one kind of trap see [7].)

(iii) An essential assumption of the two-state trapping model of Sect. 3 is that the binding of the positrons to the traps is strong enough for the escape of the positrons from the traps to be neglected. This assumption fails if the parameter $\Delta\epsilon_j/k_B T$ is not sufficiently large, i.e. if either the binding energy $\Delta\epsilon_j$ of the positrons to the j-traps is too small or the temperature too high. In the same approximation in which σ_j may be taken as time-independent [cf.(ii)] the *detrapping* may be taken into account by introducing escape frequencies ν_j. The general solution of this extension of the trapping model is complicated [39] but simple expressions exist in special cases, e.g. for the mean lifetime [39].

Taking into account detrapping correctly requires the pair-correlation-function approach alluded to in item (ii). The general solution of the problem is rather complicated and leads to simple

analytical expressions only in special cases [40]. A complete analytical solution is available under the assumption that the specific trapping rate σ_j may be taken as time-independent and that the detrapping may be described by time-independent detrapping frequencies [16].

Another important deviation from the simple trapping model caused by preferential trapping of positrons with kinetic energies, has come into the dicussion during the past few years. Brandt and Arista [3] pointed out that the ensuing removal of these positrons from the ensemble of "free" positrons will result in a "heating" or "cooling" of the remaining positrons ensemble. Brandt and Arista considered in particular the case of very long thermalization times at the low-energy end of the e^+ energy distribution. If the trap concentration is high, a considerable fraction of the positrons may be trapped before they reach thermal equilibrium. Shirai and Takamura [41,42] and McMullen and Stott [43,44] have independently considered the preferential trapping of positrons with energies close to those of virtual bound states ("resonances") at the traps. For typical potential wells describing traps of atomic dimensions such as resonances are likely to occur at energies of the order of magnitude 1 eV.

Experimental indications for the trapping of nonthermal positrons in vacancies in Al and Cu have been reported by Nielsen, Lynn and Chen [45].These authors observed the energy distribution of positrons reemitted from the specimen surface and found a considerable decrease in the fraction of positrons with energies around 1eV, in the presence of vacancies.

The question of preferential trapping of epithermal positrons is certainly important enough to warrant further investigation. Resonance trapping may, e.g., complicate the comparison of e^+-annihilation investigations of frozen-in and thermal-equilibrium vacancies.

Summarizing the current situation we may state that a complete theoretical framework is available which allows us to treat any extension of the simple two-state trapping model that at the present time appears necessary for analyzing experimental data. Reasonably simple analytical solutions have been derived in quite a number of cases of practical interest. So far relatively little use has been made of the extensions with the noticeable exception of the work of Mogensen et. al. [46] on positron trapping by halogen ions in water. At present the theory is far ahead of the experiments. However, as the experimental techniques continue to improve, more and more refined versions of the trapping model will have to be employed in the data analysis.

5 Experimental Techniques

5.1 Introductory remarks

The information of the behaviour of thermalized e^+ in condensed matter is transmitted exclusively by the annihilation irradiation. Since the annihilation of positron-electron pairs into two γ quanta according to

$$e^+ + e^- \rightarrow 2\,\gamma \qquad (21)$$

is much more frequent than that into three γ quanta, we confine ourselves entirely to the 2γ process (21).

The measuring techniques fall into two broad categories, depending on whether they give

information on the *momentum distribution* of the annihilating positron-electron pairs or on the *annihilation rate* of the positrons. The annihilation rate is determined by the overlap of the positron wavefunction with the electron wavefunctions and is thus closely related to the electron density at the annihilation sites. The momenta of thermalized positrons are small compared with the width of the momentum distribution of the electrons in condensed matter. Variations in the momentum distribution of the e^+ e^- pairs and/ or in the annihilation rate pertain therefore primarily to the *electrons* of the host material. As a consequence, the information on the *positron* behaviour has to be obtained in a more indirect way, e.g. through diffusion (Sect. 2) and trapping (Sects. 3 and 4) studies, or through depolarization experiments (Sects. 5 and 6).

It has already been argued (Sect. 3) that at a vacant lattice site the electron charge density is less than at an interstitial site in a perfect environment. Hence the annihilation rate of positrons trapped in a vacancy, τ_v^{-1}, is less than the annihilation rate τ_f^{-1} of "free" positrons. Analogous arguments hold for the momentum distribution. The absence of the ion core in a vacancy reduces the high-momentum components in the e^+e^- momentum distribution of trapped positrons compared with "free" annihilation.

5.2 e^+e^- momentum distribution

For measuring the e^+e^- momentum distributions and their changes due to e^+ trapping two techniques are available, viz,

1. the Doppler Broadening of the 2γ-annihilation photon line (Fig. 6a) and
2. the *A*ngular *C*orrelation of the *A*nnihilation *R*adiation (ACAR) (Fig. 6b).

In the rest systems of the e^+e^- pairs annihilating in the 2γ mode the laws of conservation of energy and momentum require the energies of the two photons resulting from an annihilation event to be equal and their momenta to be opposite. Owing to the velocities of the electrons, the laboratory system differs from the individual e^+e^- rest systems. This has the following consequences for observations in the laboratory system :

(i) If the e^+e^- momentum possesses a "longitudinal" component (i.e., parallel to the direction of the γ detection) the energies of the two photons are different; hence the annihilation photon line is Doppler-broadened.

(ii) In general (viz. if the e^+e^- momentum possesses a non-vanishing component transverse to the direction of γ detection) the flight directions of the two members of a photon pair deviate from 180 °. Hence the dependence of the coincidence count rate $C(\theta)$ on the angle θ between the simultaneously emitted γs (ACAR) is a measure of the e^+e^- momentum distribution.

Both types of measurements (Doppler broadening and ACAR) give in principle the same information but are in practice quite different. ACAR is capable of a very high resolution (limited only by geometry and statistics) but since it is based on coincidences the counting is slow. (This disadvantage may be alleviated by two-dimensional γ detection though at the cost of considerable expenditure.) The resolution of the Doppler broadening measurements is limited by the energy resolution of the available Ge detectors but since no coincidences are involved, data accumulation is much faster and simpler than in ACAR.

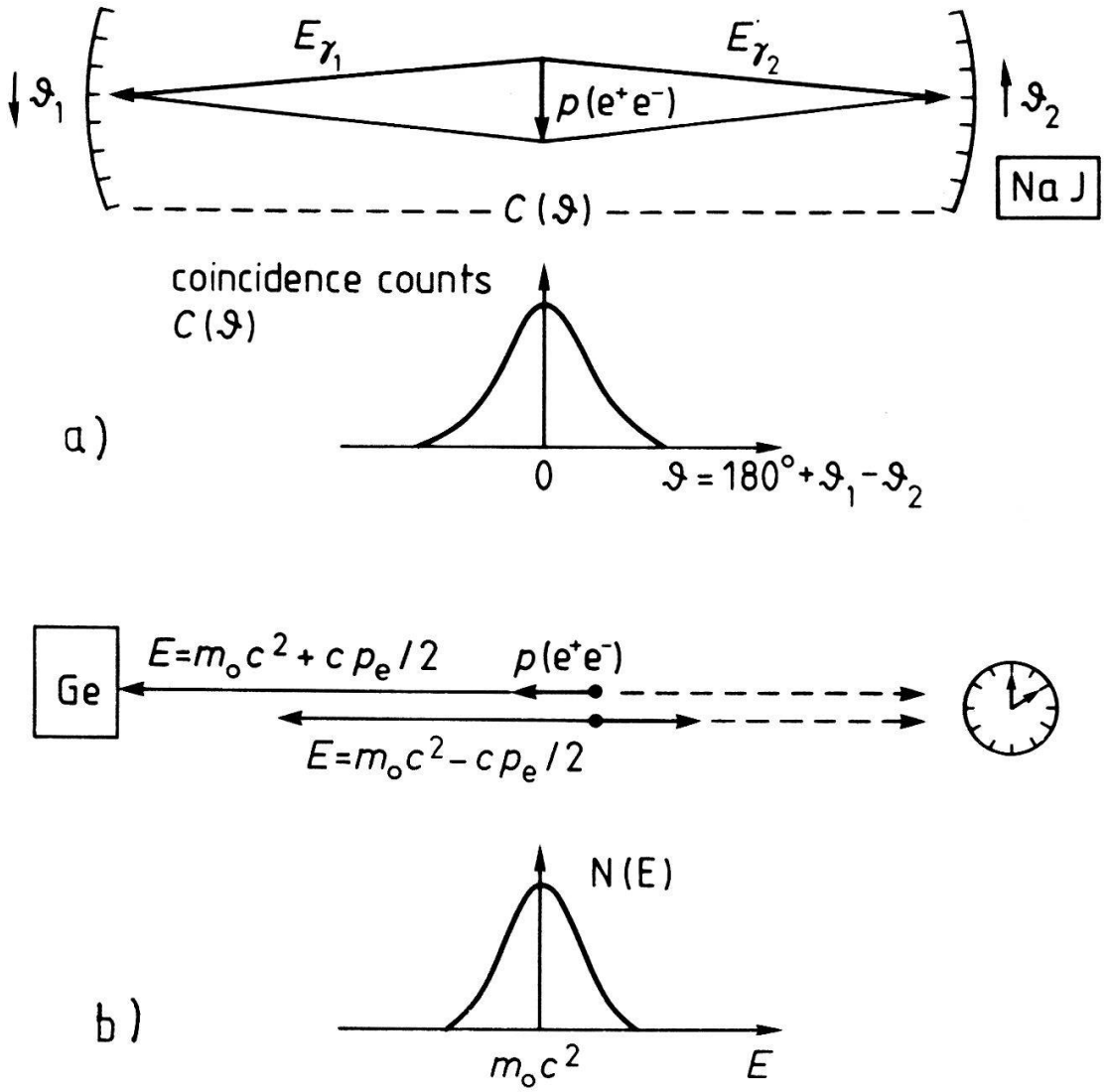

Figure 6: a): The ACAR technique for determining the distribution of the transverse components of the e^+e^- momenta $p(e^+e^-)$. E_{γ_1} and E_{γ_2} denote the photon energies in the laboratory system. NaJ = sodium iodide detector

b): The Doppler-broadening technique for determining the distribution of the longitudinal components of $p(e^+e^-)$. Ge = germanium detector. $N(E)$ = count rate. The arrows indicate the possibility to use the second annihilation photon for the determination of the positron age.

In contrast to ACAR, Doppler broadening uses only one of the two annihilation photons. The second one may be employed to stop an electronic clock that had been set going by either a "prompt" γ quantum or by the positron entering the sample (cf. Sect. 5.3.). This means that the longitudinal components of e^+e^- momenta may be *correlated* with the time that the individual positrons have spent in the target, the so-called *positron age*. Such so-called "age-momentum" measurements will be discussed below (Sect. 5.5)

5.3 Positron lifetimes

The positron is a *stable* particle. In contrast to other positively charged elementary particles with finite lifetimes, such as the positive muon (μ^+) and the positive pion (π^+), it does not *decay* with a fixed rate but *annihilates* with its antiparticle, the electron. As already emphasized (cf. Sect. 3), the e^+ annihilation rate and its inverse, the e^+ lifetime, depend on the *environment* in which the positrons annihilate. Measurements of the mean lifetime or, more generally, of the distribution of lifetimes (= lifetime spectroscopy) can therefore give information on the sites at which the positrons annihilate, e.g. on inhomogeneities at which they have been trapped. Lifetime data possess the advantage that – as long as we confine ourselves to 2γ annihilation and exclude formation of orthopositronium – their qualitative interpretation is straightforward: longer lifetimes mean smaller electron densities at the location of the positrons. If for a given material the τ_t values of a number of different traps are known, this rule helps us in finding the correct assignment of new lifetime components.

For the interpretation of e^+ lifetimes it is important to note that if the formation of ortho-positronium "atoms" (e^+e^- bound states with total spin 1) may be excluded, the positron lifetime cannot exceed an upper limit, τ_∞, given by

$$\tau_\infty^{-1} = \frac{1}{4}\,\lambda_{p-Ps} + \frac{3}{4}\,\lambda_{o-Ps}. \tag{22}$$

In (22) $\lambda_{p-Ps} = 7.994 \cdot 10^9\ s^{-1}$ is the annihilation rate of para-positronium (= e^+e^- bound states with total spin zero) [47], $\lambda_{o-Ps} = 7.0516 \cdot 10^6\ s^{-1}$ that of ortho-positronium [48].

The physical background of (22) is as follows. Because of the Coulomb attraction between positrons and electrons the electron density at the positrons cannot be smaller than in positronium atoms even if the average electron density in the environment is much smaller. A lower limit for the positron annihilation rate in the absence of positronium may thus be derived from the annihilation rates of para - and ortho-positronium, taking into account the statistical weights of the different spin states. Eq. (22) gives us for the corresponding upper limit of the positron lifetime $\tau_\infty = 500$ ps. If positron lifetime spectroscopy leads to time constants exceeding τ_∞ we have to conclude that ortho-positronium is involved.

Time constants larger than τ_∞ are familiar in insulating materials. They have also been found in nanocrystalline metals (see e.g. [49]). This indicates that these nanocrystals may contain open spaces ("microvoids") large enough to sustain positronium atoms.

From the preceding discussion it follows that the lifetimes of trapped positrons are insensitive against the nature of the positron traps if they are close to τ_∞. In lifetime spectroscopy we are thus particularly interested in "short" lifetimes, say between $1 \cdot 10^{-10}$ s and $3 \cdot 10^{-10}$ s. The

accurate measurement of such lifetimes is not easy since they are comparable with the widths of the resolution functions of the best available lifetime spectrometers.

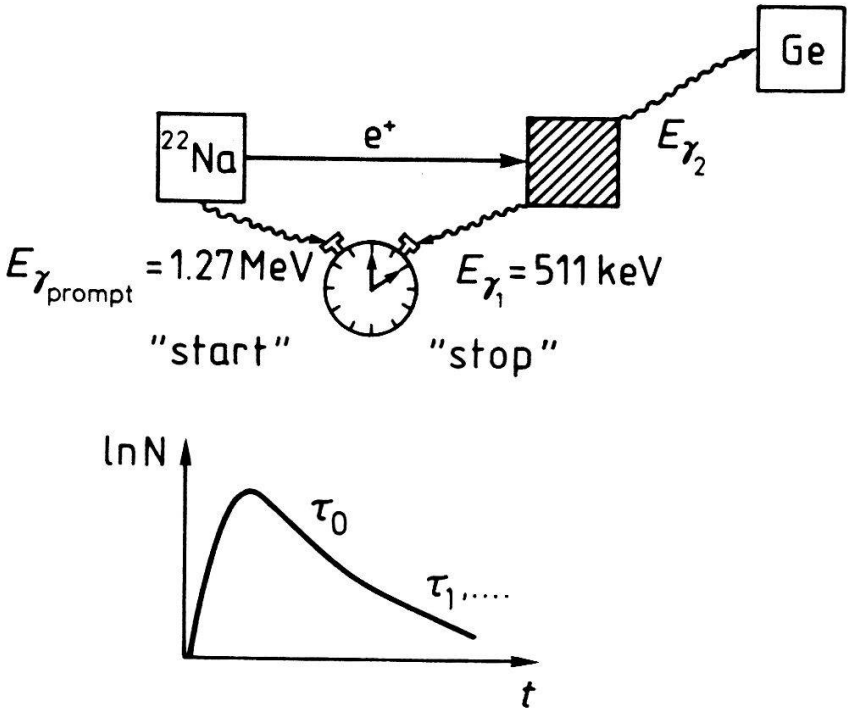

Figure 7:
Positron lifetime measurement by a $\gamma\gamma$ spectrometer. The possibility to use the second annihilation quantum for a Doppler-broadening measurement is indicated.

Positron lifetime spectrometers fall into two categories, viz. $\gamma\gamma$ spectrometers and $\beta^+\gamma$ spectrometers. The basic idea of $\gamma\gamma$ spectrometers is shown in Fig 7. The positrons are obtained from a radioactive source that emits so-called prompt γ quanta almost simultaneously with the positrons. The prompt γs are used to start an electronic clock. The clock is stopped by detecting one of the annihilation γs. One obtains a so-called time differential spectrum in which the count rate is plotted against the time spent by the positrons in the sample before they annihilate. Ideally, if the lifetime spectrum consists of only one component this plot should be exponential. In practice, however, it is always considerably distorted due to the finite resolution of the spectrometer.

For weldable materials, i.e. for solid metals and alloys, the use of the $\gamma\gamma$ method was very much facilitated by the invention of the "sealed-source" technique [50,51]. This technique, which in the meantime has become widespread, allows measurements up to the melting point of tungsten, on specimens irradiated at arbitrary temperatures or quenched from high temperatures, etc.

An intrinsic drawback of the $\gamma\gamma$ technique is the low detection efficiency of the γ detectors, which makes it rather time-consuming to achieve statistics that are good enough for the analysis of complicated lifetime spectra. The problem has recently been alleviated by replacing the conventional plastic scintillators by more efficient BaF_2 crystals [52].

If this is done, special attention has to be paid, however, to artifacts in the e^+ lifetime spectrum that may arise if the BaF_2 start detector can be reached by the companion of the annihilation γ triggering the stop signal. These artifacts may be avoided by arranging the BaF_2 detectors in a geometry, which makes it impossible for the quasi-collinear annihilation γs to reach both the start and the stop detector, or by retaining a plastic scintillator as start detector [53]. The lower detection efficiency of the plastic scintillators reduces considerably the probability that a start

pulse is recorded in which both start and stop signal of a single positron are superimposed. A preliminary set-up consisting of a start scintillator (Pilot U, diameter × height = 30 mm × 30 mm) and a stop scintillator (BaF_2, diameter × height = 40mm × 30mm) at a distance of 15 mm in a 180 °-geometry, and a positron source (activity $1.5 \cdot 10^5$ Bq) between them gives a coincidence counting rate of 250 s^{-1} and a time resolution of 250 ps (FWHM) [53].

It has been known for a long time that an alternative exists for obtaining the start signal of the lifetime spectrometer. Already in the first comprehensive study of positron lifetimes in liquids and solids by Bell and Graham [54] the γ detection was employed only for the annihilation γs supplying the stop signal; the start signal was obtained from the passage of the positrons (coming from a ^{22}Na source) through a β counter (a stilbine crystal). In order to permit a correction for the transit time of the positrons, after their passage through the entrance counter a fixed e^+ kinetic energy of 275 keV was selected by means of a β spectrometer.

In the following years the $\beta\gamma$ detection technique of Bell and Graham [54] was supplanted by the $\gamma\gamma$-technique, which allowed better time resolutions to be achieved. In 1979 Maier and Myllylä [55] pointed out that the performance of $\beta\gamma$ spectrometers can be decisively improved by employing *relativistic positrons.* If all positrons enter the sample with a speed sufficiently close to the speed of light, detection efficiency unity and high counting rates in the start detector can be achieved simultaneously with a negligible contribution of the positron transit time to the width of the resolution function.

In a pilot study using a $^{68}Ge/^{68}Ga$ source (maximum kinetic energy of the positrons 1.9 MeV) the viability of the Maier-Myllylä proposal was demonstrated [55]. Lifetime measurements on solid In gave results that compared well with those obtained with a conventional $\gamma\gamma$ spectrometer in spite of the fact that a compromise between time resolution and counting rate was unavoidable [56]. Full exploitation of the strengths of the $\beta\gamma$-techniques, however, requires a reasonably intense and well collimated beam of monoenergetic relativistic positrons. Such a beam has recently been installed at the Max-Planck-Institut für Metallforschung in Stuttgart and will be described in the next subsection.

5.4 Fast positron lifetime measurements by means of a relativistic positron beam [57,58]

A slow-positron source was installed in the high-voltage terminal of a vertical electrostatic accelerator of the pelletron type. The source consists at present of a ^{22}Na source ($6 \cdot 10^8$ Bq and a moderator comprising a tungsten foil (thickness: 3-6μm) and tungsten rings (height× diameter: 3,3 mm× 10 mm) in a combined transmission-reflection geometry. By means of a variable voltage (0-30 V), equally divided between the tungsten rings, of an extraction voltage (0-50 kV) between the moderator and the terminal, and of an electrostatic lens the positrons are focused into the accelerator tube. This arrangement delivers to the target a monoenergetic flux of about $6 \cdot 10^4$ e^+ s^{-1} in the energy range 0.5-6.5 MeV. A relative energy stability of better than $3 \cdot 10^{-4}$ can be achieved but is not necessary for the lifetime measurements. By means of deflection magnets, correction coils, and quadrupole magnets the beam can be deflected into various positions and focused onto a spot of less than 1 mm in diameter.

The start signals for e^+ lifetime measurements are obtained from a plastic scintillator (Pilot

U, thickness 3-5mm), through which the e^+ pass immediately before they are implanted into the target specimen. The stop signal is produced in a BaF_2 scintillator (diameter × height = 25 × 25 mm) by one of the 511 keV annihilation photons. A veto scintillator with a cylindrical hole (5 mm in diameter) between start detector and target is used to eliminate coincidence signals from backscattered positrons. With this setup and a beam flux of $6 \cdot 10^4 e^+ s^{-1}$ a time resolution of 180 ps (FWHM) at a coincidence count rate of 480 s^{-1} is obtained. The e^+ lifetime spectra show an exceedingly low background. This makes the spectrometer particularly well-suited for the investigation of weak long-lived components in the lifetime spectra, due to, e.g. orthopositronium.

Since the MeV positrons are implanted deeply into the material the specimen preparation for e^+ lifetime studies is considerably simplified in comparison with the above-mentioned sealed-source technique.

Generally speaking, the beam technique simplifies the specimen preparation for lifetime measurements strikingly since it virtually eliminates not only the so-called source problems but also, on account of the deep penetration of MeV positrons, any surface problems. This is particularly true of those materials to which the sealed-source technique (Sect. 5.3.) is not applicable. Examples of investigations that would have been either impossible or not at least very difficult without the beam technique are high-temperature thermal equilibrium studies on In, Al, and Ge in the solid and molten state [59,60] as well as in Si up to the melting temperature [61]. They were performed with the e^+ impinging vertically on cylindrical specimens heated by an electron beam.

By varying the e^+ beam energy the depth distribution of the implanted positrons may be changed. This should permit an extension of the "defect profiling" technique already implemented with slow-positron beams [62,63] to the investigation of defect distribution deep inside macroscopic specimens and to non-destructive testing of materials. As an example of great practical importance we mention the distribution of oxygen precipitates in as-grown Si crystals, which Doyama et. al. [64] have already successfully studied by Doppler-broadening measurements (though without the depth resolution achievable with an e^+ beam of variable energy).

A substantial futher improvement of the time resolution of the $\beta^+\gamma$ spectrometer may be expected from the development of a *positron clock* [58]. In this novel extension of the relativistic beam technique the e^+ beam is circularly deflected by means of an electromagnetic field with a frequency f in the GHz range. It will scan over a ring of scintillator segments like the pointer of a clock (hence the name) and then be refocused onto the specimen. The start pulse supplied by one of the β^+ scintillator segments supplies additional information on the position of the transmitted positron in the scintillator arrangement and on the phase of the circular GHz field. This allows us to determine the time of the start signal with considerably increased accuracy. The time resolution of the start circuit can then be calculated from the deflection frequency f and the number of scintillators segments N (e.g., for f = 1.25 GHz and N = 40 we obtain a contribution of only 20 ps from the start circuit to the total spectrometer time resolution). By means of a 1.25 GHz prototype resonator a periodic linear deflection of a 4 MeV e^+ beam by ± 14 mm over a distance of 1.8 m has been produced. The practical realization of a beam-based e^+ clock thus appears to be feasible. It should be given high priority since it promises to bring the time resolution close to the limit set by that of the stop detectors and thus to make detailed studies of very short lifetimes feasible.

5.5 Measurements of the positron age-momentum correlation

Both types of lifetime measurements, $\beta^+\gamma$ and $\gamma\gamma$, make use of only one of the two photons emitted in a 2γ annihilation event. As already mentioned (Sect. 5.2.), by simultaneously measuring the Doppler shift of the other photon a correlation between the positron age and the e^+e^- momentum may be established. From this, information on the evolution of the e^+ states during thermalization, diffusion, and trapping may be obtained. The *age-momentum correlation technique* is based on triple-coincidences and therefore rather slow. This is particularly true of the $\gamma\gamma E$ technique, which suffers from the low detection efficiency of the γ detectors as well as from the pile-up effects at high source strengths. In spite of the potential power of this method only very few investigations have so far been reported [65-68]. Earlier attempts [69,70] combined with ACAR and lifetime measurements were thus even slower.

In the $\beta^+\gamma E$ arrangement pile-up pulses in the start detector can be used to discriminate random coincidences arising from multiple annihilation signals. In a $\beta^+\gamma E$ pilot set-up [58] using the e^+ beam described in Sect. 5.4. the start detector consists of a thin plastic scintillator (d = 1 mm) coupled with two photomultipliers. The stop detector is a fast BaF_2 scintillation counter (crystal diameter × length = 51 mm × 51 mm). For the energy measurements a high-purity coaxial Ge detector crystal (diameter × length = 54.6 mm × 52.2 mm) is used. This pilot system has been optimized for high count rates with low background (a $\beta^+\gamma$ E triple-coincidence count rate of $4 \cdot 10^2 s^{-1}$ at a beam current of $6 \cdot 10^4 e^+ s^{-1}$ has been achieved) rather than for good time resolution (FWHM $\approx$ 900 ps).

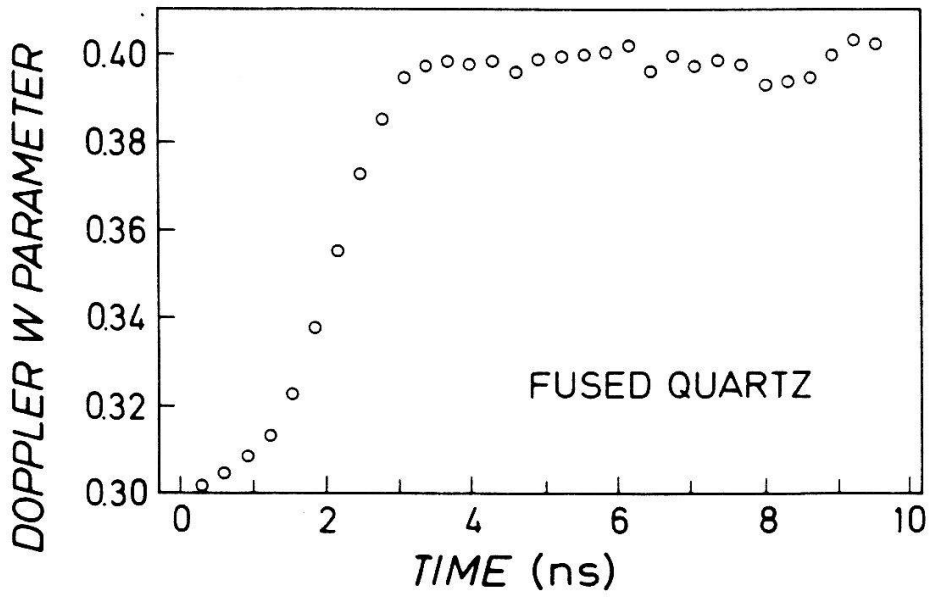

Figure 8: Age-momentum correlation in fused quartz. The Doppler-broadening parameter W characterizing the width of the annihilation γ line is measured as a function of the positron age t.

Preliminary results on fused quartz (Fig. 8) have demonstrated the potential of the $\beta^+\gamma E$ method for the investigation of positronium states. In Fig. 8 the W parameter characterizing the Doppler broadening (i.e., the width of the 2γ-annihilation line) is plotted as a function of the positron age. In the plateau regime (large broadening above $t = 3\mu s$) pick-off annihilation of ortho-positronium with crystal electrons (with high momentum) occurs. The sharp decrease of the W parameter towards shorter positron ages is considered as evidence that in the short e^+

lifetimes parapositronium is involved. We note that this investigation is in agreement with that of Bell and Graham [54], who observed long lifetime components of positrons annihilating in fused quartz and some other insulating materials and explained them in terms of the conversion of triplet positronium to the singlet state by electron spin reversing collision with electrons.

5.6 Positron spin relaxation (e^+SR) experiments

Since the main information obtainable from e^+ annihilation experiments concerns the annihilation electrons, it is difficult to investigate the behaviour of thermalized or nearly thermalized positrons in condensed matter, since their energies and momenta are small compared with those of the electrons. Spin relaxation experiments with protons [71] and muons [72,73] have provided us with rather direct insights into the dynamics of these particles in solids. Since positrons are also spin-1/2 particles, it is an intersting question whether analogous information may be expected from positron spin relaxation (e^+SR) experiments.

In e^+SR experiments [74,75] *spin polarized* positrons from radioactive sources are implanted into a ferromagnetic (more generally: ferrimagnetic) specimen. During the thermalization period, provided it does not exceed a few picoseconds, the e^+ polarization is essentially conserved. The interaction between the e^+ magnetic moments and spatially varying magnetic fields in the sample which the e^+ experience during their diffusive motion can lead to a depolarization of the e^+ ensemble and hence to a relaxation of the e^+ spin polarization towards its equilibrium value. However, since e^+e^- annihilation conserves parity, no direct information on the e^+ spin can be derived from the annihilation radiation. As shown already in 1957 by Hanna and Preston [76], ferromagnets may, nevertheless, serve as e^+ polarization detectors. In our e^+SR experiments ferromagnetic samples serve both as depolarizing medium and as polarization detectors. In order to achieve this, the magnetic structure of the sample has to satisfy several requirements [74]. They are satisfied in α-iron and some of its alloys. The observation of e^+ spin relaxation allows us to test microscopic models relating the correlation time τ_c of the magnetic fields felt by the e^+ to the e^+ diffusivity, D^+.

Theory shows that in α-Fe e^+ propagating in Bloch states cannot lead to an observable depolarization [77], whereas e^+ in metastable self-localized states that diffuse by adiabatic hopping [22] can give rise to a detectable relaxation rate. In pilot experiments using ^{68}Ge positron source (activity $\leq 3 \cdot 10^7$Bq) we have observed a small temperature-dependent depolarization in nitrogen-doped α - iron, which we have interpreted as an indication of a spin relaxation associated with the e^+ motion [75]. Further investigations of this topic should include other materials, e.g. the ferrimagnetic insulator Fe_3O_4. If a sufficiently intense beam of polarized e^+ becomes available, time-resolved depolarization experiments will become possible. Such experiments will allow us to determine the e^+ spin relaxation rate directly rather than indirectly from the dependence of the e^+ polarization on temperature and applied magnetic field as was done in the above-mentioned pilot experiments [75].

5.7 Spin-polarized positrons in positronium research

Since the pioneering work of Page and Heinberg [78] the application of *spin-polarized* positrons annihilating with electrons in magnetic fields has developed into a powerful tool in the investigation of positronium or positronium-like states ("quasi-positronium") in condensed matter (see, e.g., [79]).The formation of singlet or triplet positronium is favoured depending on whether the incoming positrons are polarized parallel or antiparallel to the magnetic field direction. In the presence of a magnetic field the annihilation characteristics of positronium atoms is modified by the mixing of the para state with the ortho state of magnetic quantum number $m = 0$. The influence of a reversal of the magnetic field on the annihilation radiation can thus be taken as a measure of the fraction of positrons forming positronium in the specimen. Herlach and Heinrich [80] employed this technique for detecting positronium in F-centers in KCl. This work demonstrated the trapping of positrons in anion vacancies (cf. [18]).

The experimental set-up for the e^+SR technique (cf Sect. 5.6.) may also be used as a sensitive system for the detection of positronium. Experiments on various solids are currently being carried out. An intensive beam of high energetic *spin-polarized* positrons will be very useful not only for e^+SR experiments but also in the field of positronium research.

6 Conclusions

During the past twenty years positron annihilation methods have been established as powerful tools for studying defects in crystals or, more generally, inhomogeneities in condensed matter. Models for the analysis of such data are available with widely different degrees of complexity and sophistication. A particularly effective technique is positron lifetime spectroscopy, since it is sensitive, defect-specific, and relatively easy to interpret. Reliable interpretation of the experimental data, also of other positron-annihilation techniques such as the angular correlation of the annihilation radiation (ACAR) or the Doppler broadening of the 511 keV annihilation, requires reliable information on the behaviour of positrons in condensed matter, e.g. on the thermalization process, on the positron diffusivity, on the process of positron capture by traps, and, at present most controversial, on the question whether and in which materials positrons may occupy metastable localized states (= acoustic polarons) in which they diffuse by hopping. Since such information is hard to come by, there is a wide field for future experimental work based on improved techniques.

With regard to novel experimental techniques the potential of positron beams of relativistic energies for lifetime measurements has clearly been demonstrated. A breakthrough not only in the rate of lifetime-data accumulation but also in the achievable time resolution appears feasible by means of the so-called positron clock. If a substantially more intense beam than that at present operative at the Stuttgart pelletron is available, further extensions of the experimental methods will become possible, e.g. routine age-momentum correlation measurements with good statistics and high time resolution.

It is highly desirable that a future intense relativistic beam should provide spin-polarized positrons, i.e., be fed by positrons from β^+-decay of radioactive nuclei rather than from pair production. Such a beam would make measurements of the rate of positron spin relaxation in suitably chosen ferro- and ferrimagnets possible. From such measurements we may expect information on

the behaviour of positrons in crystals that is difficult to obtain by other means. Application of strong magnetic fields parallel or antiparallel to the beam direction would allow us to study positronium formation in the target rather directly, since the formation of para- or ortho-positronium is favoured depending on whether the external magnetic field is parallel or antiparallel to the positron polarization.

Acknowledgements

The authors have enjoyed the support and the help of too many members, past and present, of the Stuttgart positron group to mention all their names. Special thanks for their year-long contribution and valuable discussions are due to D. Herlach, K. Maier, H.E. Schaefer, and J. Major. The authors should also like to express their appreciation to Mrs. I. Schemminger and Dipl. Phys. U. Holzwarth for their untiring efforts in the preparation of the typescript.

References

[1] A. Seeger, Nova Acta Leopoldina N.F., **64**, 21 (1989)

[2] G. E. Lee-Whiting, Phys. Rev. **97**, 1557 (1955)

[3] W. Brandt and N. Arista, Phys. Rev. B **26** , 4229 (1982)

[4] A. Seeger, Phys. Letters **40 A**, 135 (1972)

[5] A. Seeger, Phys. Letters **41 A**, 267 (1972)

[6] R. A. Smith, Wave Mechanics of Crystalline Solids, Chapman and Hall, London 1969

[7] A. Seeger, Frontiers in Materials Science-Distinguished Lectures (1973), Eds.: L. M. Murr and Ch. Stein, M. Dekker, New York and Basel (1976), p. 177

[8] J. Jäckle and K. W. Kehr, J. Phys. F: Met. Phys. **13**, 753 (1983)

[9] P. J. Schultz and K. G. Lynn, Rev. Mod. Phys. **60**, 701 (1988)

[10] E. Soisinen, H. Huomo, P. A. Huttunen, J. Mäkinen, A.Vehanen, and P. Hautojärvi, to be publ. in Phys. Rev. B

[11] A. P. Mills and L. Pfeiffer, Phys. Rev. Letters **36** 1389 (1976)

[12] A. P. Mills and L. Pfeiffer, Phys. Letters **63 A**, 118 (1977)

[13] P. Norton and H. Levinstein, Phys. Rev. B **6**, 478 (1972)

[14] W. Shockley, Bell System Tech. J. **30**, 990 (1951)

[15] T. R. Waite, Phys. Rev. **107**, 463 (1957)

[16] W. Frank and A. Seeger, Appl. Phys. **3**, 61 (1974)

[17] Y. Shirai, J. Takamura, and K. Furukawa, Materials Science Forum Vol **15 - 18**, Trans. Tech. Publ. Aedermannsdorf 1987, p. 137

[18] V. I. Gol'danskii and P. E. Prokop'ev, Sov. Phys. Solid State **6**, 2641 (1965)

[19] A. Seeger, Appl. Phys. **7**, 85 (1975)

[20] A. Seeger, Appl. Phys. **7**, 257 (1975)

[21] D. Emin, M. I. Baskes, and W.D. Wilson, Phys. Rev. Letters **42**, 791 (1979)

[22] A. Seeger, in: Positron Annihilation, Eds.: P.C. Jain, R.M. Singru, and K.P. Gopinathan, World Scientific Publ. Co, Singapore 1985, p. 48

[23] P.C. Lichtenberger, C.W. Schulte, and I.K. MacKenzie, Appl. Phys. **6**, 305, (1975)

[24] S.M. Kim and W.J.L. Buyers, J. Phys. F: Met. Phys. **6**, L 67 (1976)

[25] P. Rice-Evans, I. Chaglar, F.A.R. El Khangi, and A.A. Berry, Phys. Rev. Letters **47**, 271 (1981)

[26] W. Puff, P. Mascher, P. Kindl, and H. Sormann, Appl. Phys. A **27**, 257 (1982)

[27] H.E. Schaefer, K. Maier, M. Weller, D. Herlach, A. Seeger, and J. Diehl, Scripta Met. **11**, 803 (1977)

[28] I.Ya. Dekhtyar, D.A. Levina, and V.S. Mikhalenkov, Sov. Phys. Doklady **9**, 492 (1964)

[29] S. Berko and J.C. Erskine Phys. Rev. Letters **19**, 307 (1967)

[30] I.K. MacKenzie, G.F.O. Langstroth, B.T.A. McKee, and C.G. White, Canadian J. Phys. **42** 1837 (1964)

[31] I.K. MacKenzie, T.L. Khoo, A.B. McDonald, and B.T.A. McKee, Phys. Rev. Letters **19**, 946 (1967)

[32] B. Bergersen and M.J. Stott, Solid State Commun. **7**, 1203 (1969)

[33] D.C. Connors and R.N. West, Phys. Letters **30 A**, 24 (1969)

[34] J.C. Grosskreutz and W.E. Millett, Phys. Letters **28 A**, 621 (1969)

[35] H.E. Schaefer, in: Positron Annihilation, Eds.: P.G. Coleman, S.C. Sharma, and L.M. Diana, North Holland, Amsterdam, 1982, p. 369

[36] H.E. Schaefer, phys. stat. sol.(a) **102**, 47 (1987)

[37] A. Seeger, J. Phys. F: Met. Phys. **3**, 248 (1973)

[38] W. Brandt, in: Positron Annihilation, Eds.: A.T. Stewart and L.O. Roellig, Acad. Press, New York and London 1967, p. 155

[39] A. Seeger, Appl. Phys. **4**, 183 (1974)

[40] W. Meyberg, W. Frank, U. Gösele, and A. Seeger in: Positron Annihilation, Eds.: P.C. Jain, R.M. Singru, and K.P. Gopinathan, World Scientific Publ., Singapore 1985, p. 458

[41] Y. Shirai and J. Takamura, J. Phys. Cond. Matter **1**, SA 125 (1989)

[42] Y.Shirai and J. Takamura, Mat. Science Forum **37**, Trans. Tech. Publ. Aedermannsdorf 1989, p. 123

[43] T. McMullen and M.J. Stott, Phys. Rev. B **34**, 8985 (1986)

[44] M.J. Stott, in: Positron Annihilation, Eds.: L. Dorikens-Vanpraet, M. Dorikens, and D. Segers, World Scientific Publ., Singapore 1989, p.56

[45] B. Nielsen, K.G. Lynn, and Y.-C. Chen, Phys. Rev. Letters **57**, 1789 (1986)

[46] O.E. Mogensen, M. Eldrup, and N.J. Pedersen, in: Positron Annihilation, Eds.: P.C. Jain, R.M. Singru, and K.P. Goinathan, World Scientific Publ., Singapore 1985, p. 756

[47] D.W. Gidley, A. Rich, E. Sweetman, and D. West, Phys. Rev. Letters. **49**, 525 (1982)

[48] C.I. Westbrook, D.W. Gidley, R.S. Conti, and A.Rich Phys. Rev. Letters **58**, 1328 (1987)

[49] H.E. Schaefer, W. Eckert, O. Stritzke, R. Würschum, and W. Templ, in: Positron Annihilation, Eds.: L. Dorikens-Vanpraet, M. Dorikens, and D. Segers, World Scientific Publ., Singapore 1989, p.79

[50] D. Herlach and K. Maier, Appl. Phys. **11**, 197 (1976)

[51] K. Maier, M. Peo, B. Saile, H.E. Schaefer, and A. Seeger, Phil. Mag. **A40**, 701 (1979)

[52] W. Bauer, J. Major, W. Weiler, K. Maier, and H.E. Schaefer, in: Positron Annihilation, Eds.: P.C. Jain, R.M. Singru, and K.P. Gopinathan, World Scientific Publ., Singapore 1985, p. 804

[53] M. Forster, G. Schmid, and W. Eckert, to be published

[54] R.E. Bell and R.L. Graham, Phys. Rev. **90**, 644 (1953)

[55] K. Maier and R. Myllylä, in: Positron Annihilation, Eds.: R.R. Hasiguti and K. Fujiwara, Japan Inst. of Metals, Sendai 1979, p. 829

[56] W. Weiler and H.E. Schaefer, in: Microstructural Characterization of Materials by Non-Microscopical Techniques, Eds.: N. Hessel-Andersen et. al., Roskilde 1984, p. 565

[57] W. Bauer, K. Maier, J. Major, H.E. Schaefer, A. Seeger, H.D. Carstanjen, W. Decker, J. Diehl, and H. Stoll, Appl. Phys. **A43**, 261 (1987)

[58] W. Bauer, J. Briggmann, H.D. Carstanjen, S. Connell, W. Decker, J. Diehl, K. Maier, J. Major, H.E. Schaefer, A. Seeger, H. Stoll, and E. Widmann, Nucl. Instr. and Methods, **B50**, 300 (1990)

[59] H.E. Schaefer, W. Eckert, J. Briggmann, and W. Bauer, J. Phys. Cond. Matter. **1**, SA 97 (1989)

[60] W. Bauer, J. Briggmann, H.-D. Carstanjen, W. Decker, J. Diehl, K. Maier, J. Major, H.E. Schaefer, H. Stoll, and R. Würschum, in: Positron Annihilation, Eds.: L. Dorikens-Vanpraet, M. Dorikens, and D. Segers, World Scientific Publ., Singapore 1989, p. 579

[61] R. Würschum, W. Bauer, K. Maier, A. Seeger, and H.E. Schaefer, J. Phys. Cond. Matter **1**, SA 33 (1989)

[62] A. Vehanen, in: Positron Annihilation, Eds.: L. Dorikens-Vanpraet, M. Dorikens, and D. Segers, World Scientific Publ., Singapore 1989, p. 39

[63] E. Tandberg, P.J. Schultz, T.E. Jackman, M.W. Denhoff, G.C. Aers, K.G. Lynn, and B. Nielsen, in: Positron Annihilation, Eds.: L. Dorikens-Vanpraet, M. Dorikens, and D. Segers, World Scientific Publ., Singapore 1989, p. 708

[64] M. Doyama, Y. Suzuki, S. Ishibashi, and T. Abe, J. Phys.: Cond. Matter **1** SA 83 (1989)

[65] J.D. Mc Gervey and V.F. Walters, Phys. Rev. B **2**, 2421 (1970)

[66] I.K. MacKenzie, and P. Sen, Phys. Rev. Letters, **19**, 1296 (1976)

[67] Y. Kishimoto and S. Tanigawa,in: Positron Annihilaition, Eds.: P.G. Coleman, S.C. Sharma, and L.M. Diana, North Holland, Amsterdam, 1982, p. 815

[68] S. Linderoth and I. K. MacKenzie, in: Positron Annihilation, Eds.: P.C. Jain, R.M. Singru, and K.P. Gopinathan, World Scientific Publ., Singapore 1985, p. 833

[69] F.H. Hsu, and C.S. Wu, Phys. Rev. Letters **18**, 889 (1967)

[70] I.K. MacKenzie and B.T.A. McKee, Appl. Phys. **10**, 245 (1976)

[71] C.P. Slichter: Principles of Magnetic Resonance, Springer-Verlag, Berlin 1978

[72] J. Chappert and R.I. Grynzspan, Eds.: Muons and Pions in Materials Research, North Holland Publ. Co., Amsterdam 1984

[73] A. Schenck: Myon Spin Rotation Spectroscopy, A. Hilger Ltd., Bristol and Boston 1985

[74] A. Seeger, J. Major, and F. Banhart, phys. stat. sol. (a) **102**, 91 (1987)

[75] F. Banhart, J. Major, and A. Seeger in: Positron Annihilation, Eds.: L. Dorikens-Vanpraet, M. Dorikens, and D. Segers, World Scientific Publ., Singapore 1989, p. 281

[76] S.S. Hanna and R.S. Preston, Phys. Rev. **106**, 1363 (1957)

[77] R. Blank, L. Schimmele, and A. Seeger in: Positron Annihilation, Eds.: L. Dorikens-Vanpraet, M. Dorikens, and D. Segers, World Scientific Publ., Singapore 1989, p.278

[78] L.A. Page and M Heinberg, Phys. Rev. **106**, 1220 (1957)

[79] A. Dupasquier, in: Positrons in Solids, Ed.: P. Hautojärvi, Springer-Verlag Berlin 1979, p. 197

[80] D. Herlach and F. Heinrich, Helv. Phys. Acta **45**, 10 (1972)

Helvetica Physica Acta
Vol. 63 (1990)
0018-0238/90/040429-06$1.50+0.20/0

The Laboratory Positron Beam in Helsinki: Applications to Positron Dynamics in Solids

P. Hautojärvi and H. Huomo
Laboratory of Physics
Helsinki University of Technology
02150 Espoo, Finland

Abstract: We report experiences on a laboratory positron beam based on positron-active isotopes. Measured quantities, count rates and times are discussed. We also show applications of the beam on positron diffusion, mobility and defect profiling experiments.

1. Introduction

The development in the slow positron beam techniques has been very rapid (for a review see [1]). There are now several feasible plans for high intensity (>10^8 e^+/sec) positron beams as described elsewhere in these proceedings.

In parallel with the trend towards intense multiuser beam facilities there exists an increasing demand for simple, versatile and low-cost laboratory beams based on long-living positron active isotopes. For most experiments e.g. applications to defect studies, positron intensities of 10^5 e^+/sec are already sufficient. Also the effective use of future high-intensity beams requires that more groups have their own beams for preliminary tests and experiments.

In this paper we report experiences on the isotope-based laboratory beam in Helsinki. We give also a brief account to some experiments which are feasible with this type of positron beams.

2. The Positron Beam

Our laboratory beam became operational in 1984 [2]. It has been designed for surface and positron physics experiments. It is an all-metal system with oil-free ultra high vacuum ($p < 10^{-10}$ mbar) pumps. The beam is magnetically guided. The moderated positrons are extracted electrostatically and the non-moderated positrons are excluded by an ExB filter. The beam energy can be varied from 0 eV to 30 keV with an electrostatic accelerator.

The initial positron source was Co-58 electro-deposited onto a tungsten single crystal needle. The moderator was a W(110) single crystal in a back-scattering geometry. This source-moderator assembly had a moderation efficiency up to $3x10^{-3}$. Intensities of 10^6 -10^7 e^+/sec were easily obtained with a 100-500 mCi Co-58 source. Main disadvantages of this

arrangement were the short lifetime of Co-58 isotope (71 days) and the necessity of UHV for the W(110) moderator. In 1989 we had to give up this technique, as the supplier failed to prepare the special Co-58 sources for us.

Now we are using a 50 mCi Na-22 source prepared by the technique described elsewhere [3]. The transmission moderator is a 7000 Å thick W(100) foil obtained from Åarhus University. Initially the foil was annealed 15 min at 2000°C in $1x10^{-8}$ torr vacuum. The foil is exposed to air during mounting, which decreases the efficiency by about 20%. The present beam intensity is $1.5x10^5$ e^+/sec corresponding to the moderation efficiency of about $3x10^{-4}$. Reference [4] contains more information on thin film moderator preparation and characterization.

3. Experimental Quantities and Counting Rates

In most experiments the annihilation radiation from the sample is monitored as a function of the positron beam energy. Our detector is a HPGe with 35% efficiency. It is placed 4 cm away from the sample. In the following we give some typical counting rates and times based on a beam intensity of 10^6 e^+/sec.

(i) ***Positronium emission*** from the sample surface to vacuum is measured by $3\gamma/2\gamma$ ratio. Typically about 10^5 counts are collected to the annihilation peak in 30 sec. A whole Ps fraction curve $F_{Ps}(E)$ takes 0.5 h.

(ii) ***Positron re-emission spectrum*** is measured at a fixed incident energy E by observing the annihilation rate as a function of the grid bias V_g placed in front of the sample. A typical counting time for the re-emission spectrum $f(V_g)$ is 0.5 h.

(iii) ***Doppler broadening*** is the slowest to measure. We collect $2x10^6$ counts to the 511 keV peak to get the lineshape parameter S accurately enough. The counting rate of the Ge detector is limited to 10-20 kHz not to deteriorate the resolution. The 3 min time per a point is needed and the whole S(E) curve takes 2 h.

We see that at 10^6 e^+/sec in 0.5-2 h a whole curve $F_{Ps}(E)$, $f(V_g)$ or S(E) is measured. These data accumulation rates are much higher than in the bulk experiments with unmoderated positrons, where typical counting time for a lifetime spectrum or Doppler broadening takes several hours. Thus positron beam intensities around 10^5 and even 10^4 e^+/sec are still sufficient for most experiments described below.

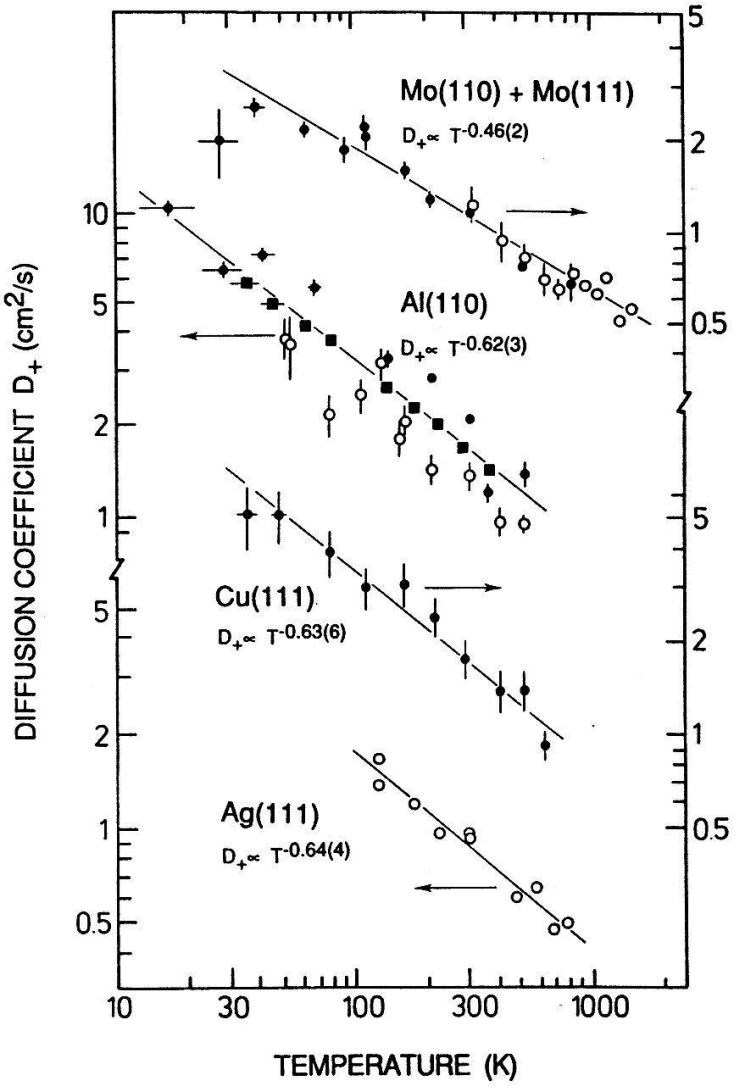

Fig. 1. The temperature dependence of positron diffusion coefficient in various metals. Open symbols indicate Ps fraction measurements and filled ones Doppler broadening measurements. From ref. [6]

4. Applications to Positron Dynamics in Solids

4.1 Positron Diffusion in metals

Positron diffusion coefficient is measured by observing the fraction of positrons returning back to the sample surface after implantation. The back-diffused fraction is determined either from Ps emission or Doppler broadening as a function of the positron implantation energy. The first parameter is faster to measure, but it requires a clean and stable surface i.e. UHV. In addition, great care must be taken to subtract properly the contribution of non-thermalized Ps which is significant at low (<5 keV) incident energies [5]. Doppler broadening measurements requires that Ps emission does not occur (dirty sample surface). Sometimes the surface S-parameter is rather close to the bulk one, which makes the analysis less accurate.

Fig. 1 shows our experimental results in several metals as function of temperature [6]. The results are in agreement with the theoretical prediction $D \propto T^{-1/2}$ due to positron scattering by acoustic phonons.

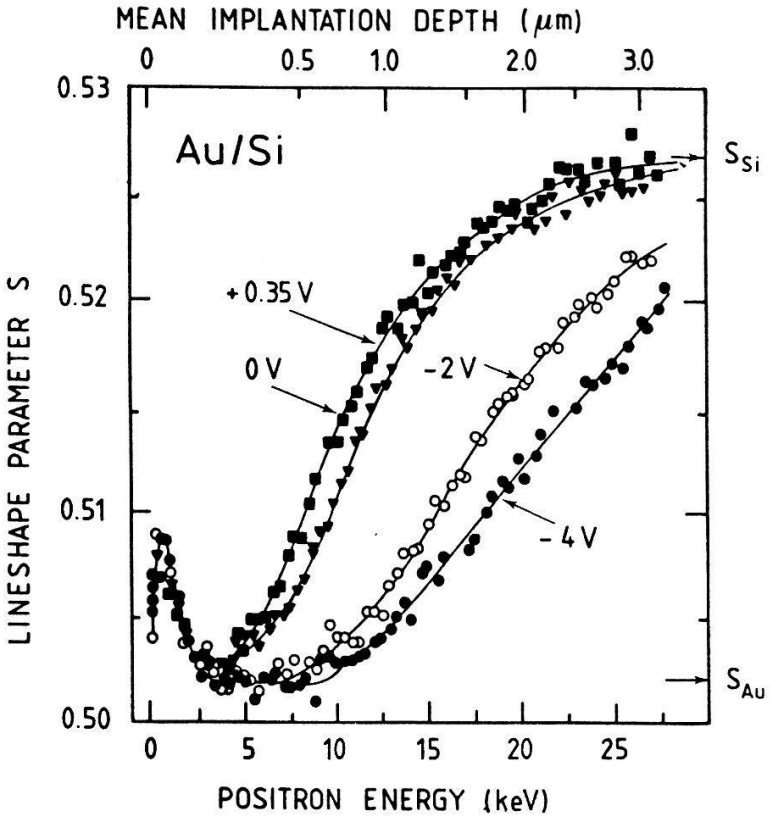

Fig. 2. The lineshape S-parameter as a function of positron incident energy for various bias voltages of the Au/Si Schottky diode. From ref. [7].

4.2 Positron Mobility in Si

Positron mobility was measured by implanting positrons into the depleted layer of a 100 Å Au/n-Si (P: 7.4 x 10^{14} cm^{-3}) Schottky diode [7]. Changing the diode bias the electric field strength and depletion depth could be varied from 10 to 30 kV/cm and from 1 to 3 μm, respectively.

At small incident positron energies (E<4 keV) the lineshape parameter S does not depend on the bias voltage, as the positrons are implanted into the Au overlayer. At higher energies (E>5 keV) the S-parameter depends strongly on the bias, i.e. on the electric field strength.The value of the S-parameter is a superposition of the Au and Si bulk S-parameters . At high negative bias the field is seen to pull positrons towards the Au layer.

The analysis of the data with drift-diffusion equation gives a value μ_+=120±10 cm^2/Vs, which corresponds to a diffusion coefficient D_+=3.0±0.2 cm^2 s^{-1}. During its mean life of 220 ps a positron in Si may drift several micrometers, i.e. distances which are 10 times longer than the thermal diffusion lenght. Long drift lengths under electric field open possibilities to new types of positron moderators.

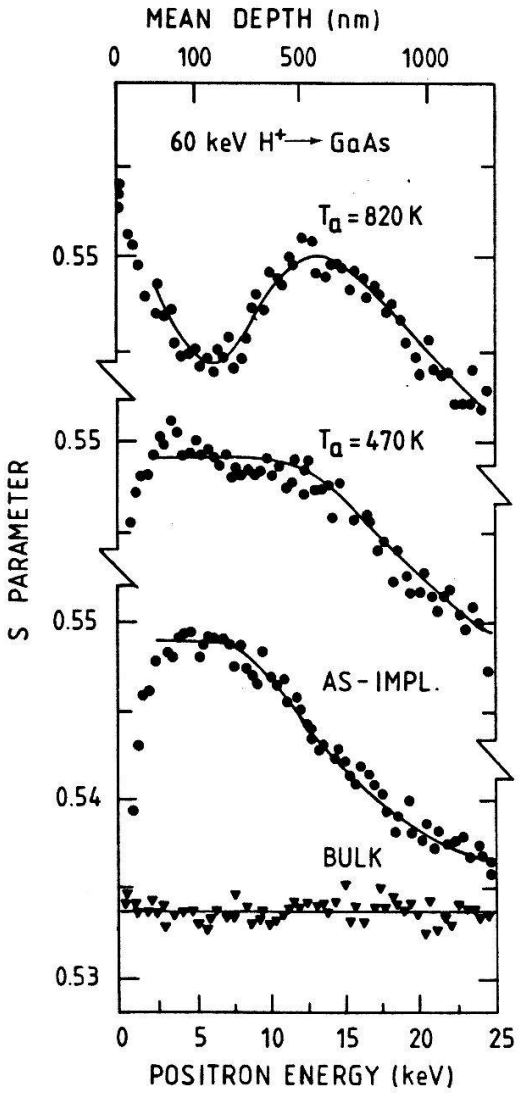

Fig. 3. Lineshape S-parameter as a function of positron incident energy in 60 keV H^+ implanted GaAs. From ref. [8].

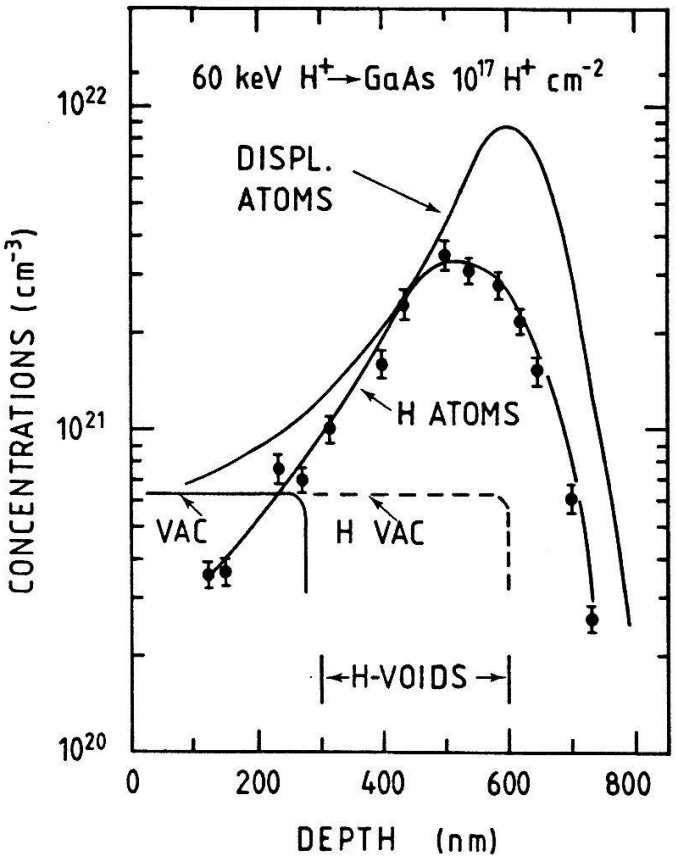

Fig.4. Depth profiles of vacancy defects in H^+ implanted GaAs compared to those of displaced atoms and hydrogen atoms. From ref. [8].

4.3 Defect Profiling

As an example of a defect study in near-surface region we consider semi-insulating GaAs implanted with 10^{17} 60 keV H^+ ions cm^{-2} [8]. Fig. 3 shows the S-parameter measured before and after implantation and after annealing treatments . In presence of vacancy defects the value of S is known to increase. This is easily seen in comparing the bulk and as-implanted curves. The plateau in the as-implanted curve is attributed to saturation trapping of positrons resulting the defect-characteristic value S_{def}. The ratio S_{def}/S_{bulk} is 1.028 showing that these defects are monovacancies. In SI-GaAs material As vacancies are positive and Ga vacancies negative. Thus we identify the positron traps as Ga vacancies.

In the near-surface region the lineshape S-parameter is a superposition of

annihilations in the surface, in the defects, and in the bulk. To calculate the fractions of positrons at various states the diffusion-annihilation equation is used. The defect profile is varied until a satisfactory fit with the calculated S(E) curve to the experiments is obtained [9].

Fig. 4 shows profiles of the H atoms obtained by nuclear resonance broadening (NRB), displaced atoms obtained by Rutherford back-scattering and vacancy defects obtained by positron beam [9]. The results on vacancy defects are understood in such a way that after implantation the vacancies between 300 and 600 nm are filled with H atoms. They become effective traps for positrons only after 470 K annealing, which is seen in Fig. 3 as the broadening of the plateau of the T_a=470 K curve compared to the as-implanted curve. The H-void complexes appear after annealing at higher temperatures. In the S(E) curve they are seen as a bump around 15 keV.

5. Conclusions

Positron motion and trapping is well understood in metals. Recently, much progress, both theoretical and experimental, has been made in these problems in semiconductors. We are reaching the state where positron beams can be applied e.g. to defect studies in near-surface regions, thin films and overlayer. For many application, only a rather modest beam capable to measure Doppler broadening vs. incident energy with intensity around 10^5 e^+/sec is sufficient.

References

1. P.J. Schultz and K.G. Lynn, *Rev. Mod. Phys.* **60**, 701 (1988).
2. J. Lahtinen, A. Vehanen, H. Huomo, J. Mäkinen, P. Huttunen, K. Rytsölä, M. Bentzon, and P. Hautojärvi, *Nucl. Instr. and Meth.* **B17**, 73 (1986).
3. H. Huomo, R. Jones, J. Hurst, A. Vehanen, J. Throwe, S.G. Usmar and K.G. Lynn, *Nucl. Instr. and Meth.* **A284**, 359 (1989).
4. E. Gramsh, J. Throwe and K.G. Lynn, *Appl. Phys. Lett.* **51**, 1862 (1987).
5. H. Huomo, E. Soininen, and A. Vehanen, *Appl. Phys. A* **49**, 647 (1989).
6. E. Soininen, H. Huomo, P.A. Huttunen, J. Mäkinen, A. Vehanen, and P. Hautojärvi, *Phys. Rev. B*, in press.
7. C. Corbel, P. Hautojärvi, J. Mäkinen, A. Vehanen, and D. Mathiot, *J. Phys.: Condens. Matter* **1**, 6315 (1989).
8. K. Saarinen, P. Hautojärvi, J. Mäkinen, A. Vehanen, J. Keinonen, E. Rauhala, J. Koponen, C. Corbel, *Proceedings of the International Conference on the Science and Technology of Defect Control in Semiconductors*, Yokohama 1989 (in press).
9. J. Keinonen, M. Hautala, E. Rauhala, V. Karttunen, A. Räisänen, J. Lahtinen, A. Vehanen, E. Punkka, and P. Hautojärvi, *Phys. Rev. B* **37**, 8269 (1988).

Helvetica Physica Acta
Vol. 63 (1990)

0018-0238/90/040435-07$1.50+0.20/0

POSSIBLE SOURCE TECHNIQUES AT PSI FOR SLOW POSITRON BEAMS

Ulrich Zimmermann
Paul Scherrer Institute, CH-5232 Villigen PSI

Abstract

The various techniques available at PSI for the primary source of a slow e^+-beam of high intensity are dicussed assuming conventional moderation. The final choice of a specific source technique depends upon the type of experiments the beam will be applied for and in some cases also upon the results of more detailed feasibility studies.

1 General Considerations

There are in principle two different ways to produce positrons, namely, by pair production or by β^+ decay. In both cases, the positrons typically have energies far above the value which is usually associated with "slow positrons" ($\sim$1eV). Therefore, it is necessary to slow the positrons down to the desired energy range. This is usually accomplished by stopping the high energy positrons in a solid with a negative positron work function such as W, Ni or solid Ne. In such a solid, the positrons are slowed down to thermal energies very rapidly compared to their lifetime in the solid. There is a certain probability that a positron, during its diffusive motion through the solid, moves back to the surface before annihilation with an electron of the solid occurs. Due to the negative work function, such positrons can escape from the solid into the vacuum with a final energy which corresponds roughly to the work function ($\sim$1eV) and with an energy spread according to the thermal motion ($\sim$0.1eV). A monochromatic positron beam of variable energy can then be formed by means of suitable magnetic or electrostatic fields. Unfortunately, this moderation procedure is a very inefficient way to slow the positrons down. This is due to the fact that the range of the fast positrons in the solid is much larger than the mean diffusion length of the positrons ($\sim$1000Å), i.e. most positrons annihilate with an electron of the solid before they can reach the surface.

A commonly used moderator is single crystal W(110). With carefully heat treated source and moderator and optimized extraction optics, a moderation efficiency of $\sim$0.3% has been achieved with good long-term stability [1]. The efficiency decreased slowly by a factor of 2 during 1 year of operation and was regained after heat treatment. Higher efficencies have been reported for solid Ne moderators (0.7%) [2]. A completely new technique is proposed at this workshop and will be treated in a separate contribution to this volume by D.Taqqu. Magnetic and electrostatic confinement of the e^+ together with a thin moderator is used in this method and efficiencies of $\geq$10% are quoted. In the present paper which deals with techniques available at PSI to produce primary β^+ sources of high intensity, conventional moderation is assumed for the estimation of the final slow positron beam intensity. $\epsilon=10^{-3}$ is assumed if not stated explicitly.

At this point it is important to note that the choice of a specific beam technique not only depends upon the intensity which can be reached but also depends upon other properties such as polarization and brightness. In principle, positrons from β-decay are

polarized, while those from pair production are not. However, for the production of a high intensity beam using β-decay sources the collection of the positrons at a large solid angle is required, i.e. a compromise has to be made between polarization, if desired, and intensity, depending upon the experiments for which the beam will be used.

Application of slow positrons to e^+-microbeams or to e^+-microscopy, on the other hand, implies small beam size and angular divergence as well as low spread in energy in addition to high intensity. These types of beam qualities can be discussed in terms of the brightness B of the beam (see the contribution to this volume by W.B.Waeber). To increase the brightness of a beam, remoderators are used [3] rather than collimation by appertures. These consist of one or more stages of acceleration to ~10keV followed by focussing the beam to moderators. In order to minimize the number of brightness enhancement stages, it is necessary to use primary beams of small diameter and low angular divergence. This implies small source size and moderators with low transversal energy E_T of the re-emitted positrons for high-brightness beams. In terms of E_T the brightness writes as $B=d^2E_T$, where d is the diameter of the beam. Often moderators with parallel W vanes are used together with electrostatic extraction parallel to the re-emitting surface. Such an arrangement results in large transversal energy since the positrons after re-emission, carry away the positron work function energy in a direction normal to the emitting surface. For W vanes, e.g. this gives E_T~2.5eV. If the moderator surface is oriented normal to the beam axis the transversal energy is E_T~kT, hence ideally two orders of magnitude lower than in the parallel geometry. High-brightness beams therefore require moderator arrangements with the extraction normal to the emitting surfaces.

From the preceding discussion it is evident that the choice of the way in which a slow positron beam is produced is highly dependent upon the kind of investigation intended. This holds for the methods to produce the fast positrons as well as the slowing down procedures and beam line considerations. In the present status of the project for a slow e^+-beam at PSI, the evaluation of possible applications is still in progress. It therefore appears not reasonable to restrict our discussion to only one specific solution for such a beam, but rather to evaluate the different possible techniques which could in principle be realized at PSI. This will be done in the following sections.

2 Facilities at PSI

2.1 SAPHIR Reactor

This facility is a 10MW swimming pool type light water reactor. It is presently used mainly as a neutron source for thermal neutron scattering experiments in crystal structure research, solid state physics and chemistry, biology etc. The fast neutron spectrum is used for radiation damage research in material science and technology (defects in metals and alloys, semiconductor conditioning, etc.). The production of isotopes using both thermal and fast neutrons and training of power reactor operators are further examples.

Among other isotopes, ^{64}Cu is produced routinely for applications in positron annihilation experiments (1D-ACAR) at PSI (formerly at ETH-Hönggerberg). These sources consist of 25μm copper sheets (~1cm^2) resulting in 1Ci ^{64}Cu after 12h irradiation at 8x10^{13}n/cm^{2}s which is the maximum available thermal neutron flux in the core of the

reactor. The maximum fast flux in the core is $10^{14}cm^{-2}s^{-1}$. It is somewhat lower at the core edge, and decreases rapidly outside the core.

The time schedule of the reactor operating sessions is such that approx. 3-4 weeks of operation at full power are usually followed by 1 week at low power for maintenance and education purposes. There are 2 longer shutdowns per year (3-4 weeks) partly also due to personnel considerations. During operation the stability of the neutron flux is excellent. The swimming pool type of construction brings about several advantages for irradiation experiments: ease of access, since not enclosed in a vessel, available space around the core, certain variability of in-core and core-edge irradiation positions.

2.2 Ring Accelerator

The proton cyclotron at PSI primarily produces a proton beam of 590MeV. Prior to injection into the high energy cyclotron, the protons are accelerated to 72MeV in an injector cyclotron. The beam current is at present $\sim 200\mu A$, and at least 1mA will be available after the 12 month shutdown during 1990. This great effort to increase the beam current was necessary mainly in order to facilitate a high flux spallation neutron source at PSI (SINQ) which is at present under construction. This intense neutron source will be available at the end of 1993 mainly for neutron scattering experiments using cold neutrons at an intensity comparable with ILL. The thermal neutron flux in the moderator tank will be comparable with SAPHIR ($10^{14}cm^{-2}s^{-1}$), but due to the lower accessibility (many m^3 of Fe) and the possible disturbance of the neutron flux for the scattering experiments, SAPHIR will certainly be superior to SINQ for isotope production with thermal neutrons. For nuclear reactions with epithermal or fast neutrons SAPHIR is expected to give the higher flux. There is, however, one possible advantage of SINQ over SAPHIR, namely in cases where high thermal but low fast neutron flux is desired. An example will be given in section 3.4.

The 590MeV pulsed beam extracted from the ring accelerator has a pulse repetition frequency of 50.7MHz and a pulse width of 1ns. The beam is used to simultaneously produce several secondary particle beams of pions, muons, neutrons and polarized protons at different targets. The final beam dump is used for the production of neutrons (SINQ) and is not available for isotope production. The injector cyclotron is already used for the production of β^+-emitters for application in positron emission tomography (PET) at PSI. For this purpose a $100\mu A$ beam of the 72MeV Injector II is split from the beam and guided to the isotope production area. Several gaseous and liquid targets have been developed together with chemical and physical isotope enrichment procedures in hot cells and radiopharmaceutical carrier compounds.

3 Possible Sources at PSI

3.1 Carbon-11

This isotope has 100% β-emission, and no γ's except 511keV are produced. Its half-life is 20.3min. and the β-spectrum has a maximum energy of 1MeV. It can be produced with protons according to the reaction

$$^{14}N(p,\alpha)^{11}C.$$

The cross section for this reaction [4] has a threshold at 5MeV. The resonance excitation function has a maximum of 280mb at 7MeV and the direct reaction has a relatively high tail at higher energies (~80mb at 15MeV). The thick target yield for 25MeV protons is 200Ci/mA. Thus, with the full 1mA proton beam at PSI Injector II and a moderation efficiency of 10^{-3}, theoretically, 0.75×10^{10} slow e^+/s can be obtained.

For PET applications at PSI, the 72MeV proton beam for ^{11}C production is reduced to 16MeV by means of a degrader [5]. The ^{14}N target consists of 15bar N_2 gas in a stainless steel bottle 18cm long. There is a steady gas flow through the target. The carbon produced reacts with traces of oxygen in the circuit to give CO_2. A cold trap in the circuit serves as a separator of the CO_2 from the N_2 carrier gas. With this existing circuit a source activity of a few Curies has already been obtained although normal operation for this application is at a much lower activity.

Due to ever present natural carbon in the circuit, the specific activity is much lower than the theoretically expected value of 9.2kCi/μmole. With the present equipment 50Ci/mmole is routinely obtained. For a 10Ci source on 1cm^2, e.g., this means that the source thickness would be 8.6mg/cm^2. Comparing this with the range ρ/μ=60mg/cm^2 for β^+ from ^{11}C, it is obvious that a continuously working $^{11}CO_2$ source of higher activity would need some effort to increase the specific activity. A continuously working source can be realized by placing a cold finger behind a β-thin window which separates the target circuit from the UHV e^+-moderator vessel. Pressure reduction from 15 to less than 1bar would probably be necessary in order to reduce the mechanical stress on the window and the β-absorption in the gas.

To summarize, we can state that with a N_2 target at a proton beam current of 100μA a slow e^+-beam intensity of $10^8 e^+/s$ can be expected using state-of-the-art techniques. The potential of the method is nearly two orders of magnitude higher. As to which extent this can be utilized, depends mainly upon the feasible beam current. This is limited by the heat transfer from the gas to the water cooled target bottle. Due to heating by stopping the protons the density of the gas is decreased in the path of the beam. To reduce this effect, the beam can be scanned or its diameter can be increased. Also, optimization of the degrader, the gas pressure, the dimensions of the target bottle, the N_2 flow and the water cooling will be indispensible in order to obtain a high intensity e^+-beam. One should however, keep in mind that the power dissipated by a 100μA/25MeV proton beam is 2.5kW. In addition, increasing the current to the full 1mA of Injector II would interrupt all other experiments at the ring accelerator. This would perhaps only be acceptable for short periods of time, say for 1h each day.

3.2 Fluorine-18

Similar to ^{11}C, this isotope is a 100% β^+-emitter, and it has no γ's except 511keV. The maximum β-energy is 0.6MeV and the half-life is 110min. It is produced according to

$$^{18}O(p,n)^{18}F$$

using liquid ^{18}O enriched water targets [6]-[9]. ^{18}O enriched water is commercially available but very expensive (~100$/g). It is now also produced at PSI for PET applications. The cross section for the above (p,n) reaction is similar to that of ^{14}N but with narrower resonances and lower tail at high energy [10]. The thick target yield for 15MeV protons

is 180Ci/mA, thus close to the result for ^{11}C. The problems connected with the power dissipated by the beam at high current seem to be more worse for liquid targets than for gas targets. This comes from the formation of gas bubbles in the liquid due to local boiling and radiolytic decomposition. Vogt et al. [8] in their experiments observed a linear decrease of the ^{18}F yield by a factor of 2 on going from 20 to 40μA beam current.

Using state-of-the-art techniques, practical yields would result in $\sim 10^8$ slow e^+/s for this reaction as was the case for ^{11}C. On the other hand, high specific activities seem to be possible (50Ci/μmole [9]). Losses due to self absorption are therefore less important. However, the separation from the liquid target and the deposition of ^{18}F in a continuous way is more difficult than in the case of $^{11}CO_2/^{14}N$. Operation in a batch mode is therefore the more probable solution.

3.3 Cobalt-58

As an alternative to ^{64}Cu (see chapter 2.1), the SAPHIR reactor can be used to produce ^{58}Co according to the reaction

$$^{58}Ni(n,p)^{58}Co.$$

At PSI, a wet chemical procedure was developed to separate ^{52}Fe from Ni [5]. It is believed that a similar technique can be used to separate ^{58}Co from Ni. Using the cross section of 113mb [11] and the fast flux at SAPHIR, one obtaines 1Ci^{58}Co/g Ni after 70 days of irradiation or 150mCiβ^+/g Ni (branching ratio: 15%β^+), i.e. a few kg of Ni would be necessary to irradiate in the reactor and to chemically separate in order to produce $\sim 10^{10}$slow e^+/s with conventional moderators. This large amount of Ni and the relatively high γ background makes ^{58}Co an unattractive isotope for intense e^+-beams. It may, however, be useful for lower e^+-intensities ($10^8 e^+/s$) if ^{22}Na or ^{64}Cu can not be used. The situation is also more attractive for a high flux reactor. It is planned to make some test runs at PSI in 1990 to produce ^{58}Co. During irradiation in the reactor, shielding of the thermal neutron flux by Cd is necessary in order to suppress the concomitant reaction $^{58}Co(n,\gamma)^{59}Co$(stable) [11].

3.4 Pair Production Using γ's from Cd(n,γ)

If Cd is placed in a thermal neutron flux, a very strong γ-source can be obtained from the prompt γ's of the reaction $^{113}Cd(n,\gamma)^{114}Cd$ (σ=20000b for thermal n-spectra of light water reactors [11]). These γ's, having energies up to 6MeV, can be used for pair production. Such an e^+-source was proposed for the high flux reactor at ILL/Grenoble (see the contribution to this volume by W.Triftshäuser). One problem of this method is that the moderator must be placed close to the Cd-target. If an in-core position is chosen at SAPHIR, the high flux of fast neutrons would cause a high radiation damage rate in the moderator material and a corresponding decrease in moderation efficiency. Frequent heat treatments would therefore be necessary or even permanent operation at high temperature ($\sim$2000°C for W) which would also decrease the moderation efficiency. The ILL e^+-source will be at a position of much lower fast n-flux. This is not feasible at SAPHIR.

Another possibility at PSI will be SINQ. At present it is being investigated whether there is an accessible position in the moderator tank of SINQ with high thermal flux

($10^{14}cm^{-2}s^{-1}$) and sufficiently low fast flux. At such a position, a Cd-tube of 2cm diameter, 20cm long and with a wall thickness of 0.1mm, surrounded by a W-tube with 0.25mm wall thickness for pair production/moderation would yield $6x10^{13}\beta^+/s$. Additional concentric W-tubes can help to increase this yield. An axial electrostatic field is needed in order to extract the slow e^+ from the arrangement. This can be accomplished by dividing the tubes into several longitudinal sections and applying a voltage to each section. The relative large volume of such a source, limits the application for high brightness beams.

3.5 Electro-Production

There are efforts at PSI for the installation of an e^+/e^--collider storage ring operating at a lower energy than LEP at CERN, but at a higher current. Besides the interesting features of such a machine for experiments in elementary particle physics, it would also provide usful tools for other scientific fields, e.g. synchrotron radiation for investigations in solid state physics and surface science. Since the positrons for these machines will be produced by means of an e^--Linac using bremsstrahlung and pair production in a target, it would be possible to use this Linac also as a source for slow e^+. Such a combined use would be economical because the Linac is needed only during short periods of time to load the storage ring. For the time between these periods (several hours) the Linac would be available for other applications.

In a recent study (B-factory) [12], a 200MeV Linac was proposed for e^+-production with an averaged e^--current of 1.5μA ($1.9x10^{11}e^-/s$, 12ns pulse length, 50pulses/s). Assuming the highest reported conversion efficiency of $8x10^{-6}e^+/e^-$ [13], a slow e^+-intensity of $8x10^7s^{-1}$ can be expected. It follows that an increase of the beam current to ~200μA would be necessary in order to reach 10^{10} slow e^+/s which is believed to be the limit of this technique set by thermal power dissipation in the target [13]. Such high intensity e^+-beams based on dedicated Linacs are planned in different laboratories (see the contribution of S.Tanigawa in this volume and ref. [13] and the references given therein).

4 Conclusions

Pair production seems to be the most promising method if 10^{10}slow e^+/s are desired, provided that a suitable position in the SINQ moderator tank will be available or the current of the Linac for the planned meson factory can be increased to 200μA. Proton induced β^+-emitters such as ^{11}C or ^{18}F are limited by the available beam current of 100μA at Injector II and by power dissipation in the targets at higher currents. However, this type of sources as well as ^{58}Co produced at SAPHIR would be useful for laboratory based beams of lower intensity ($10^8e^+/s$).

Acknowledgements: I wish to acknowledge R.Weinreich, H.-H.Braun and F.Hegedues for many suggestions and detailed informations. I am also indebted to M.Peter, A.Manuel, W.B.Waeber and K.Ghazi Wakili for helpful comments and discussions.

References

[1] J.Lahtinen, A.Vehanen, H.Huomo, J.Mäkinen, P.Huttunen, K.Rytsölä, M.Bentzon and P.Hautojärvi, Nucl. Instr. Meth. Phys. Research B17 (1986), 73

[2] A.P.Mills,Jr. and E.M.Gullikson, Appl. Phys. 49 (1986), 1121

[3] A.P.Mills,Jr., Appl. Phys. 23 (1980), 189

[4] V.R.Casella, D.R.Christman, T.Ido and P.Wolf, Radiochimica Acta 25 (1978), 17

[5] R.Weinreich, private communication

[6] I.Huszár and R.Weinreich, J. Radioanal. Nucl. Chem., Letters 93 (1985), 349

[7] C.Vandecasteele and K.Strijckmans, Nucl. Instr. Methods Phys. Res. A236 (1985), 558

[8] M.Vogt, I.Huszár, M.Argentini, H.Oehninger and R.Weinreich, Appl. Radiat. Isot. 37 (1986), 448

[9] R.Iwata, T.Ido, F.Brady, T.Takahashi and A.Ujie, Appl. Radiat. Isot. 38 (1987), 979

[10] T.J.Ruth and A.P.Wolf, Radiochimica Acta 26 (1979), 21

[11] G.Erdtmann: Neutron activation tables, Weinheim, New York: Verlag Chemie (1976)

[12] H.-H.Braun, private communication

[13] J.Dahm, R.Ley, K.D.Niebling, R.Schwarz and G.Werth, Hyperfine Interactions 44 (1988), 151

Helvetica Physica Acta
Vol. 63 (1990)
0018-0238/90/040442-06$1.50+0.20/0

HIGH EFFICIENCY POSITRON MODERATION

D. Taqqu
Paul Scherrer Institute, CH-5232 Villigen PSI, Switzerland

ABSTRACT

A new positron moderation scheme is proposed. It makes use of electric and magnetic fields to confine the β^+ emitted by a radioactive source forcing them to slow down within a thin foil. A specific arrangement is described where an intermediary slowed-down beam of energy below 10 keV is produced. By directing it towards a standard moderator optimal conversion into slow positrons is achieved. This scheme is best applied to short lived β^+ emitters for which a 25% moderation efficiency can be reached. Within the state of the art technology a slow positron source intensity exceeding $2 \cdot 10^{10}\ e^+/sec$ is achievable.

1. INTRODUCTION

With the steady increase of interest in the applications of slow positron beams, various schemes have been proposed in order to produce beams of high intensity ($> 10^{10}\ e^+/sec$) [1]. In this paper, a method is presented where the high intensity is achieved by optimizing the conversion of the β^+ emitted from a radioactive source into slow positrons. The basic idea is to collect most of the β^+ emitted by the source and slow them down to quite low energy before directing them onto the moderator. In this way no positron can enter very deep into the moderator thereby minimizing the moderation losses.

The main features of the method are:

1. The β^+ source is deposited as a thin layer on a thin foil so that almost all positrons escape from it.

2. Confining fields force the high energy positrons to return towards the foil and slow down in it.

3. Just before the positrons have slowed down to energies at which they may stop in the foil, they are moved out from the slowing down path and directed towards a moderator operated in the back reflection mode.

4. The slow positrons emitted by the moderator are extracted from the confining field to form a standard slow positron beam.

The basic principles underlying these various steps are described in the next two paragraphs. The achievable moderation efficiency and beam intensity are discussed in the last paragraph.

2. CONFINEMENT

The source is deposited on the center of a thin foil over a diameter d_s. The foil is placed on the axis of a high field solenoid (at field B_o) perpendicular to it. The emitted positrons follow spiralling trajectories around the field lines so that they remain transversally confined within a diameter d which exceeds d_s by about twice the cyclotron radius

of the highest energy positrons.

To this transverse confinement, a first longitudinal confining configuration is added by increasing the axial field on both sides of the foil to a maximal value B_m. This introduces a mirror action [2] so that all positrons emitted with an angle to the axis greater than

$$\theta_c = arc\ sin\ \sqrt{B_o/B_m} \tag{1}$$

are reflected back to the foil and slow down into it. Such a magnetic bottle configuration is an efficient energy independent confining device, but only as long as multiple scattering effects that inevitably accompany the slowing down do not move the reemission angle to $\theta < \theta_c$. The so-called escape cone ($\theta < \theta_c$) is reached diffusively and the positrons will flow out from the magnetic bottle slowly at high energy and increasingly faster as they decellerate towards the lowest energies.

In order to conserve optimal longitudinal confinement at lower energies, another kind of reflection element is added in the form of a positive electrostatic column at both extremities of the solenoidal field (at $B = B_r$). This end cap, made of a serie of ring electrodes connected via a resistive voltage divider to a high voltage supply V_r, form an electrostatic mirror for positrons emitted from the foil with energy

$$E < \frac{eV_r}{1 - sin^2\theta \cdot B_r/B_o} \tag{2}$$

so that all positrons slowed down to $E < eV_r$ will be reflected.

Use of a high voltage parallel to a B field may require special measures to inhibit discharges but as a 100 kV HV has already been routinely used [3] it can be anticipated that the 100-200 kV positive HV range should be easily achievable. Under these conditions, both magnetic and electrostatic mirrors contribute in a complementary way to obtain a high confinement efficiency.

3. MODERATION AND EXTRACTION

As a result of confinement and because of the possibility of using very thin source foils, positrons of 5-10 keV kinetic energy are still able to travel back and forth between foil crossings. This is an energy range for which high conversion efficiency to slow positrons have been measured. Best results have been obtained for the solid neon moderator in the back reflection mode [4]. This moderator has also a re-emission probability distribution for slow positrons which is optimally suited to the present extraction scheme so that it will be adopted as the element on which the slowed-down positrons will be directed after having been moved away from the slowing-down path.

The specific problem to be solved is how to achieve a selective displacement of the low energy positrons with the simultaneous requirement that the operation takes place without affecting the slow-down of the higher energy positrons. The solution proposed here, together with the procedure used for the extraction of the slow positron beam, will be described with reference to Fig. 1 which shows the overall system in a schematic form together with the field distributions and some beam trajectories.

Between the two HV end caps, one has on the left side the magnetic bottle with the source placed at its centre and the moderator close to it slightly moved downwards. On

the right side a long solenoid operated at a field $B' \ll B_o$ contains longitudinal electrodes (E1 to E5) in which the positrons will be subjected to various electric fields. These fields are made to vary sufficiently slowly to ensure a high degree of adiabaticity in the change of transverse momentum.

A first requirement, the full transparency of the right magnetic mirror to low energy positrons, is achieved by placing the foil at a positive potential relative to that of a cyclindrical electrode that extends over the region of increased magnetic field. With ΔV being this potential difference (ΔV equals the foil potential V_o in the configuration of Fig. 1) the positrons exiting from the foil are longitudinally accelerated and the reflection condition (1) is modified to an expression similar to (2):

$$E > \frac{-e\Delta V}{1 - sin^2\theta \; B_m/B_o} \tag{3}$$

or

$$\theta > arc\, sin \sqrt{(B_o/B_m)(1 + e\Delta V/E)} \quad . \tag{3'}$$

This ensures the passage of all positrons emitted with an energy below the selected cut-off energy:

$$E_c = e\Delta V/(B_m/B_o - 1) \quad . \tag{4}$$

These positrons, together with many others of much higher energy, exit the magnetic bottle and enter the B' field region with $\theta < arcsin \sqrt{B'/B_o}$ [2]. By using $B' \ll B_o$ the longitudinal velocity $v_{||}$ is very close to the particle velocity.

As the positrons pass between the first set of vertical electrodes (E1), they are subjected to an horizontal electric field E, drift downwards with a velocity E/B' and exit this field region of length ℓ displaced downwards by

$$d' = \frac{1}{v_{||}B'} \int_o^\ell E dz \quad .$$

The next set of electrodes (E2) with a maximal positive voltage V' at the middle have the special task to separate between the higher energy positrons that pass it, get reflected by the HV mirror and return toward the source foil whereas those with energy below the cut-off energy E_c (which equals here $e(V' - V_o)$) are returned towards the moderator.

The positrons that pass E2 continue their path towards the HV end cap. On their way, they transverse drifts in the three other directions (upwards, right and left) of the same amount as the initial downwards drift. Full drift compensation is achieved in this way for positrons initially centered on (or spiralling around) the magnetic field axis. For off-axis trajectories, the well known $\vec{E} \times \vec{B}$ drift inhomogeneity effect [5] cumulates in the present configuration into a slow rotation (by an angle $\sim 1/v_{||}^2$ for each pass) around the axis.

Positrons slowed down to a kinetic energy smaller than E_c will not pass the V' potential hill in E2 and are reflected back into E1 thereby increasing their downward drift to $2d'$. They then return into the centre of the magnetic bottle displaced downwards by $d_o = 2d'\sqrt{B'/B_o}$.

With d' sufficiently high to ensure that d_o is greater than the slowing down beam diameter d (at B_o), complete separation is achieved and the moderator can be placed with its upper edge at a distance $d/2$ from the magnetic axis so that all returning positrons impinge on it. This takes place with an angular distribution that extends from 0° to 90°, so that an appreciable part of these positrons will backscatter before full moderation is achieved. Together with the re-emitted slow positrons they return into the B' field region, get reflected at E2 and return toward the moderator, displaced further downwards by about d. A slight increase of the moderator potential in the downward direction (by less than 1V per d) is introduced so that the lowest energy positrons (whose re-emission probability in solid neon is significantly less than 100% according to Fig. 1 of ref. [4]) will not reach the moderator. The higher energy positrons reimpinge the moderator and get re-emitted with a further reduced energy distribution. By allowing this downward drift and remoderation to repeat itself a few times a highly efficient conversion into slow positrons of a few eV energy width is achieved.

The trapping and downward drift of the slow positrons between moderator and E2 terminates when the positrons reach a special downward extension of E2 in which V' is reduced to $V'' < V_o$. Positron reflection is thereby inhibited and a beam with width of the order of $d\sqrt{B_o/B'}$ is formed, passes below the HV end cap and exits the solenoid via a magnetic guide where the field B is made to decrease slowly to a very low value. Beam size increases thereby like $1/\sqrt{B}$ but divergence decreases by the same amount leaving the beam brightness constant [2]. As most experiments or remoderation stages require a prior beam extraction into a field-free region, it is necessary to correct for the angular momentum resulting from the axial magnetic field (Busch theorem, see for example ref. [6]). This will be done in a low field solenoid by imparting to the positrons the Larmor transverse angular velocity $eB/2m$ in such a way that a beam focus is achieved on the solenoid axis. This operation, which will be described in more details elsewhere [7], should be achievable without important intensity losses and without great increase in beam emittance. Thereafter the beam exits the solenoid with a final emittance only slightly worse than that of a standard slow positron beam emitted from a 1 cm^2 moderator.

4. AN INTENSE SLOW POSITRON SOURCE

Application of this high moderation efficiency scheme to the realisation of a high intensity slow positron source is made possible by the availability of strong positron sources with high specific activity. The optimal source material appears to be ^{18}F from which, according to ref. [8], .06 $\mu mole$ can be produced at a specific activity of 50 Curies/$\mu mole$ in a few hours irradiation of a $H_2^{18}O$ target with 20 μA of a 20 MeV proton beam. By depositing $Li^{18}F$ over 4 mm diameter on a thin 5 $\mu g/cm^2$ self supported carbon foil, a 3 curies source foil with 17 $\mu g/cm^2$ is obtained. For an axial field of $B_o = 3\ T$ the emitted β^+ remain transversally confined during slowing down within a diameter $d \sim 6$ mm (at $B = B_o$). Averaging the foil thickness over the beam diameter d results in an average $t \sim 12\ \mu g/cm^2$ which is significantly less than the average range of a 5 keV positron for any angle of incidence [9]. The positron losses in the source foil can be estimated by computing the probability (averaged over the incident angular distribution) for a positron with energy $E > E_c$ to stop in a foil of thickness $2t$ instead of exiting (either by backscat-

tering or by transmission) with an energy less than E_c. This source of positron losses falls rapidly with the increase of E_c. On the other hand, optimal conversion efficiency in the moderator requires minimizing E_c. The optimal value of E_c for the source and moderator considered here can be estimated to be between 5 keV and 10 keV. It should result in an efficiency of converting the confined positrons into slow positrons of the order of 50%.

The other relevant efficiency factor, the confinement efficiency, depends on B_m/B_o, V_R and the source properties (end energy and Z). A gross estimate for the $Li^{18}F$ source, $B_m/B_o = 3$ and $V_R = 200$ kV gives a result significantly greater than 50%.

Taking into account some other small losses, a resulting overall conversion efficiency of the order of 25% can be expected.

The development of the proposed scheme will lead to the possibility of realizing a slow positron source of about $2{\cdot}10^{10}$ e^+/sec intensity at most common cyclotrons. The required β^+ source production system which has been routinely in use for many years [10], does not appear to have reached a fundamental intensity limitation of any kind. It can therefore be anticipated that a significant increase in proton beam current will result in an almost proportional increase in both absolute and specific source activity so that the present method could lead to the achievement, in a not too distant future, of a slow positron beam with intensities in the range of 10^{11} e^+/sec.

References

[1] See for example the various contributions to this workshop in the present issue.

[2] See for example J.D. Jackson, Classical Electrodynamics, chapt. 12, John Wiley & Sons, 1962.

[3] See for example K.G. Lynn, B. Nielsen and J.H. Quaterman, Appl. Phys. Lett. **47** (1985) 239.

[4] A.P. Mills Jr. and E.M. Gullikson, Appl. Phys. Lett. **49** (1986) 1121.

[5] S.M. Hutchins, P.G. Coleman, A. Alam and R.N. West, in Positron Annihilation, edited by P.C. Jaim et al., 1985 Word Scientific Publ. Co., Singapore.

[6] J.D. Lawson, The Physics of Charged Particle Beams, p. 16, Clarendon press, Oxford 1977.

[7] D. Taqqu, to be published.

[8] R. Iwata et al., Appl. Radiat. Isot. **38** (1987) 979.

[9] S. Volkealakti and R.M. Niemenen, Appl. Phys. **A32** (1983) 95 and Appl. Phys. **A35** (1984) 51.

[10] R. Iwata, pivate communication.

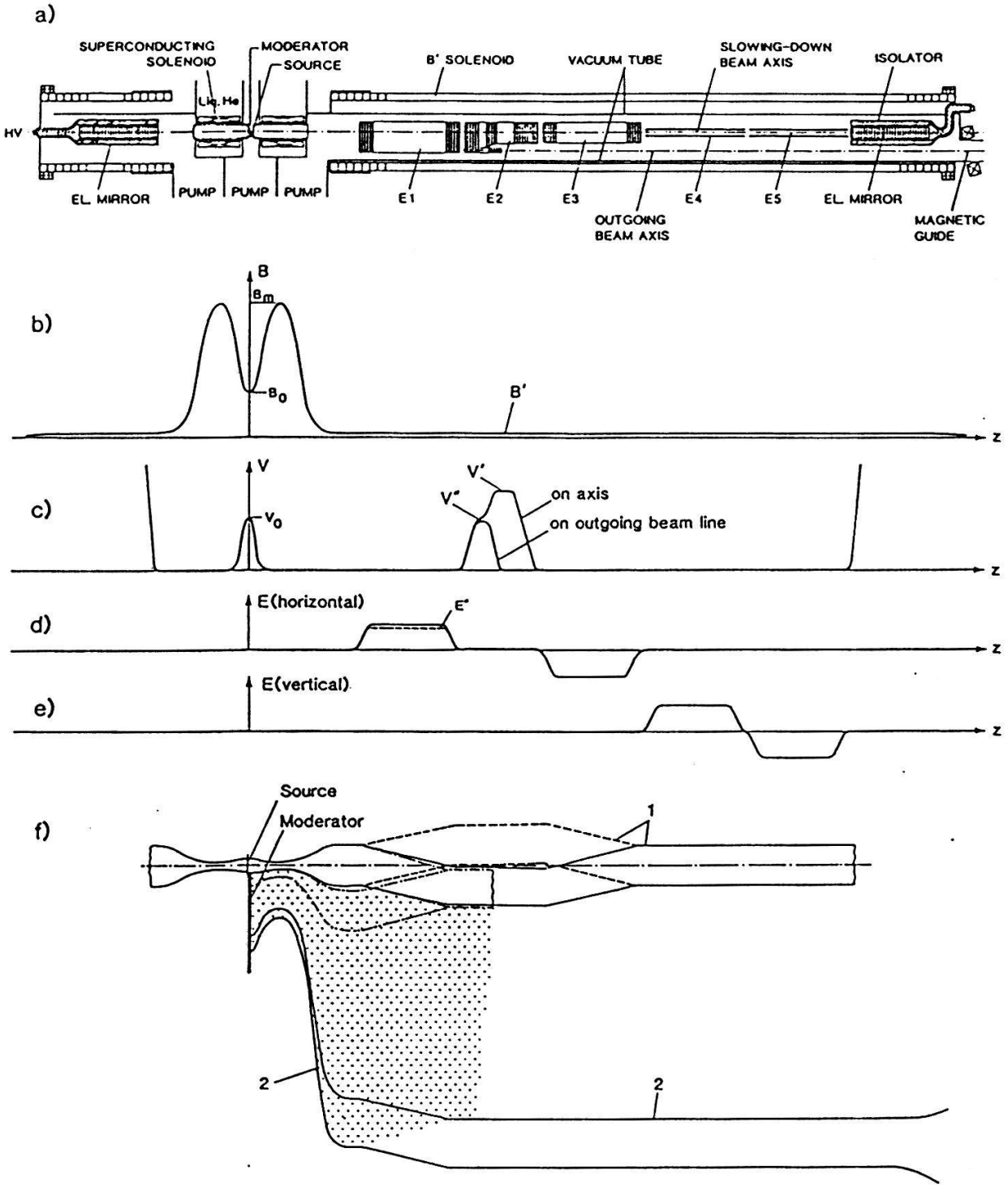

Figure 1:
a) *Schematic overall arrangement showing the main components.*
b) *Longitudinal magnetic field distribution.*
c) *Axial electric potential. In E2, the distribution along the extraction path (with V'' maximal potential) differs from that on the slowing down path.*
d) *Horizontal transverse electric field (E'' on extraction path).*
e) *Vertical transverse electric field.*
f) *Various beam envelopes drawn with vertical scale increased by a factor of 20.* —— *(1) Leftward slowing-down beam emitted at E slightly greater than* E_c. - - - *(1) Same beam rightward* -.-.- *Left bound beam envelope after* $E < E_c$. -..-..- *Same after reflection from E2. Shaded area: region of downward movement of backscattered and slow positrons trapped between E2 and moderator.* —— *(2) Exiting slow positron beam.*

Helvetica Physica Acta
Vol. 63 (1990)

0018-0238/90/040448-10$1.50+0.20/0

POSITRON MICROSCOPY, A POSSIBLE NEW EXPERIMENT AT PSI

W.B. Waeber

Paul Scherrer Institute, CH–5232 Villigen PSI

ABSTRACT The state of the art of positron microscopy is reviewed in this paper, highlighting the topics such as the basic physical processes in the various modes of imaging and in particular the natural and technical limits of the new technique. Trends of its further development and anticipated improvements, the main fields of applications in condensed matter physics and materials sciences and also new types of experiments with no analogues in electron microscopy are discussed and put into perspective with relation to future slow positron beam technology.

1 Introduction

'Positron microscopes offer a new view of things' – this is the title of a short note which recently appeared in Physics Today [1]. Indeed, this statement has been demonstrated by a number of exciting new publications on the subject during the year of 1988.

An immediate question arises as to why the positron probe interacting with matter should be able to produce images of the same or even a better quality than many other existing imaging techniques using above all electrons, but also ions and other primary beams such as γ's, resulting in some secondary particles for imaging. An answer to this question is that even if the structure of condensed matter viewed with positrons might not be as finely resolved as with electrons, for example, it might possibly reveal a qualitatively different picture. The so–called positron reemission microscope (PRM) as first proposed by Hulett et al [2] in 1984 produces contrasts by more or less readily emitting positrons from different surface regions. It is known that positrons in solids are strongly attracted and preferentially trapped by defects [3]. Without scanning a large number of atoms as needed for example with the scanning tunneling microscope in order to single out one defect at the surface of a crystal, the positron microscope may be able to image individual sites or spatial distributions of monovacancies in 'one single shot' [1]. Of course, with the currently available slow positron laboratory beam intensities (state of the art $\sim 10^6$ e^+/sec) such a single shot would take several hours for the imaging process. Hence, the basis for any practical positron microscope is an intense source and a bright beam of low–energy positrons. This is one important instance that calls for very bright, highest intensity slow positron beams.

With respect to radiation damage of biological samples, for example, there is a distinct advantage of a PRM over the transmission electron microscope since it is eV energies of positrons versus energies several orders of magnitude times greater, which traverse the specimen material. Other applications, above all in surface and thin film physics and in defect physics are indicated, as well as sophisticated combinations of microscopic imaging with positron annihilation or spectroscopy techniques for studying spatially resolved trapping sites, for example.

In this reviewing note the state of the art of positron microscopy is summarized by referring mainly to the work of two leading groups in the field: those at the Michigan University and at the Brandeis University–Bell Labs respectively, who independently realized the successful operation of PRM instruments. It will become evident that positron microscopy experiments at PSI would open up an exciting new field of applications in condensed matter physics provided an intense slow positron beam facility were available [4]. In the following sections the various types of positron microscopes are presented, a discussion of the limits of the technique follows, and some fields of specific applications are mentioned, also by showing various possibilities to combine other more conventional positron techniques with space resolving positron imaging and microbeam techniques.

2 Positron versus Electron Microscopy

With respect to transmission microscopy any quantitative comparison between positron and electron microscopy is somewhat unbalanced, because positrons can hardly ever compete with electrons which already offer very high resolution. Nevertheless, it may be interesting to look at the scattering behaviour of positrons interacting with matter in order to isolate the gradual differences between positrons and electrons, resulting for example, in pronounced amplitude and phase contrast changes.

The reemission microscope (PRM), however, exploits unique features of the positron, which leads to differences that are much more of a qualitative than of a quantitative nature. The basic design of such a microscope was first suggested in 1984 by Hulett, Dale and Pendyala of Oak Ridge National Laboratory [2]. Variants of such a PRM have been built and are reviewed below.

2.1 The Transmission Positron Microscope

Van House and Rich at Michigan University have realized a transmission positron microscope TPM [5] in which a positron beam of intensity 3.5 x 10^5 e^+/sec, focused into a 1.7 mm spot at the target, passes through the sample without thermalizing within the sample material. They produced images with a beam energy set at 1.3 keV for polymer foils $\sim$ 400 Å thick with a magnification factor of 55, a resolution of 4000 nm and a 4 h running time. As in transmission electron microscopy, the TPM samples primarily bulk properties of thin targets; good contrast is obtained for positron interactions at energies $E \geq 2$ keV.

The scattering interactions with matter for positron energies in the range 1 keV $< E <$ 1 MeV are governed by a much more effective screening of the nuclei than would be experienced by electrons, especially for $E <$ 100 keV, resulting in a substantially reduced small–angle scattering and in a strongly Z–dependent difference in the amplitude contrast: between 10 % for Z = 8 and 130 % for Z = 80 at E = 50 keV. For lower positron energies these differences would even become 2–3 times larger. As further pointed out in reference [5], a comparison between TPM and TEM images could provide information on atomic form factors and an enhanced sensitive microanalysis is indicated, due to the mentioned screening differences and the strong Z–dependence, respectively. For $E >$ 100 keV the range of positrons in the bulk solid is a factor of 1.3 larger than for electrons

as a consequence of the reduced elastic scattering. This means that thicker targets or lower energies for a given contrast could be used in the positron case. Furthermore, due to the strong repulsion of positrons by the nuclear charge, an equally pronounced Z–dependence in the phase contrast differences as found for the amplitude contrast is the result. Of course, there are several further substantial differences between the electron and the positron behaviour in solids, such as the relative contributions of elastic and inelastic scattering to the contrast, as well as a larger positron energy loss per unit length due to the increased inelastic scattering resulting in a more intense secondary electron production. These differences and other intrinsic positron properties in solids could prove to be of use in specific applications with no analogue in the electron microscopy case. For a further reaching discussion, reference [5] and the references therein should be consulted.

2.2 The Positron Reemission Microscope

The PRM is clearly distinct from a standard electron microscope. In a reemission microscope a positron beam with initial energies of 1 – 10 keV is implanted within a diffusion length of the sample surface ($\sim$ 100 – 1000 Å). The positrons become thermalized and a fraction of up to 50 % of the incident positrons may be reemitted spontaneously as slow positrons ($\sim$ 1 eV) from the surface if the sample has a negative affinity (work function) for positrons. For an extended table of work functions see e.g. reference [6]. A fairly small energy spread of the emitted positrons facilitates sharp images by subsequent acceleration and focusing of the positrons to form an image of the reemitting surface on a detector which is sensitive to the position of the emerging positrons. The nature of the low energy positron emission process, and the short depth of the small accelerating fields for imaging combine to make the PRM an extremely surface– and near–surface–sensitive device, sampling positron interactions occurring at eV energies.

The Michigan group PRM [7] is designed in a reflection geometry (Figure 1). An off–axis positron beam illuminates the sample at an angle from the front, and the positrons are reemitted from the sample's front surface. Hence, this design allows direct imaging of thick targets. The reflection geometry also allows an energy dependent, and thus depth controlled, implantation of the incident positrons into the sample, thus resulting in the possibility of depth profiling subsurface features. Van House and Rich studied tungsten and molybdenum foils whose surfaces had been masked by a grid prior to bombardment with ions. The near–surface defect sensitivity of the PRM contrast between the bombarded and masked portions was clearly demonstrated. Images were taken of a variety of targets, among them the image of an N_2 bombarded Mo foil was taken at a magnification factor of 56 and a resolution of 2300 nm. It required 30 h to accumulate at an incident beam intensity of 5 x 10^5 e^+/sec and an incident energy of 2 keV.

The Brandeis–Bell Labs PRM instrument [8] closely follows the original Oak Ridge conception [2] in which the sample was to be placed on a 1 – 10 nm thick substrate. Positron beam back illumination of the substrate, thermalization of the positrons in the substrate and reemission from the front side would allow to image the sample by a shadowing effect. By contrast, in the device of Brandes, Canter and Mills, a 150 nm thick Nickel film replaces the above mentioned substrate and sample. The positron beam used in their experiment

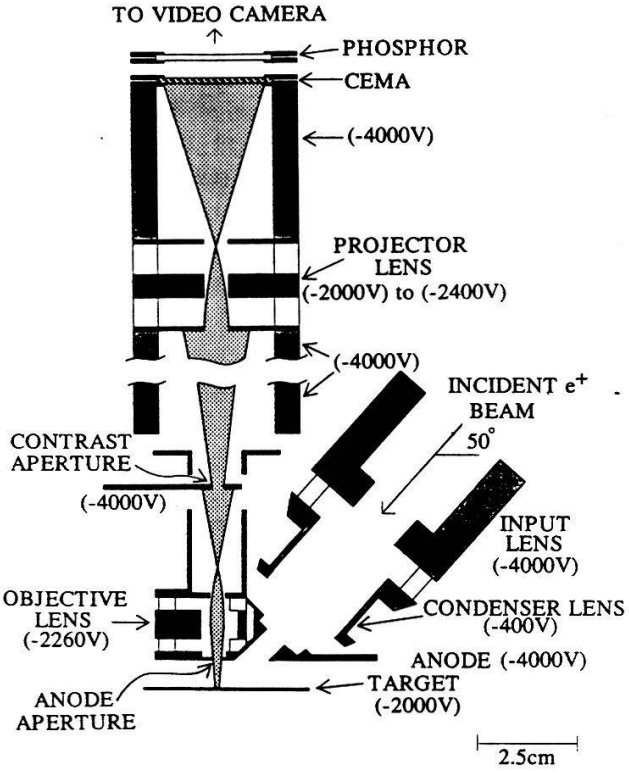

Figure 1: *Reflection mode PRM as realized by the Michigan group; details of performance can be found in [7]. Incident beam generation as well as the image analysis system are discussed in detail in reference [5].*

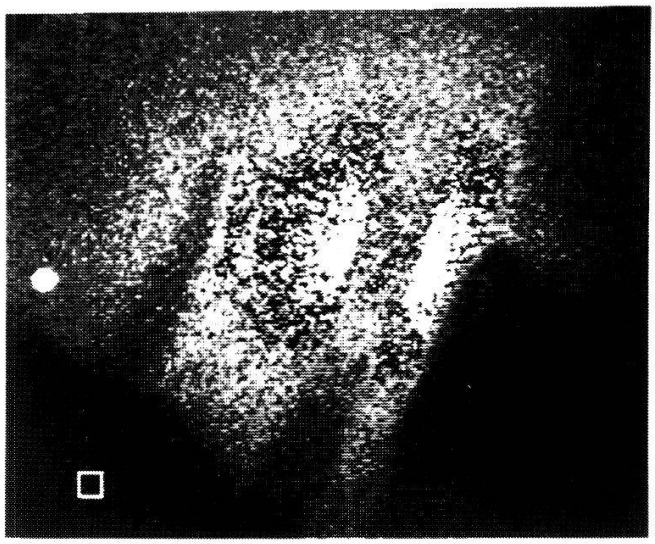

Figure 2: *Image of a nickel film as produced by the Brandeis–Bell Labs group [8] with their PRM. Brandes et al assume that the different patches of emissivity are due to the trapping of positrons by various low angle or tilt boundary layers parallel to the surface of the sample material.*

employed two stages of brightness enhancement (see section 3). With an attained intensity of 10^4 e^+/sec, accelerated to 5 keV and brought to a focus of 20 μm diameter on the back of the sample, the positrons emitted from the front were magnified by objective and projector lenses by a magnification factor of 1150 producing an image (Figure 2) in a 14 h running time with an experimental resolution of 300 nm. As pointed out by Brandes et al [8], a flux increase by several orders of magnitude would be feasible by installing a 100–mCi ^{22}Na instead of a 80–mCi ^{58}Co source, a solid Ne positron moderator and cooled remoderators for the two brightness enhancement stages.

3 Positron Microscopy and its Limits

Spatial resolution, positron beam properties and restrictions in the preparation of the samples and their environmental conditions are important items to be considered when discussing natural and technical limits in positron microscopy. Detailed discussions of the influence of various instrumental parameters on the resolution can be found in references [5,7,8]. In this reviewing note we shall concentrate on the various physical mechanisms that will determine the resolving power of positron microscopes.

3.1 Resolution of positron microscopes

In direct imaging of features, the overall resolution will be determined, generally speaking, by a convolution of the characteristics of physical processes in the target and the instrumental characteristics such as aberrations of the positron optical system, primary beam properties and detector properties. As for the PRM, the physical effects in the target which enter this convolution are determined by the combined variation in the positron implantation depth, the positron diffusion prior to reemission and an energy dependent positron reemission probability ϵ, averaged over the microscope's field of view. By comparison, for the TPM the role of the target is taken over by the moderator or remoderator (see section 3.2) used to generate the primary positron beam. Whence, in the case of the transmission microscope the diffusion length of positrons in the target does *not* enter the resolution function, because there is no thermalisation of positrons in the target.

In the TPM case, where the resolution depends on instrumental characteristics and target properties through chromatic aberration only, it can easily be shown [5] that there exists a 'diffraction limit' of the resolution, scaling with the de Broglie wavelength as $\sim \lambda^{3/4}$, while neglecting chromatic aberrations (variation $\Delta E \ll E$ at the target). For a primary beam energy $E = 100$ keV at the target, this amounts to ~ 2 Å. If the prerequirements of sufficiently bright and intense beams were fulfilled (see below and Figure 3) this limit would easily compare with resolution limits achieved with modern TEM's.

Contrast in a PRM image may be provided by variations in bulk defect densities, different crystal orientations and various surface phenomena that attenuate the emitted positrons or affect the positron work function and hence the reemission probability ϵ.

If bulk positron interactions determine the features of an image, their resolution is then limited by the positron thermal diffusion length (100–1000 Å). Both the reflection mode and the transmission mode PRM employ the same contrast mechanisms for bulk defect imaging, because defects which trap or scatter positrons diffusing back to the surface will be imaged, regardless of the mode of implantation.

On the other hand, only defects within a few nm from the surface can be imaged effectively. The further a defect is below the positron emitting surface, the more difficult it is to observe it due to lateral diffusion around the defect. Surface and near surface phenomena like defects, adsorbates, overlayer islands or thin film overlayers give rise to variations in the reemission rate near the point of positron emission, which in turn result in higher resolution (as small as a few Å [7], in any case < 10 Å, the de Broglie wavelength of the emitted positrons [8])[1] depending on the details of the positron interactions with such surface phenomena. This makes the PRM extremely surface–sensitive. The resolution will be limited in this case by the instrumental resolution alone since, again, there is no target specific thermal diffusion involved in this imaging process. The ultimate resolution of the Michigan group PRM is in fact limited by geometry (Figure 1): the off–axis incident beam prevents one from moving the imaging lens closer to the sample. In the transmission mode PRM the positrons are introduced from behind an overlying structure. It has the

[1] In references [8,12] Canter et al hope that the reemission microscopy technique might lead to a form of holographic imaging by interference between emitted positrons from the substrate and scattered positrons from adsorbed atoms or molecules. Thus, the 1 nm resolution limit could eventually be circumvented.

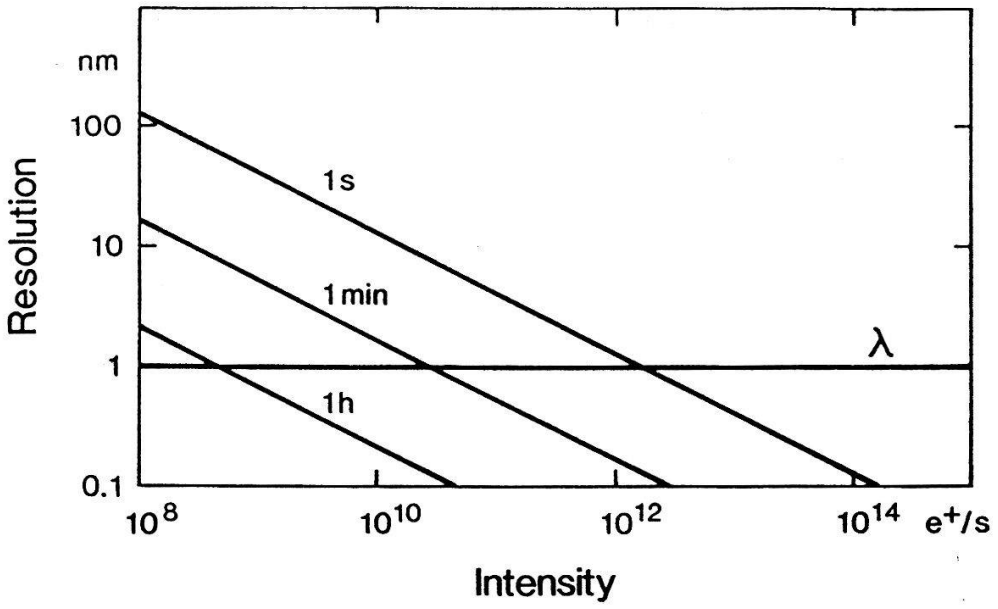

Figure3: *The horizontal line at 1 nm resolution gives the de Broglie wavelength λ of 1.5 eV positrons. λ determines the diffraction limit to the resolution. The inclined lines give the resolution limit due to positron statistics as a function of the intensity of the slow positron beam.*

advantage that surface features are illuminated only by $\sim$ 1 eV positrons, an important aspect when concerned with biological sample material. Hence, a PRM installed at a high flux facility ($> 10^{10}$ e^+/s) would allow to observe the dynamics of monovacancy diffusion [12], early stages of precipitate nucleation and of radiation damage, for example.

Last but not least, one of several contributions to the resolution of a positron microscope is a counting–statistics limited term proportional to the inverse square root of the positron flux density. Figure 3 shows the resolution limit due to positron statistics as a function of slow positron beam intensity and exposure time. The limit is given for 3 different exposure times under the same assumptions as in reference [8] but with cooled remoderators for the brightness enhancement (see section 3.2).

3.2 Brightness enhancement of positron beams

Equally important as beam intensity is flux (i.e. intensity per unit area) incident on the sample in a microscope or microprobe application. For high magnification positron reemission microscopy it is an absolute necessity that sufficient brightness of the primary beam is available. This means that questions about phase space characteristics of positron beams are essential: In order to focus a beam down to a small spot (typically > 1 μm) the brightness of the primary beam moderator has to be given equal attention as is given to maximizing the beam intensity. Brightness is a measure not only of the intensity of the

beam but of its diameter and angular divergence. Thus, in order to convert a quoted beam intensity of, say, 10^{10} e^+/sec into an optimal flux at the sample in a microscope, one has to know more about the details of the actual beam design [9].

Various phase space issues and corresponding limits are discussed in the references [10,11]. The brightness of a beam is defined as a current per unit area per unit solid angle; per unit energy it can be written as $R = I/(\Gamma^2 E)$, where I is the intensity, $\Gamma = 2\theta d$ is the phase space occupied by the slow positrons in the beam with longitudinal particle kinetic energy E, beam diameter d and half angular spread θ. It is appropriate now to mention the statement of the Liouville theorem: The particle density in phase space is constant if the beam is only acted upon by conservative forces. For a constant longitudinal energy spread ΔE this means, that the brightness per unit energy is also a constant. Hence, in analogy to the above formulation, considering a moderator of diameter D and transverse energy $E_T \ll E$, and by using the relation $\Gamma\sqrt{E} = 2D\sqrt{E_T}$, the brightness (per unit energy normalized to source activity) of a moderator can be written as [12]

$$R_m = \varepsilon/(4D^2 E_T) \quad ,$$

where ε is the moderator efficiency.

Yet, brightness *enhancement* of positron beams can be achieved and a method for this has been proposed by Mills [13] in 1980. He recognized that the moderation used to generate a positron beam (i.e. the thermalization process of positrons in a solid) is not a conservative process and that Liouville's condition should not apply to it. Mills proposed that a beam with enhanced brightness could be obtained by

$$accelerating(\text{to a few keV}) + focusing(\text{down to} \sim 10^{-2}D) + remoderation$$

of the positrons by a small crystal, which would thermalize and reemit the low–energy positrons from a small area with low angular divergence. Canter et al [12] estimated with the above figures a 10^3 increase in R_m and a loss down to one tenth of the original intensity by assuming a 10 % remoderation efficiency. Further details of such enhancement stages can be found e.g. in [12].

Mills's enhancement concept was experimentally verified in 1985 by Frieze et al [14]; Canter et al [8] used such enhancement stages in their PRM to reduce the beam area by several 10^5 and to increase the beam brightness by a factor of 500. Their final result was a 5 keV beam with $\sim 10^4$ e^+/sec whose full width at half maximum was 12 μm. They anticipated an improvement in the resolution by increasing the brightness enhancement factor to 25'000 when using more intense radioactive sources, switching to more efficient primary moderator and cooled remoderator stages.

3.3 Specimen preparation and environmental conditions

Appreciable change of $\epsilon(E)$, the reemission probability, may result from heat treatments and from vacuum condition changes, which have, of course, to guarantee reproducible values of ϵ. On the other hand, for biological materials high vacuum required in any particle microscope technique may be a limit to study such samples.

The reflection mode PRM offers a wide spectrum of choice and preparation of targets, it is thus particularly useful in surface physics and materials sciences. This geometry allows an energy dependent implantation of positrons, and therefore the possibility exists to perform depth profiling of subsurface features. However, its resolution is limited by geometry (see section 3.1).

Sample preparation for the transmission type PRM is more critical, because targets have to be thin enough to allow the passage of positrons and thick enough to allow for thermalization to occur. Depth profiling is also possible, however, there is the restriction in sample thickness.

Positron microbeam technology is useful to apply to positron surface and bulk spectroscopies as well as ACAR or life time spectroscopy on small samples, or in a spatially resolved mode for inhomogeneous samples (certain high T_c compounds, for example) [15]. Microbeams can also be used to improve the angular resolution of ACAR instruments.

4 Applications of Positron Microscopy Techniques

The TPM should have a variety of new applications as a result of the different contrast which appears when positrons rather than electrons are used as the imaging particles (see section 2.1 and reference [5]). Furthermore, as a consequence of a larger energy loss per unit length for positrons than for electrons, the secondary electron intensity of a thin target in a TPM will be increased and the spectral composition altered when positrons are incident on the target. When combined with a secondary electron analysis technique, the TPM will provide a different sensitivity to target composition from that of a TEM.

The areas of application of a PRM are radically different from those of the TPM. We have seen that resolutions of a few Å are possible in a PRM, especially when imaging surface and near surface features, for example, to image single vacancies in a crystal or overlayer molecules of biological interest [8]. The defect sensitivity of the PRM may also be useful in studies of the role of surface defects in materials science applications. Surface sensitivity will also be present in the scanning positron microprobe. In reference [16], Brandes et al discuss applications to defect spectroscopy and observation of small samples, a problem which is discussed also in [15].

An experimental combination of positron microscopy with annihilation techniques would result in a method that has no analogue in electron microscopy. Such a combination would allow to obtain new information such as distinguishing various types of positron trapping sites, like monovacancies, grain boundaries or misfit dislocations at precipitate interfaces, in a spatially resolved mode. In addition, the Michigan group [7] considers the incorporation of an energy analyser with an energy resolution of about 0.1 eV in their PRM so that high spatial resolution imaging could be combined with reemitted positron spectroscopy [17] of thin metal films and multilayer systems. One could then selectively image layers of specific material (depth profiling), alloyed or pseudomorphically deformed layers [18] or overlayer islands for nucleation or growth studies [17].

PSI is considering the feasibility of applying positron reemission microscopy charac-

terized by 'high spatial resolution imaging in seconds', and by a combination of positron imaging with annihilation techniques. A first objective of such experiments would be to study space resolved positron trapping sites in low temperature irradiated iron–copper alloys.

5 Conclusions

Positron microscopy views things differently, it offers **new applications** in materials science, in particular for defect analysis and surface physics. Positron microscopy is less destructive for biological material or molecules on top of the reemitting surface, for example, since it is eV energies of positrons which image objects in positron reemission microscopes.

The availability of an **intense slow positron beam facility** is essential. It gives positron reemission microscopy the unique ability to observe the dynamics of monovacancy migration and aggregation in the earliest stages of precipitate nucleation or metal fatigue, for example. An efficient way to realize such instruments at PSI is indicated by collaborative ventures with experienced university groups and interested industry research laboratories.

A **combination** of positron microscopy **with annihilation techniques** would add new and necessary information for distinguishing between positron trapping sites in a spatially resolved way. The combination of high spatial resolution imaging **with reemitted positron spectroscopy** of thin metal films and multilayer systems would offer the selective imaging of layers of specific material, i.e. a kind of depth profiling.

Positron microscopy is still in an early phase of development. It tends to become a new and powerful technique with great potential for materials science applications. Moreover, positron beam technology has reached a level of development where studies in certain cases begin to go beyond the capabilities of electrons, in particular in surface and defect structure determinations. Considering the already existing infrastructure at PSI (cryophysics, UHV technology, charged particle beam technology, detector technology) together with important user group interests, this is the right moment to enter **an exciting new area of research.**

Acknowledgement

I would like to acknowledge the critical reading of the manuscript and the numerous helpful discussions with U. Zimmermann, H. Grimmer, G. Solt and P. Tipping. I would also like to thank A.A. Manuel, M. Peter and H.R. Ott for continuous suport.

References

[1] B. Goss Levi, Physics Today, **12** (1988) 17.

[2] L.D. Hulett, J.M. Dale, S. Pendyala, Mater. Sci. Forum **2** (1984) 133.

[3] A. Seeger, this volume.

[4] U. Zimmermann, this volume and D. Taqqu, this volume.

[5] J. Van House, A. Rich, Phys. Rev. Lett. **60** (1988) 169.

[6] P. J. Schultz, K.G. Lynn, Rev.of Modern Phys. **60** (1988) 701.

[7] J. Van House, A. Rich, Phys. Rev. Lett. **61** (1988) 488.

[8] G.R. Brandes, K.F. Canter, A.P. Mills Jr, Phys. Rev. Lett. **61** (1988) 492.

[9] see e.g. D. Taqqu, this volume.

[10] A.P. Mills Jr, in 'Positron Scattering in Gases', p. 121, eds: J.W. Humberston, M.R.C. McDowell, Proceedings of the NATO Advanced Research Workshop on Positron Scattering in Gases, July 19–23, 1983, Plenum Press New York and London, 1984.

[11] K.F. Canter, Proceedings of the workshop on researches using positrons, Japan Atomic Energy Research Institute, February 7–8, 1989, p.1.

[12] K.F. Canter, G.R. Brandes, T.N. Horsky and A.P. Mills.Jr., ibid, p.55.

[13] A.P. Mills, Jr., Appl. Phys. **23**, (1980) 189.

[14] W.E. Frieze, D.W. Gidley, K.G. Lynn, Phys. Rev. B **31**, (1985) 5628.

[15] A.A. Manuel, M. Peter, this volume.

[16] G.R. Brandes, K.F. Canter, T.N. Horsky, P.H. Lippel and A.P. Mills, Jr., Rev. Sci. Instrum., **59**, (1988) 228.

[17] D.W. Gidley and W.E. Frieze, Phys. Rev. Lett. **60**, (1988) 1193.

[18] D.W. Gidley, Phys.Rev.Lett., **62**, (1988) 811.

Helvetica Physica Acta
Vol. 63 (1990)
0018-0238/90/040458-07$1.50+0.20/0

SUMMING UP

M. Peter and A.A. Manuel
Département de Physique de la Matière Condensée, Université de Genève,
24 quai E. Ansermet, CH-1211 Genève 4, Switzerland

The purpose of the workshop on high intensity positron beams held at the Paul Scherrer Institute (PSI) was to obtain the opinion of some of the world's experts on the potential interest for the development, at the PSI, of a large scale effort for the production (and the detection) of positrons for the investigation of condensed matter. The program was organised around three topics:

- Intense sources around the world,
- Applications of positrons in condensed matter physics,
- Possible techniques and experiments at PSI.

1. Recent positron beam technology[1]

Among the sources of positrons we can distinguish between 1) pair production in heavy targets and 2) the use of radioactive isotopes. We briefly summarize some typical characteristics of the facilities which have been presented or mentioned during the workshop, keeping in mind that exact comparisons are difficult and sometimes misleading.

A. Pair production based facilities.

In this category there is one exception to LINAC-based systems. It is the project of the **Laue Langevin Institute**[2]. The $^{113}Cd(n,\gamma)^{114}Cd$ nuclear reaction will be used to create high energetic γ-rays which will be converted in 10^{13} positron-electron pairs per second in W moderators inserted in a "positron bottle". After remoderation and extraction a flux of 10^{10} slow positrons/sec is expected[3].

Six LINAC-based systems actually in operation were outlined:

1) **Livermore:** 120MeV LINAC, flux 7 10^9 (instantaneous) 2 10^7 (average) monoenergetic positrons/sec. The energy of positrons may be fixed between 740eV and 18keV[4]

2) **Oak Ridge:** 150-180MeV, 50-60kW LINAC with pulse width of 2-40ns and repetition frequency of 30-1000Hz. Using W moderator, 1.1 10^8 positrons/sec (at 33kW) are

obtained with a typical energy of 3keV[5].

3) **Giessen:** The Giessen facility to produce slow positrons (TEPOS) is using a 65MeV LINAC. At 34keV it delivers a maximum current of 200μA (time average), used to produce a monoenergetic positron beam of 10^8 positrons/sec (time average). The diameter of the beam is of the order of 10mm (50% of the flux) and the energy can be fixed between 10eV and 80keV[6]. A separate new beam line is under construction[7].

4) **Mainz**: a LINAC of 200MeV is used[8] to project electrons on a watercooled Ta target. Using W moderator, a beam of about 2 10^7 positrons of about 60eV are produced per second. The spot is collimated to a diameter of 5mm at the sample.

5) **ETL Tsukuba:** a 75MeV, 4μA LINAC is used to produce[9] a beam of 10^7 slow positrons/sec after pulse stretching[10] using a Penning trap. Monoenergetic positrons up to ~35keV are available.

6) **JAERI Tokai:** Here[11], the 100MeV LINAC has a peak intensity of 6A for pulse width of 25ns at the frequency of 600Hz. Using Ti moderator, a beam of 10^6 positrons/sec is obtained. The energy of positrons is 2eV (peak) 2eV (FWHM). Pulse stretching available.

One LINAC-based facility is under study. It is the **Positron Factory Project in Japan**[12]. With a 100kW, 100MeV (max.) LINAC producing pulses up to 100μsec width at 1000Hz, 10^{10} slow positrons/sec are expected from this large scale facility which will be equipped with various kind of instrumentation. We have not quoted high-energy physics facilities like the SLC[13] etc.

B. Use of radioactive isotopes.

Three positron emitters are commonly used: ^{64}Cu ($T_{1/2}$=13 hours, positron yield= 19%), ^{58}Co ($T_{1/2}$=71 days, positron yield=15%) and ^{22}Na ($T_{1/2}$=2.6 years, positron yield=89%). The following laboratories have been presented or mentioned during the workshop:

Tsukuba, University: 25mCi of ^{22}Na irradiate a W vane moderator. Monoenergetic positron beam of 0-50keV is available[14]. This group is actually planning to use a mini-cyclotron to produce short-lived positron emitters with high intensities.

NIRIM, Tsukuba: T. Akahane and T. Chiba are now testing a micro-beam[15].

Stuttgart: From 16mCi of ^{22}Na and W moderator, a beam of 4mm in diameter having a flux of 6 10^4 slow positrons is formed. It is available for various kind of studies. From this beam, using a Pelletron accelerator, relativistic (0.5-6.5MeV) positrons may be sent on various beam lines. One is equipped with a "positron clock" to perform lifetime measurements with a resolution of 175ps (FWHM)[16].

East Anglia: Using 20mCi of ^{22}Na, a 1-8keV flux is obtained. Remoderation and focalisation lead to a sub-millimetre beam[17].

Munich: Using a 30mCi ^{22}Na source and W(100) single crystal of 1μm thickness as transmission moderator (efficiency of 4 10^{-4}), a beam of 2mm in diameter is formed having a flux of 4 10^5 positrons/sec (dc) and 6 10^4 positrons/sec in pulses of ~ 135ps (FWHM) duration. The energy range is 50eV - 40keV for the dc beam and 500eV - 40keV for the pulsed one[18]. The pulsed beam permits to increase the resolution of lifetime measurements up to 240ps.

Helsinki: a 4x7mm^2 beam of 4.7 10^6 positrons/sec is obtained using 300mCi of ^{58}Co and a W moderator with an efficiency (including transport) of 0.28%. The energy of the beam may be tuned from 1eV to 35keV[19].

Trento: Solenoid beam, ^{22}Na 5mCi, 4μm thick W film as transmission moderator, intensity ~10^5 positrons/sec, continuous, diameter of the beam: 5mm, energy: 100eV-30keV[20].

Brookhaven: This laboratory is exploiting beams of various kinds. We quote two of them. The first uses ^{64}Cu as positrons source. The low half-life and high activation cross-section of this isotope are used to produce very intensive sources (22Ci, total activities of 115Ci) with a flux of 2.4 10^{15} thermal neutrons per cm^2 and per sec. Using Cu as moderator, a beam of 10^8 monoenergetic positrons per sec. is obtained[21]. Another installation[22] produces an adjustable, 0.5 to 3.0MeV, beam of 3 10^5 monoenergetic positrons per sec., from a 70mCi ^{22}Na source. The diameter of the beam is 1.1 mm FWHM at 2.2MeV.

Brandeis and AT&T: These groups have developed a micro-beam of 5keV positrons having a diameter of 12μm FWHM. This is achieved from 100mCi of ^{58}Co by successive moderation-focalisation to finally obtain a brightness enhancement of 500x[23].

Wayne: W moderators are used to produce a beam of > 10^5 positrons/sec with an energy of 200eV (spread of 2eV) from a 50mCi ^{22}Na source[24].

The above list is far to be complete. Here again, we have not considered high-energy physics positron sources. In solid state, atomic, and molecular physics, other developments have been made in Europe, US and Japan. More information may be found in the proceedings of ICPA-8, Gent, 1988[25].

2. Motivations for the construction of an intense positron beam at PSI

Positron annihilation opens up to wide domains of physics. The **lifetime** of positrons in matter correlates with the spatial **electron density**. Hence lifetime data are used for the measurements of samples quality. The **Angular Correlation** (ACAR) measures **electron**

momentum density (EMD), or, more exactly the electron-positron momentum density. The information is therefore less direct than the EMD obtained by **Compton** scattering but still, it is an efficient method which in favourable cases can be implemented in ordinary laboratory conditions. **Fermi surfaces** can be deduced from EMD's. The experimental EMD's can be checked against the available numerical predictions. **De Haas-van Alphen** measurements give also information on Fermi surfaces, but this method is only applicable if the collision rate is smaller than the cyclotron frequency: ACPAR is not subject to such extrinsic limitations. In addition, deviations from the single particle models can be detected, which allows calibration of different theoretical models.

Positrons from common beta-emitting sources penetrate tens to hundreds of microns into the samples before annihilation: ACAR is thus a **bulk** method. This is again a considerable advantage over competing methods like for instance SPARPES where results are subject to the question of the relevance of results from the surface to the bulk properties.

While the positrons penetrate into the sample, they dissipate their kinetic energy and assume in many cases the temperature of the sample. This is particularly true for metals, less so in insulators. Also, the positrons retain their spin polarisation, which makes possible spin-resolved EMD measurements.

Sources of **increased intensity** will allow essential improvements in the ACPAR techniques. And, for reasons of self-absorption and lifetime, the essential breakthrough will necessitate proximity of a large device; either a reactor or a powerful beam. (We noticed however in the focusing techniques explained by **Triftshäuser** a possibility of concentrating positrons from a larger surface of conventional emitters). Increased intensity brings a much needed gain in measurement speed: at present, a full analysis of a substance takes months! Such increased intensity will necessitate improved detectors (shorter response time), this appears to be technically possible. The surface of the detectors has direct bearing on the measuring speed, this underlines even more the necessity of maximize detector performances in parallel with the development of high performance sources.

Monoenergetic positrons will allow selection of penetration depth and hence ACPAR at controlled depth. The advantage for the investigation of surface properties is evident. Selection of monoenergetic positrons is however rather inefficient, which means again the necessity of a very intense beam to start with. The highest efficiency is actually obtained using Ne moderators[26]. The possibility of a spatial decomposition of the beam into components of different energies with possibility of simultaneous observation is to be studied.

Strong **spatial focusing** of the positron beam is another obvious advantage. In many materials it is difficult or impossible to prepare large single crystals of good quality, and with homogeneous properties. Or, if it is possible, then only after annealing periods of the order of

months. Hence rapid investigation of samples of different compositions and preparations is rarely compatible with the necessity for large crystals.

The possibility of **time bunching** of positrons offers in addition the possibility of dynamic studies. The presence of very high positron densities could open more exotic possibilities such as the possibility of the **positron-electron laser** and the **transmission positron microscope** which is discussed by Waeber. It is clear that the possibilities offered by high flux sources will have to be paid for by considerable disadvantages: High price of the beam, intermittent availability as opposed to the continuous presence of the laboratory source. But these are inconveniences proper to all large scale solutions - to be offset by the power of the instrument and also by the concentration of the best specialists in cooperative efforts.

Coordination is possible: At present it is not clear which method of positron production will produce the best results. Different schemes are presently proposed and should be tried. No system is in view which would be so powerful in satisfying all experimental need. For these reasons, the participants to the workshop arrived to the following proposition:

proposition:

Scientists assisting the workshop on intense beams of slow positrons and applications, considering that:

- *the interest for positrons grows both in research and industry,*
- *present sources are far from attaining theoretical performance,*
- *most interesting problems exist in metals, semiconductors, surfaces, which could be studies with an intense beam,*
- *great efforts are undertaken in several institutions, that the problem is timely and that coordination is possible,*

recommend that PSI seriously consider the construction of an intense slow positron source. This would present an essential contribution to the contemporary research in condensed matter physics.

Acknowledgements:

All the participants to this workshop are very grateful to W. Waeber and U. Zimmermann who have perfectly organized, with the efficient help of Mrs. E. Huber, this day of fruitful exchanges. The authors are grateful to P. Hautojärvi, G. Kögel, K.G. Lynn, H.-E. Schäfer, H. Schneider and A. Zecca for communicating to them useful informations. The workshop was sponsored by the Paul Scherrer Institute and the University of Geneva, with the support of the Swiss National Science Foundation.

References:

1. A general reference is *Intense Positrons Beams*, E.H. Ottewitte and W. Kells, eds, World Scientific, 1988.
2. W. Triftshaüser, these proceedings.
3. K. Schrekenbach, *Meeting on the use of a high flux source of moderated positrons*, Grenoble, France, June 27, 1989, unpublished.
4. R.H. Howell, P. Meyers, I.J. Rosenberg and M.J. Fluss, Phys. Rev. Lett. **54**, 1698, (1985) and R.H. Howell, M.J. Fluss, I.J. Rosenberg and P. Meyer, Nucl. Instr. and Meth. in Phys. Res. **B10**, 373 (1985).
5. L.D. Hulett, Jr, T.A. Lewis, D.L. Donohue and S. Pendyala, in Ref. 25, p.586 and 589.
6. F. Ebel, W. Faust, C. Hahan, S. Langer, M. Rückert, H. Schneider, A. Singe and I. Tobehn, Nucl. Instr. Meth. in Phys. Res., **A272**, 626 (1988).
7. H. Schneider, private communication.
8. R. Ley, K.D. Niebling, R. Schwarz and G. Werth, in Ref. 25, p. 289 andJ. Dahm, R. Ley, K.D. Niebling, R. Schwarz and G. Werth, *Electro-Porduced Slow Positrons* in Proc. of the Conf. on the Production and Investigation of Atomic Antimatter, Karlsruhe, Germany, 1987, to be published in Hyperfine Interactions.
9. T. Akahane and T. Chiba, in Ref. 25, p.31
10. T. Akahane, T. Chiba, N. Shiotani, S. Tanigawa, T. Mikado, R. Suzuki and M. Chiwaki, in Ref. 25, p.592
11. Y.Ito, O.Sueoka, M.Hirose, M.Hasegawa, S.Takamura, T.Hyodo, Y.Tabata, in Ref. 25, p. 583
12. Y. Tabata and S. Okada, in Ref. 25, p.34
13. S. Ecklund, in Ref. 1, p.42.
14. S. Tanigawa,Y. Iwase, A. Uedono and H. Sakairi, J. Nucl. Mater. **133&134**, 463 (1985) and these proceedings
15. T. Akahane, private communication.
16. W. Bauer, J. Briggmann, H.D. Carstanjen, W.Decker, J. Diehl, K. Maier, J. Major, H.-E. Schaefer, A. Seeger, H. Stoll, and R. Würshum, in Ref. 25, p.589 and R. Würschum, W. Bauer, K. Meier, A. Seeger and H-E. Schaefer, J. Phys. Cond. Mat. **1**, SA33 (1989).
17. I.R. Farthing and P.G. Coleman, in Ref. 25, p.606
18. D. Schödlbauer, P. Sperr, G. Kögel and W. Triftshäuser, Nucl. Instrum. and Meth. in Phys. Res. **B34**, 258 (1988).
19. J. Lahtinen, A. Vehanen, H. Huomo, J. Mäkinen, P. Huttunen, K. Rystölä, M. Bentzon and P. Hautojärvi, Nucl. Instr. Meth. in Phys. Res. **B17**, 73 (1986)
20. R.S. Brusa, A. Dupasquier, R. Grisenti, S. Liu, S. Oss and A. Zecca, J. Phys.: Condens. Matter **1**, 5411 (1989)

21. M. Weber, S. Berko, K.F. Canter, K.G. Lynn, A.P. Mills, Jr, A.R. Moodenbuagh and L. O. Roellig, in Ref. 1, p. 51 and p.11.
22. H. Huomo, P. AsokaKumar, S.D. Henderson, B.F. Phlips, R. Mayer, J.McDonough, H. Hacker, S, McCorkle, P. Schnitzenbaumer, J.S. Greenberg, M.S. Lubell, K.G. Lynn and A. Vehanen, in Ref. 25, p. 603
23. G.R. Brandes, K.F. Canter, T.N. Horsky, P.H. Lippel and A.P. Mills Jr, J. Phys. Condens. Mat. **1**, SA135 (1989).
24. G.M.A.Hyder, M.S. Dababneh, Y.F.Hsieh, W.E.Kauppila, C.K.Dwan, M.Mahdavi-Hezaveh and T.S. Stein, Phys. Rev. Lett. **57**, 2252 (1986)
25. L. Dorikens-van Praet, M. Dorikens and D. Segers, eds, *Positron Annihilation*, World Scientific, Singapore, (1988)
26. A.P. Mills Jr and E.M. Gullikson, Appl. Phys. Lett. **49**, 1121 (1986)

Helvetica Physica Acta
Vol. 63 (1990)

0018-0238/90/040465-01$1.50+0.20/0

PAUL SCHERRER INSTITUTE

Workshop on Intense beams of slow positrons and applications in condensed matter physics and other scientific disciplines

20 November 1989, lecture room PSI-west
5232 Villigen PSI

Programme

08.45	Welcome address and aim of workshop	H.R. Ott	PSI
	USA intense sources and e^+ microscopy	K.G. Lynn	Brookhaven
	FRG beams and proposal 'Grenoble'	W. Triftshäuser	Munich U
	Present and future e^+ beams in Japan	S. Tanigawa	Tsukuba U
10.45	*Coffee break*		
11.00	Applications in solid state physics	A. Manuel	Geneva U
	Applications in defect physics	A. Seeger	Stuttgart U
	Efforts around the Finland e^+ source	P. Hautojärvi	Helsinki U
12.45	*Lunch*		
14.00	Possible source techniques at PSI	U. Zimmermann	PSI
	High efficiency moderation	D. Taqqu	PSI
	Joint venture: e^+ microscopy at PSI?	W.B. Waeber	PSI
15.45	*Coffee break*		
16.15	General discussion (30 min)		
	Summary talk	M. Peter	Geneva U
17.00	*End of workshop*		*WW/UZ*

Sponsors of this workshop: *PSI and Geneva University*

Helvetica Physica Acta
Vol. 63 (1990)

0018-0238/90/040466-05$1.50+0.20/0

List of Participants

Workshop on Intensive Positron Sources and Applications of Positrons
in Condensed Matter Research and Other Scientific Disciplines

at Paul Scherrer Institute, PSI-West, 5232 Villigen PSI, Switzerland
on Monday, November 20, 1989

BELYAEV, V.N., Dr.
Moscow Engineering Physics
Institute
Kashirskoye Chaussee 31
115409 Moscow
USSR

BIASINI Maurizio Dr.
ENEA
C.R.E. "Ezio Clementel" Bologna
Viale G.B. Ercolani, 8
40138 Bologna
Italy

BRAUN Hans-Heinrich
Research Dept. F1
PSI
5232 Villigen PSI
Switzerland

BRUNNER Jean Dr.
Physik Departement
ETH-Hönggerberg
8093 Zürich
Switzerland

BRUSA Roberto S. Dr.
Dipartimento di Fisica
Università degli Studi di Trento
38050 Povo (Trento)
Italy

CARTIER Eduard Dr.
IBM, Thomas J. Watson Research
Center
P.O. Box 218
Yorktown Heights, NY 10598
USA

CHARLTON Michael Dr.
Dept. of Physics and Astronomy
University College London
Gower Street
London WCIE 6BT
England

CHAWLA Rakesh Dr.
Research Dept. F4
PSI
5232 Villigen PSI
Switzerland

CHO Yang-Koo Dr.
Department of Materials Sciences
University of Tsukuba
c/o Taedok Science Town
P.O. Box 3
Taejon 300-31
Korea

COLEMAN Paul G. Dr.
School of Physcis
University of East Anglia
Norwich NR4 7TJ
United Kingdom

CORBEL Catherine, engineer
I.N.S.T.N.
CEN Saclay
91191 Gif-sur-Yvette
France

DANNEFAER Steen Dr.
Institut für Kernphysik
Technische Universität Graz
Petersgasse 16
8010 Graz
Austria

DE LIMA Adriano P. Dr.
Physics Institute
University of Coimbra
3000 Coimbra
Portugal

DORIKENS-Vanpraet, Liliane Dr.
Lab. for Nuclear Physics
Rijksuniversiteit Gent
Proeftuinstraat 86
9000 Gent
Belgium

DORIKENS Maurice Dr.
Lab. for Nuclear Physics
Rijksuniversiteit Gent
Proeftuinstraat 86
9000 Gent
Belgium

DU PASQUIER A. Dr.
Politecnico di Milano
Istituto di Fisica
Piazza Leonardo da Vinci 32
20132 Milano
Italy

ELDRUP Morten Dr.
Metallurgy Dept.
Risö National Laboratory
4000 Roskilde
Denmark

FUJINAMI Masanori Dr.
Nippon Steel Corporation
R & D Laboratories–I
1618 IDA, Nakahara-Ku
Kawasaki 211
Japan

FURRER Albert Prof.
Lab. für Neutronenstreuung
c/o PSI
5232 Villigen PSI
Switzerland

GÄGGELER Heinz Dr.
Research Dept. F3
PSI
5232 Villigen PSI
Switzerland

GARREAU Yves Dr.
Département de physique
de la matière condensée
24, quai Ernest-Ansermet
1211 Genève
Switzerland

GAVILLET Didier Dr.
Research Dept. F3
PSI
5232 Villigen PSI
Switzerland

GENOUD Patrick Dr.
Département de physique
de la matière condensée
24, quai Ernest-Ansermet
1211 Genève
Switzerland

GRIMMER Hans-Konrad Dr.
Research Dept. F3
PSI
5232 Villigen PSI
Switzerland

GYGAX Fredy Dr.
Inst. für Mittelenergiephysik
c/o PSI
5232 Villigen PSI
Switzerland

HAMMER Johannes Dr.
Research Dept. F4
PSI
5232 Villigen PSI
Switzerland

HAUTOJÄRVI Pekka Prof.
Laboratory of Physics
Helsinki University of Technology
02150 Espoo
Finland

HERLACH Dierk Dr.
Research Dept. F3
PSI
5232 Villigen PSI
Switzerland

HIRT Wilfred Dr.
Substitute Director
PSI
5232 Villigen PSI
Switzerland

HOFFMANN Ludger Dr.
Département de physique
de la matière condensée
24, quai Ernest-Ansermet
1211 Genève
Switzerland

KOCH Markus Dr.
Institut für Physik
Max-Planck-Institut für Metallforschung
Heisenbergstrasse 1
Postfach 80 06 65
7000 Stuttgart 80
Federal Republic of Germany

KÖGEL Gottfried Dr.
Institut für Nukleare Festkörperphysik
Universität der Bundeswehr München
Werner-Heisenberg-Weg 39
8014 Neubiberg
Federal Republic of Germany

KOSTORZ Gernot Prof.
Institut fúr Angewandte Physik
ETH-Hönggerberg
8093 Zürich
Switzerland

KRENKE Mike
Universität Stuttgart
c/o PSI
5232 Villigen PSI
Switzerland

LEY Richard Dr.
Institut für Physik
Universität Mainz
Staudinger Weg 7
6500 Mainz
Federal Republic of Germany

LOU Yongming Dr.
Physics Department
Uppsala University
P.O. Box 530
75121 Uppsala
Sweden

LYNN Kelvin G., Prof.
Department of Applied Science
Head of Materials Science Division
Group Leader Physics Department
Brookhaven National Laboratory
Upton, Long Island, NY 11973
U.S.A.

MAIER Karl Dr.
Institut für theoretische und
angewandte Physik der
Universität Stuttgart
Pfaffenwaldring 57
67000 Stuttgart 80
Federal Republic of Germany

MANUEL Alfred A., Dr.
Département de physique
de la matière condensée
24, quai Ernest-Ansermet
1211 Genève
Switzerland

MEIER Peter F. Prof.
Physikinstitut
Universität Zürich-Irchel
Winterthurerstr. 190
8057 Zürich
Switzerland

MORENZONI Elvezio Dr.
Research Dept. F1
PSI
5232 Villigen PSI
Switzerland

NEUSKI Pavel Dr.
Moscow Engineering Physics
Institute
Kashirskoye Chaussee 31
115409 Moscow
USSR
c/o CERN, EP Division
1211 Genève
Switzerland

OTT Hans Rudolf Prof.
Head Research Dept. F3
PSI
5232 Villigen PSI
Switzerland

PARIDAENS, Johan Drs.
Lab. for Nuclear Physics
Rijksuniversiteit Gent
Proeftuinstraat 86
9000 Gent
Belgium

PETER Martin Prof.
Département de physique
de la matière condensée
24, quai Ernest-Ansermet
1211 Genève
Switzerland

PUFF Werner Dr.
Institut für Kernphysik
Technische Universität Graz
Petersgasse 16
8010 Graz
Austria

RICE-EVANS P. Dr.
Dept. of Physics
Royal Holloway College
University of London
Egham, Surrey TW20 0EX
England

SCHAEFER Hans-Eckhardt Prof.
Institut für theoretische und
angewandte Physik der
Universität Stuttgart
Pfaffenwaldring 57
67000 Stuttgart 80
Federal Republic of Germany

SCHENCK Alexander Dr.
Inst. für Mittelenergiephysik
c/o PSI
5232 Villigen PSI
Switzerland

SCHNEIDER Hans Prof.
Strahlenzentrum der
Justus Liebig-Universität
Abt. Angewandte Kernphysik
Leihgesterner Weg 217
6300 Giessen
Federal Republic of Germany

SCHRECKENBACH Klaus Dr.
Institut Laue Languevin
B.P. 156X
38042 Grenoble Cedex
France

SEEGER A. Prof.
Institut für Physik
Max-Planck-Institut für Metallforschung
Heisenbergstrasse 1
Postfach 80 06 65
7000 Stuttgart 80
Federal Republic of Germany

SOLT Gyoergy Dr.
Research Dept. F3
PSI
5232 Villigen PSI
Switzerland

STEFANON Mario Dr.
ENEA
C.R.E. "Ezio Clementel" Bologna
Viale G.B. Ercolani, 8
40138 Bologna
Italy

STOLL Hermann Dr.
Institut für Physik
Max-Planck-Institut für Metallforschung
Heisenbergstrasse 1
Postfach 80 06 65
7000 Stuttgart 80
Federal Republic of Germany

SURBECK Heinz Dr.
KUeR c/o
Institut de physique de
l'Université Fribourg
Pérolles
1700 Fribourg
Switzerland

TANIGAWA Shoichiro Prof.
Institute of Materials Science
University of Tsukuba
Tsukuba, Ibaraki 305
Japan

TAQQU David Dr.
Research Dept. F1
PSI
5232 Villigen PSI
Switzerland

TRIFSTHÄUSER W. Prof.
Institut für Nukleare Festkörperphysik
Experimentalphysik
Universität der Bundeswehr München
Werner-Heisenberg-Weg 39
8014 Neubiberg
Federal Republic of Germany

VICTORIA Max Dr.
Research Dept. F3
PSI
5232 Villigen PSI
Switzerland

WESOLOWSKI Pavel
Institut für Physik
Max-Planck-Institut für Metallforschung
Heisenbergstrasse 1
Postfach 80 06 65
7000 Stuttgart 80
Federal Republic of Germany

ZIMMERMANN Ulrich Dr.
Research Dept. F3
PSI
5232 Villigen PSI
Switzerland

VAN VEEN Tom Dr.
Interfaculty Reactor Institute (IRI)
Delft University of Technology
Mekelweg 15
2629 JB Delft
Netherlands

WAEBER Waldemar Dr.
Research Dept. F3
PSI
5232 Villigen PSI
Switzerland

ZECCA Antonio Prof.
Dipartimento di Fisica
Università degli Studi di Trento
38050 Povo (Trento)
Italy